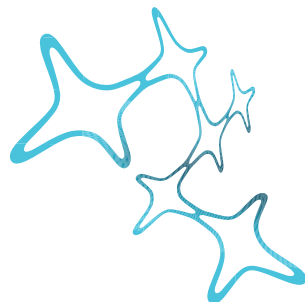


---

# Age-related changes of the cortical visual-vestibular interaction in healthy subjects

Iskra Stefanova

---



Graduate School of  
Systemic Neurosciences

LMU Munich

München 2012



---

# Age-related changes of the cortical visual-vestibular interaction in healthy subjects

Iskra Stefanova

---

Dissertation  
an der Graduate School of Systemic Neurosciences  
der Ludwig-Maximilians-Universität  
München

vorgelegt von  
Iskra Stefanova  
aus Skopje

München, den 7.11.2012

Erstgutachter: Prof. Dr. Marianne Dieterich

Zweitgutachter: Dr. Thomas Stephan

Tag der mündlichen Prüfung: 10.01.2013

## Summary

The visual and vestibular systems play one of the central roles in the perception of verticality, spatial orientation, maintenance of balance and distinguishing self-motion from motion of the environment. As the brain continuously and simultaneously receives an enormous quantity of information through their receptor organs, collaboration between these systems at different levels of information processing is crucial for the proper execution of the above mentioned functions. Psychophysical and neuroimaging research in humans has provided support for the concept of a reciprocal inhibitory visual-vestibular interaction, the functional significance of which lies in suppression of potential mismatch between incongruent sensory inputs delivered from the two systems. Functional magnetic resonance imaging (fMRI) enabled visualization of this interaction through detection of blood-oxygen-level-dependant (BOLD) signal increases or signal decreases in the visual and vestibular networks during unisensory stimulation. Specifically, visual stimulation related to the percept of self-motion, such as optokinetic stimulation, was shown to elicit BOLD signal increases in areas involved in visual processing along with BOLD signal decreases in areas involved in vestibular processing.

Increasing age was shown to alter the morphological and functional properties of the sensory, motor and cognitive systems. Previous research has revealed that senescence associates with deterioration of both, visual and vestibular functions, as well as a change in the psychophysical measurements related to their interaction. However, the effects of age on the BOLD signal pattern reflecting the visual-vestibular interaction have not yet been investigated. Exploring these effects in healthy subjects could offer the possibility to detect early age-related changes in the cortical function occurring before a decline in behavioural measurements can be detected. Aside broadening the scientific knowledge on the physiological changes with age in the sensory systems and their interactions, such research would also help to better understand the pathophysiological processes underlying various visual and vestibular disorders investigated in neuroimaging studies. Therefore, the aim of this doctoral thesis was to explore how the BOLD signal related to the visual-vestibular interaction during optokinetic nystagmus (OKN) changes with age in healthy subjects. It specifically aimed to investigate the age-related changes in the spatial and temporal patterns of the signal during unaltered oculomotor performance. In order to obtain information on the diverse effects of age, the changes in the mean of the BOLD

signal, as well as the changes in its temporal variability were analyzed. For the purpose of differentiating between global and task-related changes with age, the alterations of the BOLD signal during OKN were compared to the alterations of the BOLD signal elicited by a pure visual and a pure motor task.

In the frame of this work, we were able to show that significant age-related changes in the mean of the BOLD signal and in its temporal fluctuations occur prior to any measurable decline in OKN performance. The changes in the mean of the BOLD signal were task-specific and possibly reflected age-related alterations in neurovascular coupling and neural processing related to OKN. They were found only in cortical and subcortical areas of the visual system. The changes in the temporal fluctuations of the BOLD signal were not specific for the OKN task, but rather region-specific, affecting mostly areas known to be part of the multimodal vestibular processing network.

# Contents

<b>Summary</b>	<b>v</b>
<b>1 Introduction</b>	<b>1</b>
1.1 Visual system . . . . .	1
1.2 Vestibular system . . . . .	2
1.3 The visual-vestibular interaction . . . . .	3
1.4 Optokinetic nystagmus - a probe into the visual-vestibular interaction . . . . .	5
1.5 Age-related changes of the signal measured in imaging studies . . . . .	9
1.6 Age-related changes of OKN performance and oculomotor function . . . . .	12
1.7 Methodological aspect: functional magnetic resonance imaging and the blood-oxygen-level-dependent (BOLD) signal . . . . .	13
1.8 Aim of the thesis . . . . .	16
<b>2 Methods</b>	<b>19</b>
2.1 Subjects . . . . .	19
2.2 Experimental design, tasks and stimuli . . . . .	19
2.3 Video-oculography (VOG) . . . . .	21
2.4 Functional MRI acquisition . . . . .	21
2.5 Data analysis . . . . .	22
2.5.1 VOG data analysis . . . . .	22
2.5.2 fMRI data analysis . . . . .	22
<b>3 Results</b>	<b>31</b>
3.1 Video-oculography data . . . . .	31
3.2 Covariates analysis . . . . .	31
3.3 Dynamics of the positive BOLD response (PBR) and their age dependencies . . . . .	31
3.3.1 Group fMRI data analysis of PBR amplitude, latency to peak and dispersion . . . . .	31
3.3.2 Age-related changes of PBR dynamics . . . . .	34
3.4 Dynamics of the negative BOLD response (NBR) and their age dependencies . . . . .	38
3.4.1 Group fMRI data analysis of NBR amplitude, latency to peak and dispersion . . . . .	38
3.4.2 Age-related changes of NBR dynamics . . . . .	41
3.4.3 Voxel-based-morphometry . . . . .	42
3.5 Temporal variability of the BOLD signal (SD) and its alteration with age . . . . .	42
3.5.1 Differences between the temporal variability during stimulation and during rest . . . . .	42
3.5.2 Age-related changes of the temporal variability during stimulation and during rest . . . . .	44

---

<b>4 Discussion</b>	<b>51</b>
4.1 Age-related changes of the positive BOLD response (PBR) during OKN . . .	51
4.1.1 Interpretations of the age-related changes in PBR dynamics . . . . .	52
4.1.2 Task-specific changes of PBR dynamics with age . . . . .	53
4.2 Age-related changes of the negative BOLD response (NBR) during OKN . .	55
4.3 Temporal variability of the BOLD signal . . . . .	56
4.3.1 Differences between SD <sub>rest</sub> and SD <sub>stimulation</sub> . . . . .	56
4.3.2 Age-related changes of SD <sub>rest</sub> and SD <sub>stimulation</sub> . . . . .	58
4.4 Conclusions . . . . .	60
4.5 Future research . . . . .	60
<b>Bibliography</b>	<b>61</b>
<b>Acknowledgements</b>	<b>71</b>
<b>Appendix</b>	<b>73</b>

# 1 Introduction

## 1.1 Visual system

The visual system provides humans with crucial sensory information about the environment, as it enables the perception of objects, shapes, colours and motion of the surrounding. The visual receptors (photoreceptors) are located in the retina, and transform light energy into neural signals. These signals are then carried through the retinofugal projection (consisted of the optic nerve, optic chiasm and optic tract) to the lateral geniculate nucleus (LGN). From LGN, ascending pathways lead to the primary visual cortex (V1) where discrimination of changes in visual orientation, spatial frequencies and colours, as well as global organization of the scheme takes place (Lamme and Roelfsema, 2000). From V1, two large-scale cortical streams originate: the 'dorsal stream', projecting towards the parietal lobe, and the 'ventral stream', projecting towards the temporal lobe. The 'dorsal stream' includes the areas V2, V3, V5 and the medial superior temporal area (MST). It has been assumed to be involved in the analysis of visual motion, visual control of action and navigation. The 'ventral stream' includes the areas V2, V3, V4 and part of the inferior temporal lobe (IT) and has been assumed to be involved in the perception of the visual world (Bear et al., 2006). The LGN, V1 and the higher visual areas are not only interconnected with driving feed-forward connections, but also with modulatory feedback projections which modify and shape the respective neural responses.

Parts of the axons from the optic tract do not project cortically, but end in the pretectum of the midbrain and control the pupil size and certain types of eye movements. Other axons of the optic tract project to the superior colliculus of the midbrain and control the eye and head movements through indirect connections with motor nuclei in the brain stem, thereby stabilizing the image on the retina during visual motion. Although the initiation of these reflexes is not under cortical control they can be modified by top-down projections from the cortex.

The visual system cooperates tightly with the other sensory as well as motor systems at different levels of information processing. Through these inter-sensory and sensory-motor interactions, it is involved in the performance of simple actions, such as the optokinetic nystagmus, as well as in that of higher functions such as orientation in space, perception

of verticality or self-motion.

## 1.2 Vestibular system

The vestibular system provides information on the accelerating movements of the head. The vestibular end organ is located in the inner ear of each side and it consists of two otolith organs (utricle and saccule) and the three semicircular canals (anterior, posterior and horizontal canal). The otolith organs are sensitive to linear acceleration and the force of gravity, while the semicircular canals sense rotational accelerations. Each pair of semicircular canals is positioned in such a way that the canal on one side lays almost parallel to its counterpart on the other side. In this way, they work in a push-pull manner during acceleration in a certain direction. For example, rightward head rotation stimulates the right horizontal semicircular canal and at the same time inhibits the left horizontal semicircular canal. This simultaneous excitation on one side and inhibition on the other makes the vestibular afferents, which are active even at rest, highly sensitive to accelerating motion in different directions. Through combined activation of the receptors in both, the otolith organs and the semicircular canals, a vast range of physical motions experienced in everyday life can be sensed. The neural signals from the vestibular receptors are carried through the vestibular nerve and the vestibular nuclei located in the medullary brain stem to the ocular motor nuclei (i.e. vestibulo-ocular reflex) as well as to the cerebellum. From here, feed-forward ascending (cortical) and descending (spinal) pathways originate. The vestibular nuclei also receive modulatory projections from the cerebellum, the visual and the somatosensory cortical areas, and combine vestibular information with information from other sensory modalities.

It is characteristic for the vestibular system that its central processing is highly convergent and multimodal (Angelaki and Cullen, 2008). Because it can only sense accelerating motion, the vestibular system alone cannot provide information on position and self-motion, and therefore cannot give rise to a separate conscious sensation. In fact, unlike in the case of the other sensory systems, no primary (unimodal) vestibular cortex can be identified. Rather, a multimodal network of cortical areas receiving vestibular input, where extensive multimodal convergence with other sensory and motor signals occurs, executes the highest functions of this system. Animal studies have identified the area 2v at the tip of the intraparietal sulcus (IP), area 3aV in the central sulcus, area 7 in the inferior parietal lobule, the parieto-insular vestibular cortex (PIVC) in the monkey (Grüsser et al., 1990a,b), and the anterior suprasylvian sulcus and the temporo-parietal cortex in the cat (Andersson and Gernand, 1954) as part of this multimodal vestibular network. Imaging

studies in humans using caloric or galvanic vestibular stimulation have identified a similar network of the temporo-parietal cortex, the posterior insula, the anterior cingulate cortex, the precuneus, the supramarginal gyrus, the hippocampus, the thalamic pulvinar and the cerebellar vermis comprising the human homologue of this multimodal vestibular network (Bottini et al., 1994; Bucher et al., 1998; Deutschländer et al., 2002; Stephan et al., 2005; Dieterich, 2007).

Through collaboration with the other sensory and the motor systems, the vestibular system helps to form the sense of balance and verticality, contributes to the coordination of head, body and eye movements, as well as to the adjustments of the body posture and the perception of self-motion. Thereby, just as the visual system, it plays a crucial role in everyday life as it enables the performance of important reflexes, such as the vestibulo-ocular reflex, and variety of precepts.

### **1.3 The visual-vestibular interaction**

As discussed above, the visual and vestibular systems, both contribute to the perception of verticality, maintenance of balance, spatial orientation and distinguishing self-motion from object motion. Together with the somatosensory system they cooperate to determine the internal representation of space and subjective body orientation in unique 3-D coordinates, which are either egocentric (body-centered) or exocentric (world-centered) (Brandt and Dieterich, 1999). Proper execution of these functions requires continuous transformation and integration of the information coded in the coordinates of the peripheral sensory organs of each system. It has been proposed that a potential mismatch between incongruent sensory information from the both systems could be resolved by reciprocal inhibitory inter-sensory interaction (Brandt et al., 1998). The functional significance of such interaction would be to allow suppression of a potential mismatch between two incongruent or misleading sensory inputs by shifting the sensorial weight to the dominant or more reliable modality (Brandt et al., 2002).

The role of the visual-vestibular interaction can be demonstrated in the example of self-motion perception. Self-motion perception can be dominated either by vestibular or visual input. On the one hand, vestibular stimulation invariably leads to sensation of body motion, however, only during acceleration or deceleration. Visual motion, on the other hand, provides information on motion during constant velocities and can lead to two perceptual interpretations: self-motion or motion of the surrounding. Therefore, motion perception during constant velocity, is mainly dependent on the visual system. The actual horizon-

tal direction and speed perceived during constant velocity motion are transduced only by the relative optic flow of the surroundings. Concurrent vertical vestibular stimulations and secondary involuntary head accelerations provide vestibular information that is inadequate or even misleading with respect to self-motion perception in the horizontal direction. It is therefore desirable, under this condition, that they are suppressed by deactivation of the input from the vestibular system (Brandt and Dieterich, 1999).

The visual-vestibular interaction plays also a crucial role in the perception of verticality by matching the cortical visual and vestibular 3-D coordinate maps. A mismatch between these maps has been assumed to underlie room tilt illusions, transient upside-down vision or apparent 90-degree tilts of the visual scene occurring in central vestibular disorders. As two different verticals - visual and vestibular - cannot be perceived at the same time, a cortical mechanism which integrates visual-vestibular input is necessary to determine the current percept of a unique verticality (Brandt, 1999). In the case of room tilt illusions, the plasticity of the visual-vestibular interaction enables vision to 'dominate and correct' the spatial orientation, based on the empirical spatial cues for upright contained in the visual scene (Brandt and Dieterich, 1999).

Support of the concept of reciprocal inhibitory visual-vestibular interaction has been found in previous behavioural and imaging studies. Probst et al. (1985) have shown that thresholds for detecting vestibular body accelerations (vestibular system) are increased during optokinetically induced vection (visual system). Straube et al. (1987) demonstrated that somatosensory and vestibular stimulation inhibits optokinetically induced self-motion perception when applied simultaneously. Imaging studies using functional magnetic resonance imaging (fMRI) and positron emission tomography (PET) have visualized this interaction, by showing signal increases in the cortical areas of the stimulated system, along with simultaneous signal decreases in the cortical areas of the system not receiving any input. Stimulation of the vestibular system, using galvanic or caloric stimulation, elicited signal increases in the multisensory vestibular areas and simultaneous signal decreases in the visual cortex (Bense et al., 2001; Deutschländer et al., 2002; Stephan et al., 2005). Conversely, visual optokinetic stimulation, which is linked to the perception of self-motion, elicited signal increases in the visual cortical areas and simultaneous signal decreases in the areas of the multimodal vestibular cortex (Brandt et al., 1998; Deutschländer et al., 2002; Dieterich et al., 2003; Konen et al., 2005; Kikuchi et al., 2009).

Based on this, it can be concluded that both, vestibular stimulation, as well as visual stimulation linked to the percept of self-motion, can be used to explore various aspects of

---

the visual-vestibular interaction.

## **1.4 Optokinetic nystagmus - a probe into the visual-vestibular interaction**

Visual optokinetic stimulation presents the coherent and continuous movement of targets across the visual field, either due to actual motion of the surrounding, or due to relative motion during self-motion. As such, it is closely related to the perception of self-motion and therefore, presents a useful tool for investigating the interaction between the visual and vestibular systems. Optokinetic nystagmus (OKN) is the oculomotor reflex elicited by optokinetic stimulation; its function is to stabilize the retinal image during visual motion. It is comprised of slow tracking eye movements and fast resetting saccades. The tracking eye movements are the slow component of OKN in the direction of the visual stimulus which enable following of the moving targets. The saccades are the fast component of OKN in the direction opposite to that of the visual stimulus, which reset the eye to its original position. Brain areas involved in the generation of saccades and slow tracking movements are located in the occipital cortex, the adjacent visual-motion areas (MT/MST complex), the frontal eye fields (FEF), the supplementary eye fields (SEF), the parietal eye fields (PEF), the cerebellum and the brain stem (Büttner and Büttner-Ennever, 2006)(Fig. 1.1).

Imaging studies in humans have shown consistent results by demonstrating signal increases in these visual and oculomotor areas during performance of OKN (Bucher et al., 1997; Dieterich et al., 1998, 2003; Konen et al., 2005; Bense et al., 2006; Della-Justina et al., 2008; Kikuchi et al., 2009). It was further revealed that OKN does not only elicit signal increases in the visual and oculomotor cortex areas, but also concurrent signal decreases in the multimodal vestibular brain regions. In an fMRI study using small-field optokinetic stimulation, (Dieterich et al., 2003) found decreases of the blood-oxygen-level-dependant (BOLD) signal in the posterior insula, retroinsular cortex, superior temporal gyrus, precentral gyrus, inferior parietal lobule, anterior cingulate gyrus, hippocampus and corpus callosum (Figs. 1.2 and 1.3).

This pattern of BOLD signal increases in visual and oculomotor areas and simultaneous signal decreases in multimodal vestibular areas was interpreted as a correlate of the reciprocal inhibitory visual-vestibular interaction. The interaction between the visual, vestibular and oculomotor systems can be demonstrated during combined visual and vestibular stimulation such as during self-rotation, which induces OKN. As the rotation

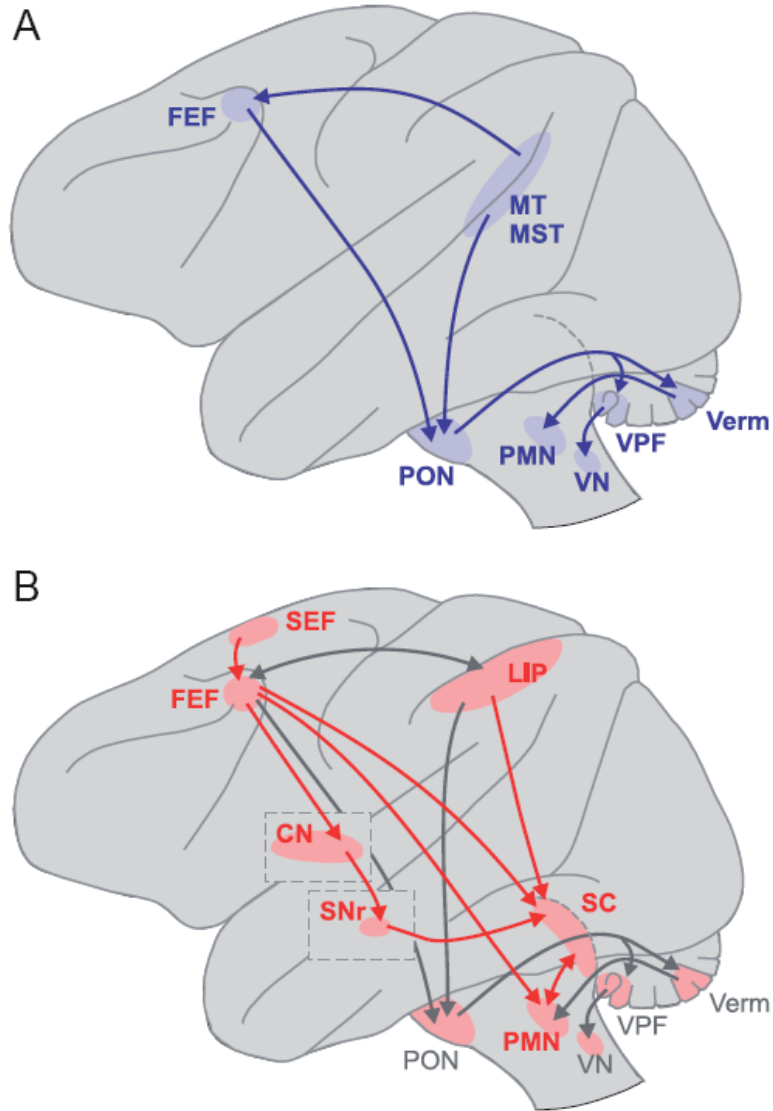


Figure 1.1: Outline of the traditional descending pathways for pursuit (A) and saccades (B). Diagram depicts a lateral view of the monkey brain. Shaded regions indicate specific areas within the cerebral cortex, cerebellum, and brain stem, and arrows indicate the anatomical connections between these areas. Regions demarcated with dashed lines indicate structures normally covered by the cerebral cortex. For clarity, not all relevant areas are depicted and arrows do not always correspond to direct anatomical connections (Krauzlis, 2004) (reprinted with kind permission from The American Physiological Society).

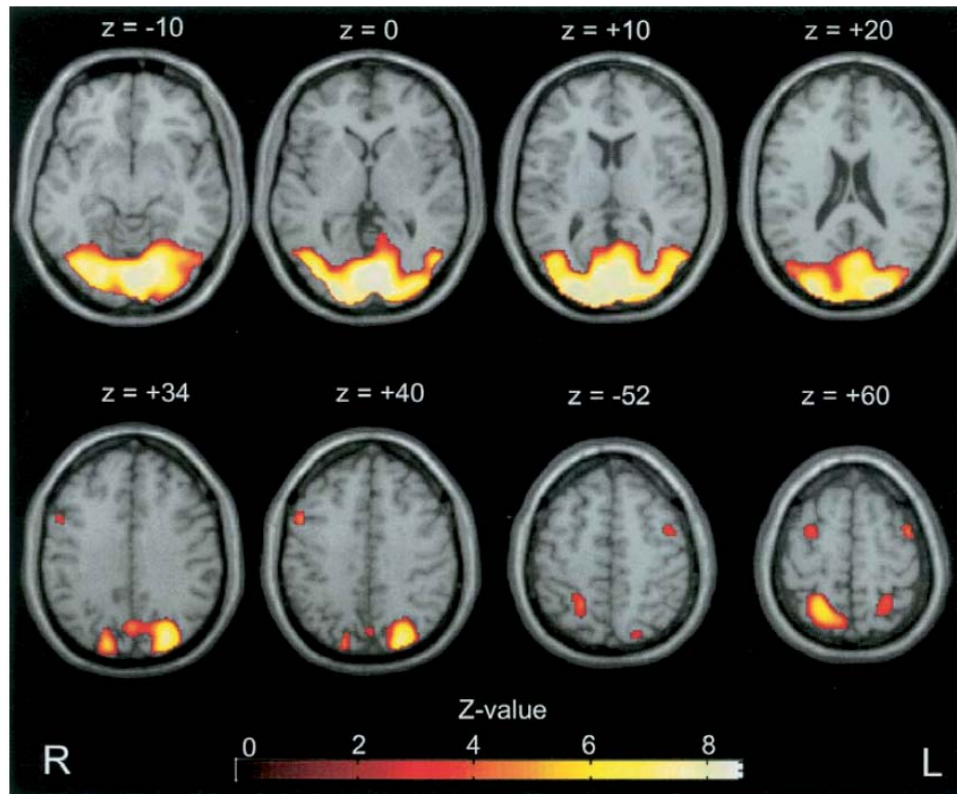


Figure 1.2: Activation areas during horizontal visual optokinetic stimulation of a restricted field of view obtained by statistical group analysis ( $n=7$ ). Activation maps were superimposed onto selected transverse sections of a standard brain template and thresholded at  $P=0.001$  (uncorrected). Activations were found bilaterally in the striate and extrastriate visual cortex areas with the maximum in the lingual gyrus, inferior and medial occipital gyri, inferior temporal gyrus, cuneus, as well as in the temporo-occipital areas, the occipital gyrus, and the precuneus. In addition, significant increases were found in the precentral gyri in both hemispheres at two different sites, one in the rostral and medial parts (BA 6) at the junction of the superior frontal sulcus with the precentral sulcus and the other in caudal and lateral parts (BA 9) at the border to the medial frontal gyrus (Dieterich et al., 2003) (reprinted with kind permission from Springer Science and Business Media)

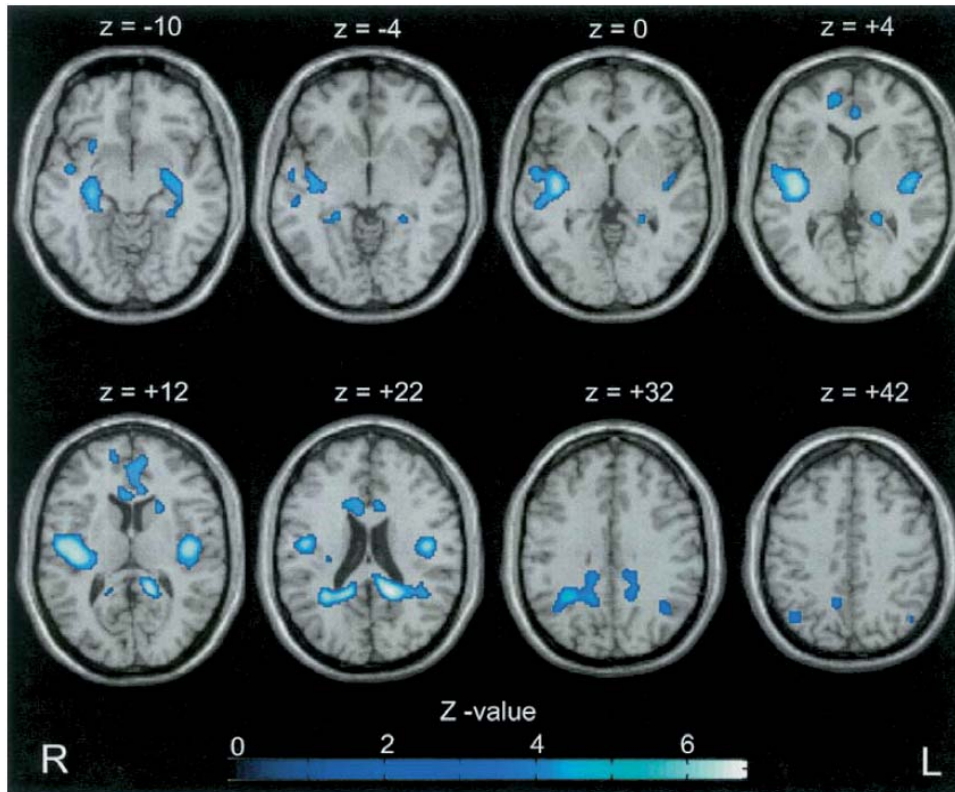


Figure 1.3: Areas with signal decreases during visual optokinetic stimulation of a restricted field of view obtained by statistical group analysis ( $n=7$ ). Activation maps were superimposed onto selected transverse sections of a standard brain template and thresholded at  $P=0.0001$ , corrected for multiple comparisons. Signal decreases were found in clusters of the temporo-parietal lobe bilaterally, including the posterior insula (first and second long insular gyri), retroinsular areas, the transverse temporal gyri (BA 41), superior temporal gyri (BA 22), and pre- and postcentral gyri (BA 4 and 6). Additional signal decreases were seen in rostradorsal parts of the superior temporal gyri (BA 22) in the right hemisphere, reaching into the inferior parietal lobule (BA 40), the inferior-anterior insula, as well as bilaterally in the hippocampus with the adjacent optic radiation, the corpus callosum, and the anterior cingulate gyri (BA 24, 22). In the rostral brain regions signal decreases of the precentral gyrus extended into two Brodmann areas, bilaterally into BA 4 and on the left side into BA 6 (not mapped) (Dieterich et al., 2003) (reprinted with kind permission from Springer Science and Business Media).

---

reaches constant velocity, the vestibular drive for OKN declines and the optokinetic stimulation becomes the main source of input for the oculomotor response. Previous animal studies have shown that this occurs as optokinetic stimulation activates the velocity storage mechanism (indirect component of OKN) in the vestibular nuclei through the nucleus of the optic tract (NOT) located in the pretectum (for review on the direct and indirect components of OKN refer to (Cohen et al., 1977) and for review on NOT function refer to (Cohen et al., 1992)). This functional cooperation of the visual and vestibular systems was pointed as an explanation for the observed BOLD signal changes in the study of Dieterich et al. (2003). Namely, visual optokinetic stimulation is linked to the visual perception of self-motion. Such unimodal stimulation, as discussed in Brandt et al. (1998), could theoretically lead to a potential mismatch between the sensory inputs from the visual and vestibular systems and would therefore, require shifting of the sensorial weight to the more dominant sensory modality, in this case the visual system. It was suggested that in imaging studies this would consequently result in the observed pattern of BOLD signal increases in the visual cortical areas and signal decreases in the cortical network receiving vestibular input. Later imaging studies have offered supporting results (Konen et al., 2005; Kikuchi et al., 2009).

Based on these findings and the fact that OKN offers directly measurable parameters of performance, this reflex can be utilized for exploring the effects of age on the visual-vestibular interaction in human imaging studies.

## **1.5 Age-related changes of the signal measured in imaging studies**

Imaging studies in humans investigating the effects of age on the signal related to sensory, motor and cognitive functions have demonstrated age-related changes in the brain's spatial and temporal activation patterns related to a specific task. Increasing age was shown to associate with task-specific and region-specific signal decreases, accompanied by decline in behavioural performance. Such signal decreases were suggested to reflect age-related primary deficits in neural function (Rajah and D'Esposito, 2005). Beside age-related signal decreases, signal increases in task-related and non-task-related brain regions have widely been demonstrated. Park et al. (2001) classified these age-related signal increases in three types of functional changes: contralateral recruitment, in which younger adults recruit a brain area in one hemisphere, while older subjects additionally use the homologous area in the contralateral hemisphere (Cabeza et al., 2002); unique recruitment, in which older adults additionally recruit brain areas not homologous to any brain region activated in the younger adults (McIntosh et al., 1999); and substitution, in

which older adults do not recruit a brain area usually activated in the younger adults, but use different brain regions for the performance of the same function (Hazlett et al., 1998).

The observed signal increases together with the accompanying changes in the behavioural performance led to the forming of two hypotheses, the 'functional compensation' and the 'dedifferentiation' hypothesis, aiming to explain the neural background of the observed age-related changes. The 'functional compensation' hypothesis refers to the signal increases in non-task related brain areas which correlate with better behavioural performance in the older adults. According to this hypothesis, while older adults recruit both, task related and non-task related brain areas, the activity in the task related regions might be decreased compared to the activity in the younger adults. The recruitment, however, of the non-task related brain areas should result in concomitant improvement of task performance (Rajah and D'Esposito 2005). This hypothesis was originally conceptualized in the PET study of (Cabeza et al., 1997), who observed that aside age-related signal decreases, older adults also showed age-related signal increases and a bilateral pattern of prefrontal cortex (PFC) activity during verbal recall compared to a rather unilateral pattern found in younger subjects. Other studies have similarly demonstrated age-related BOLD signal increases, as well as recruitment of additional brain networks during specific task performance, and suggested that these could present a reflection of neuronal compensatory mechanisms which counteract cognitive or sensorymotor decline (Madden et al., 1999, 2004; Reuter-lorenz et al., 2000; Cabeza et al., 2002; Ward and Frackowiak, 2003; Heuninckx et al., 2008). The observation of age-related reorganization of the cortical activation has been further supported by other PET and electrophysiological studies (Levine et al., 2000; De Sanctis et al., 2008). Studies on age-related changes of the multisensory interactions have broadened this concept by showing reduction of the inhibitory reciprocal interaction and increase of the multimodal integration with advancing age (Laurienti et al., 2006; Peiffer et al., 2009; Zwergal et al., 2010).

The 'dedifferentiation' hypothesis in the broader sense of its meaning posits that increasing age correlates with an increase in brain areas recruited to perform a specific task or with a recruitment of different brain regions than the ones used in the younger adults. Unlike the 'functional compensation' hypothesis, the 'dedifferentiation' hypothesis could encompass not only signal changes reflecting functional compensation which improves performance, but also changes which have no effect on the performance, or changes which reflect age-related dedifferentiation of neural function (Park et al., 2001; Rajah and D'Esposito, 2005; Voss et al., 2008). The latter refers to a decrease of the signal-to-noise ratio in the

cortical processing which would lead to a decrease in regional process-specificity and an age-related increase in non-specific cortical activations during different tasks (Li et al., 2001). Such changes would lead to diffuse signal increases in cortical regions in a non-selective manner, which does not correlate well with the behavioural performance in the older adults (Logan et al., 2002).

Most of the above mentioned studies addressed the effects of age on the spatial pattern of cortical activation and interpreted these signal changes as a reflection of age-related changes in neural function. Many studies, however, have also explored the effects of age on the temporal pattern of the BOLD signal, as well as the effect of age on the neurovascular coupling as a reason for changes in the measured signal (Taoka et al., 1998; D'Esposito et al., 1999; Buckner et al., 2000; Huettel et al., 2001; Hesselmann et al., 2001; Harris et al., 2011). Studies using pure motor or pure visual tasks demonstrated age-related changes in the BOLD signal latency and duration, in the absence of any amplitude alterations (Taoka et al., 1998; Huettel et al., 2001; Richter and Richter, 2003). They suggested that these findings rather reflect changes in neurovascular coupling due to age-related degenerative alterations in the brain's vasculature, structure and neural metabolism, than isolated changes in neural function.

Although there is an extensive literature on the age-related changes of the BOLD signal correlated to sensory, motor and cognitive tasks, no study is available on the changes of the BOLD signal reflecting visual-vestibular interaction. Previous research has demonstrated that both, the visual and the vestibular system, deteriorate with increasing age (Allison et al., 1984; Baloh et al., 2001; Jahn et al., 2003; Snowden and Kavanagh, 2006). Behavioural studies on age-related changes in the interaction between these systems have shown an altered gain modulation in senescence (Paige, 1994; Deshpande and Patla, 2007). Yet, changes in the visual-vestibular interaction which develop prior to any evident decrement in performance cannot be assessed solely based on behavioural measures, but require additional imaging parameters. As the effects of age on the spatial and temporal BOLD signal pattern, reflecting visual-vestibular interaction, have not yet been investigated, it remains unclear whether age-related changes of this signal can be observed during preserved task performance, and whether they, under such conditions, reflect global or task-specific effects of age.

## 1.6 Age-related changes of OKN performance and oculomotor function

Behavioural studies on the effects of age on OKN have shown a decrease in its performance with increasing age. This decrease, however, seems to be dependent on the velocity and type of applied optokinetic stimulation. Most of the previous studies demonstrated a decline in OKN performance when stimulus velocities above  $40^\circ/\text{s}$  were used. Simons and Büttner (1985) investigated the effects of age on the maximal OKN slow phase velocity (SPV) and found that it closely followed stimulus velocity up to  $40 - 50^\circ/\text{s}$ , but then progressively decreased with increasing age. They noted that this decrease was not restricted to ages above 60, but rather a continuous process already affecting subjects in the fourth and fifth decade. Baloh et al. (1993) found that the OKN gain (defined as the ratio of OKN slow phase velocity and stimulus velocity) rapidly decreased when higher stimulus velocities were applied in subjects above 75 years. During lower stimulus velocities, however, the OKN gain was normal and reached one. Kato et al. (1994) further showed that the age-related changes in the OKN SPV were not only dependent on stimulus velocity, but also on whether stimulation with constant or linearly increasing velocity was applied. Namely, when using linearly increasing stimulus velocity significant decrease in OKN SPV was observed at  $40^\circ/\text{s}$ , whereas during constant velocity stimulation this decrease occurred at velocities of above  $60^\circ/\text{s}$ . Significant age-related decline of OKN gain during stimulus velocity of  $60^\circ/\text{s}$  was further demonstrated in the study of (Kerber et al., 2006). These studies suggest that OKN performance remains unaffected by senescence during relatively low velocity stimulation, but decreases significantly when higher stimulus velocities are used.

Although the effects of age on the OKN performance have been thoroughly investigated, the age-related changes of the BOLD response pattern elicited by this reflex remain to be explored. Previous research on aging effects on the BOLD signal during non-reflexive oculomotor tasks (prosaccades and antisaccades) has shown a shift in the spatial pattern of the BOLD response, accompanied by an overall decrease in its amplitude, while demonstrating only a moderate decrease in the oculomotor performance (Raemaekers et al., 2006). Investigating the effects of age on the BOLD signal pattern during OKN would not only offer new information on how the brain changes with increasing age during performance of common reflexive tasks, but will also provide an insight into the effects of age on the visual-vestibular interaction.

---

## 1.7 Methodological aspect: functional magnetic resonance imaging and the blood-oxygen-level-dependent (BOLD) signal

As the name implies, magnetic resonance imaging is a technique that generates images of biological tissues by usage of strong magnetic fields. Through application of a series of changing magnetic gradients and oscillating electromagnetic fields energy is being absorbed by the atomic nuclei of the tissue. The MRI scanners are tuned to the frequency of the hydrogen nuclei (essentially containing one proton), which are the most prevalent nuclei in the human body and possess their own spins. When a subject is placed in the scanner, all the protons in the body align with the applied magnetic field ( $B_0$ ). Additional application of a specific radiofrequency (RF) pulse disturbs the protons and changes their orientation. As the RF pulses are switched off, the protons tend to return to their original position, during which they emit energy in form of radio waves which are then measured. The BOLD (blood-oxygen-level-dependent) signal, which is the basis of fMRI, essentially presents the change in the emission of RW due to changes in the ratio of deoxygenated ( $Hb$ ) and oxygenated ( $HbO_2$ ) haemoglobin in a certain part of the tissue. It presents a relative measure as it is always estimated in relation to the ratio of deoxygenated and oxygenated haemoglobin during a baseline condition. Haemoglobin is an iron-containing oxygen transport metalloprotein in the red blood cells of all vertebrates. It consists of four globular subunits (2 $\alpha$  and 2 $\beta$ ), each one containing a cofactor - heme, which is a porphyrine structure containing iron molecules with different valences ( $Fe^{2+}$  or  $Fe^{3+}$ ). Depending on the current valence of the iron molecule, the heme can temporarily and reversibly bind  $O_2$  and deliver it for use in the cell metabolism. The oxygenated and deoxygenated haemoglobin possess different magnetic properties when placed in a magnetic field, such as in the MRI scanner.  $Hb$  has the properties of a paramagnetic substance, which means that its atoms have a net magnetic moment, but are oriented randomly throughout the sample, resulting in zero magnetization. During application of an external magnetic field, the moments tend towards alignment along it, giving a net magnetization which increases with the strength of the applied magnetic field. Therefore,  $Hb$  creates magnetic inhomogeneities which consequently lead to a lower signal emission. The  $HbO_2$  has the properties of a diamagnetic material as its atoms possess no magnetic moments and therefore have no magnetization in a zero field. When a magnetic field is applied, a small negative moment is induced on the diamagnetic atoms, which is proportional to the applied field strength. This magnetic moment, however, is small and can be even neglected, because of which  $HbO_2$  does not change the local homogeneity of the magnetic field. Therefore, a decrease of the  $Hb/HbO_2$  ratio will result in a decrease of local field inhomogeneity and consequently a relative increase in RW emission from this part of the tissue (Huettel et

al., 2004).

Taking this into consideration, the origin of the BOLD signal can be explained in a very simplified manner with several sequential steps (Fig. 1.4). First, an increase in the neural activity leads to an increased demand on energy (in form of adenosine-triphosphat ATP) and oxygen ( $O_2$ ). Extraction of oxygen from the  $Hb$  molecule initially increases the  $Hb/HbO_2$  ratio. However, certain neural and astrocytic factors accompanying increased neural activity lead to a change in the regional vascular tonus (dilatation of arteries and capillaries), which then causes an increase in the regional cerebral blood flow (CBF) and cerebral blood volume CBV, and through that, an increase in the delivery of  $HbO_2$ . The delivery of  $HbO_2$ , however, overpasses the demands on  $O_2$  from the cells' metabolism, which results in an increase in  $HbO_2$  concentration in the local tissue. Based on this change of the  $Hb/HbO_2$  ratio in certain part of the brain at a given moment, as well as the structure of the tissue, changes in the emitted RW can be used to make assumptions about the neural activity in this part of the brain. From the above mentioned, it can be resumed that the BOLD signal presents a correlate of the neural processes one aims to investigate. The relationship between these neural processes and the subsequent vascular response leading to changes in the measured BOLD signal is known as neurovascular coupling. For proper interpretation of the BOLD signal it is of crucial importance to understand the complexity of the mechanisms underlying neurovascular coupling.

Recent studies strongly suggest that it is rather the changes of synaptic state that affect the blood flow than the changes in neural output (Logothetis et al., 2001; Logothetis, 2008). As both, neural input (integration and processing) and neural output (conduction, spiking) require energy, it is important to have in mind the energy budget of the neurons. Attwell and Laughlin (2001) estimated that the biggest energy is required at the synaptic level and is mainly used for restoring ionic gradients after uptake of glutamate. Consequently, the BOLD signal need not directly be dependent on spiking activity, but rather reflect a constellation of factors associated with neural activity in a certain area. Harris et al. (2011) discussed that neurotransmitters released during synaptic activation directly influence blood flow and therefore, the BOLD signal might most closely reflect excitatory synaptic activity. The neurovascular coupling which is the base of the BOLD signal, is mediated via neural and astrocytic vasoactive ions ( $K^+$ ,  $Ca^{++}$ , and  $H^+$ ), metabolites (adenosine, lactate), diffusible gases ( $NO$ ,  $CO$ ), vasoactive neurotransmitters (acetholine, dopamine, vasoactive intestinal peptide) and arachidonic derivatives. Studies on the correlation between the BOLD signal and the neural electrophysiological recordings in a certain area have immensely contributed to the understanding of this signal. Logothetis

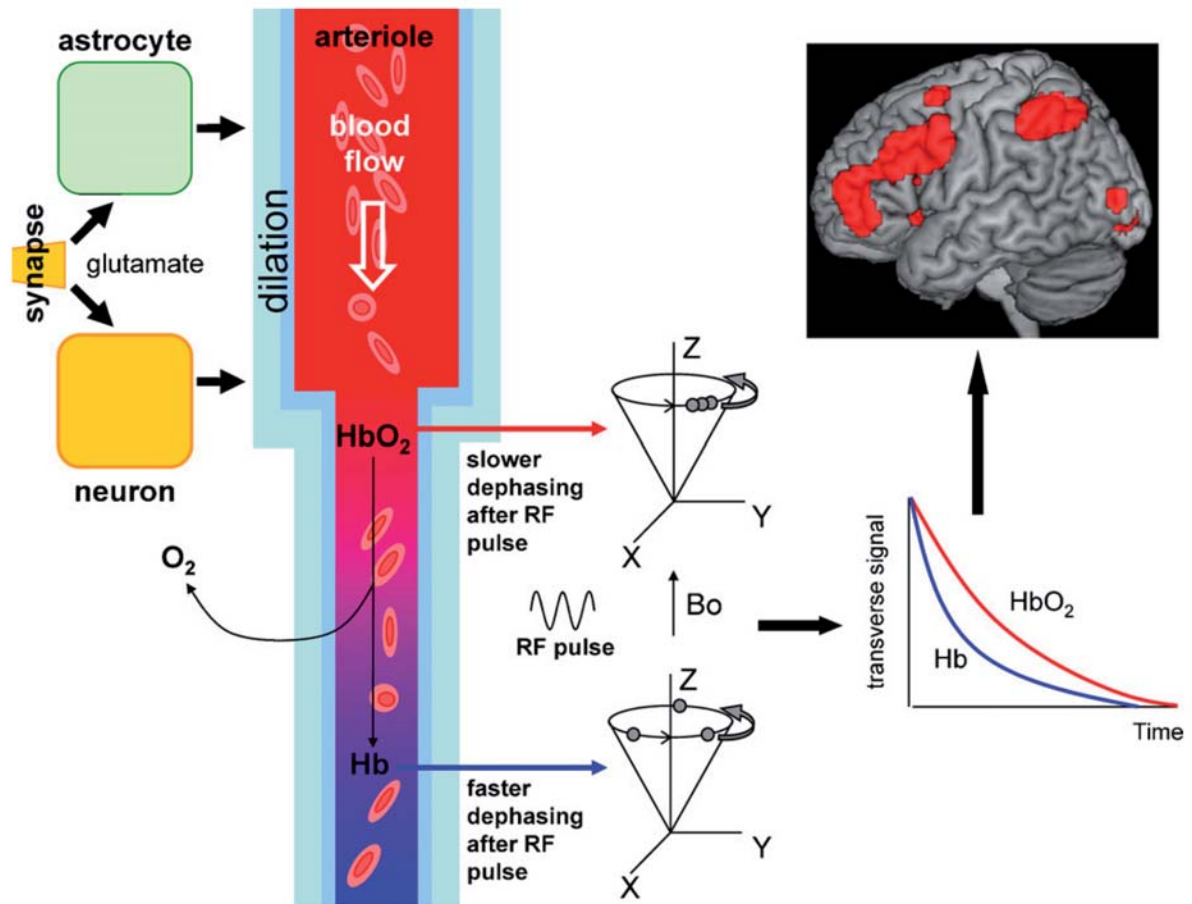


Figure 1.4: Schematic diagram showing the different stages of how BOLD signals are generated, from neurobiology through physics to data analysis. On the left, neural activity releases transmitters (glutamate) which act via neuronal and astrocytic signalling systems to trigger an increase of local blood flow. Neuronal activity also leads to  $O_2$  consumption and generation of paramagnetic deoxygenated haemoglobin ( $Hb$ ) from diamagnetic oxygenated haemoglobin ( $HbO_2$ ). The blood flow increase brings in fresh oxygenated blood which (in adults) lowers the local concentration of  $Hb$ . This decreases the non-homogenizing effect that  $Hb$  has on the local magnetic field which protons in  $H_2O$  experience. As a result, after radiofrequency (RF) pulse is applied transverse to the magnetic field used to align the proton spins ( $B_0$ ), the synchronised spin precession in the transverse plane dephases more slowly (graph on right). The difference in decay time between the red ( $HbO_2$ ) and blue ( $Hb$ ) curves in the graph generates the increased MRI signal from protons in areas where neurons are active, which is represented as the red spots superimposed on a structural image of the brain at the top right (Harris et al., 2011) (reprinted with kind permission from Elsevier).

et al. (2001) recorded the single unit activity (SUA), the multi unit activity (MUA) and the local field potentials (LFP) in the visual cortex of monkeys while simultaneously performing fMRI. This study demonstrated a positive correlation between the BOLD signal and all of the three electrophysiological parameters. However, the correlation between the BOLD signal and the LFP was stronger and the LFP showed to be a better predictor of the signal. This was not because the correlation coefficient for MUA was smaller than the one for LFP, but because of the dissociation between LFP and MUA (which is always correlated to SUA). Therefore, they concluded that the BOLD signal rather reflects the neural population's input and processing (as LFP) than the neural spiking (reflected in SUA). In order to further investigate these claims, studies have been performed to explore the relation between MUA and LFP. Goense and Logothetis (2008) showed dissociation between the two parameters through neural adaptation. Namely, the neural spiking rate decreased shortly after stimulus onset, while the LFP remained increased for a longer period of time. Rauch et al. (2008) further showed that such dissociation can also be seen after serotonin injection in the visual cortex, which caused a decrease in MUA, but no change of LFP or the BOLD signal. As these results, however, were obtained from primary sensory areas, it is possible that higher cognitive areas might show different relations between the BOLD signal and the electrorecordings. Furthermore, it must be noted that these correlations can be non-linear, dependent on the investigated brain area and task, as well as on the functional context. Therefore, as concluded by Raichle and Mintun (2006), for the interpretation of imaging studies it is important to see the brain not as a system primarily responding to changing contingencies, but as one operating on its own, intrinsically, with sensory information interacting with rather than determining the operation system.

## 1.8 Aim of the thesis

As the functions of the visual and vestibular systems deteriorate with increasing age (Allison et al., 1984; Baloh et al., 2001; Jahn et al., 2003) the question arises how the interaction between these systems conforms to those changes. Determining the functional and structural alterations of the visual and vestibular networks in normal aging would render a solid ground for the future investigations of the functional changes seen in neuroimaging studies on peripheral and central disorders of these systems. This doctoral thesis thus attempts to explore the effects of age on the visual-vestibular interaction elicited by visually induced OKN and investigate how these effects manifest in fMRI. Specifically, it aims to investigate whether age-related changes in the spatial and temporal pattern of the BOLD response occur before alterations in the OKN performance

can be detected. Aside from exploring the age-related changes in the mean of the BOLD signal, this work also investigates the age dependencies of its temporal variability. Of further interest is to distinguish between the global and the task-specific effects of age on the BOLD signal. Therefore, we compare the aging effects on the OKN-elicited BOLD response with the aging effects on the BOLD response elicited by two control tasks: a purely visual task where coupling of visual and motor information, such as during OKN, is not required, and a motor task which activates brain areas that are not involved in OKN. The purpose of the visual control task is to test whether age-related changes are task-specific or specific for one functional system (i.e. the visual); whereas the purpose of the second control task is to further test whether age-related changes are system specific or global. The performed analyses have focused on three aspects of BOLD signal changes:

1. Age-related changes in the positive BOLD response (PBR) during OKN. The purpose of this analysis was to investigate the effects of age on the visual and multi-sensory areas showing PBR during visual optokinetic stimulation. It particularly intended to differentiate between global effects of age, possibly explained by age-related changes in the brain's structure, vasculature and metabolism, and changes specific for the OKN task.
2. Age-related changes in the negative BOLD response (NBR) during OKN. This analysis aimed to extend the findings from the first analysis to the concept of the visual-vestibular interaction. Therefore, the effects of age on the NBR in the multi-sensory vestibular network were explored and compared to the aging effects in the areas showing PBR. The purpose was to investigate whether the changes in the visual-vestibular interaction comply with the findings on the aging effects demonstrated in other multisensory interactions.
3. Age-related changes in the temporal variability of the BOLD response during OKN. The purpose of this analysis was to assess the temporal fluctuations of the BOLD signal and explore the aging effects which could not be addressed with the previous two analyses.



## 2 Methods

### 2.1 Subjects

Sixty-eight right-handed healthy subjects, evenly distributed between 20 and 80 years, were examined. Twenty-three subjects had to be excluded from the analysis after inspection of data quality (see 2.5.2). Consequently, 45 subjects, evenly distributed between 20 and 76 years ( $47.6 \text{ years} \pm 17.9$ ) were included in the study. All subjects were free of neurological, psychiatric and cerebrovascular disorders and received no medication known to affect the neural function. In order to ensure that all subjects were free of neuropsychological deficits and able to sufficiently perform the visual tasks, cognitive deficits using the Montreal Cognitive Assessment Test (MoCA), visual acuity using the Snellen chart, and fixation ability were tested prior to the experiment and all the subjects meet the required criteria. Forty-two participants were right-handed and three participants were ambidextrous according to the 10-item inventory of the Edinburgh test (Oldfield, 1971). The mean handedness score of the whole group was  $88.66\% \pm 24.90$ .

### 2.2 Experimental design, tasks and stimuli

Three different functional imaging experiments have been performed by all subjects. Beside the horizontal-OKN experiment, we conducted two additional fMRI experiments as we intended to differentiate between age-related differences specific to OKN and general age effects on BOLD-excitability. As OKN is an oculomotor reflex which requires coupling of visual and motor information, we chose a purely visual and a purely motor task as our control experiments. For the purely visual task we chose checkerboard stimulation, in order to obtain data from the visual system during a task where coupling of visual and motor information, such as during OKN, is not required. For the purely motor control experiment, we chose a finger-tapping task in order to acquire data from the motor system which is not involved in OKN.

During the experiments, subjects laid supine in the MRI scanner, while visual stimuli were back projected on a screen in front of them using an LCD video projector. The stimuli were produced by a laptop running Matlab and the Cogent 2000 Toolbox

(<http://www.vislab.ucl.ac.uk/cogent.php>).

The OKN experiment contained two conditions of OKN stimulation (translational movement towards right or towards left) and one rest condition (stationary pattern). It was conducted in two imaging runs, each run containing ten blocks of OKN stimulation (five in each direction) and ten blocks of the rest condition. We used a stimulus pattern that consisted of 600 black and white dots (diameter =  $0.5^\circ$ ), randomly positioned on a grey background. During the OKN stimulation, the pattern was moving rightwards or leftwards with a constant velocity of  $15^\circ/\text{s}$ , whereas during rest condition the pattern remained stationary. We chose a velocity of  $15^\circ/\text{s}$  in order to ensure that all subjects, independent of age, were able to easily perform the task. The field of view was restricted to  $25^\circ$  in the horizontal and  $19^\circ$  in the vertical axes (small field of view) and therefore did not induce apparent self-motion perception (vection). During the OKN stimulation, subjects were instructed to passively look at the middle of the screen, without following the dots from one side to the other and without fixating the background, thereby eliciting 'stare' type of optokinetic nystagmus (Konen et al., 2005; Kashou et al., 2010). During the rest condition the subjects were instructed to fixate a dot in the middle of the screen in order to prevent after-nystagmus. Additionally, in order to ensure that all subjects were able to produce OKN at  $15^\circ/\text{s}$ , prior to the OKN experiment, we determined the individual maximal velocity of the OKN stimulus at which subjects still produced OKN. For this purpose we used the same stimulus pattern as for the OKN experiment, this time however, moving rightwards with continuously increasing velocity starting at  $12^\circ/\text{s}$  (OKN velocity test).

The checkerboard experiment contained one active (flickering-checkerboard) condition and a rest condition, during which the checkerboard pattern remained stationary. We used a circular black-and-white checkerboard stimulus (inner diameter  $1^\circ$ , outer diameter  $17.5^\circ$ ) with a fixation point at the centre. During the active condition, the black and white fields were interchanging at a rate of  $18\text{Hz}$ , whereas during the rest condition they remained stationary. The subjects were instructed to fixate the centre point of the checkerboard during the whole time. The experiment was conducted in one imaging run, containing seven blocks of active condition and seven blocks of rest condition. The finger-tapping experiment contained one active (self-paced finger-tapping) condition, during which subjects had to repetitively press a button with the index finger of the dominant hand, and a rest condition, during which subjects did not perform the motor task. Subjects were trained to perform the finger-tapping task with a frequency of  $2\text{Hz}$  prior to scanning. The beginning of each active condition was announced by the appearance of the command 'GO' on the screen, whereas the beginning of each rest condition was announced

---

by the appearance of the command 'rest'. The experiment was conducted in one imaging run, containing seven blocks of active condition and seven blocks of rest condition. The performance of the subjects was controlled by a button-pressing response device. All participants included in the study were trained to perform the experimental tasks prior to measurement.

## 2.3 Video-oculography (VOG)

The performance of the subjects during the OKN experiment, checkerboard experiment and OKN velocity test was controlled on-line and recorded by VOG. Eye movements were recorded from the right eye using an analog MRI compatible infrared camera (MRC Systems GmbH, Heidelberg) that was mounted on the head coil of the scanner. EyeSeeCam software ([www.eyesecam.com](http://www.eyesecam.com)) was used for real-time image processing and recording of VOG data at a sampling frequency of 60 Hz. For synchronization purposes, the EyeSeeCam software recorded stimulus onsets and onsets of MRI volumes along with the VOG data. For transformation of the eye movement data into degrees of horizontal and vertical axes, a 5-point calibration was performed at the beginning of the recording. During calibration subjects repeatedly fixated a sequence of given gaze directions: the central position and four lateral positions in the horizontal and vertical axis ( $\pm 8.5^\circ$ ).

## 2.4 Functional MRI acquisition

Magnetic resonance imaging was performed on a 3 T scanner (GE Signa Excite HD, Milwaukee, USA), equipped with an 8-channel head coil. In order to minimize head motion, the subject's head was fixated in the MR head-coil with a fixation band on the forehead and fixation cushions on both sides of the head. The subjects wore hearing protection. Functional images were acquired using echo-planar imaging (EPI) with a T2\*-weighted EPI sequence (TE = 40ms, TR = 2800ms, FOV = 200x200mm, matrix = 64x64x42 and voxel size 3.125 x 3.125 x 3.5mm).

The OKN experiment contained two imaging runs of alternating blocks of rightward or leftward OKN stimulation with rest conditions in between. Each run started with a rest condition. The block length was 16.8 seconds (6 scans) and each run lasted 5.6 minutes. One run contained 120 MRI volumes. The checkerboard and finger-tapping experiments contained one imaging run of alternating blocks of active and rest conditions, each run started with an active condition. The block length was 16.8 seconds (6 scans) and each run lasted 3.9 minutes. One run contained 84 MRI volumes.

Each volume in the three experiments consisted of 44 transversal slices that covered the whole brain including the cerebellum. Additionally, a 3D gradient-echo sequence (fast-spoiled gradient recalled, FSPGR) was used to obtain a T1-weighted anatomical image with a resolution of  $0.86 \times 0.86 \times 0.7$  mm.

## 2.5 Data analysis

### 2.5.1 VOG data analysis

Analysis of the eye movement recordings included estimation of the mean slow phase velocity (SPV), the mean saccadic frequency and the mean saccadic amplitude during OKN for each subject. The mean SPV was used to calculate the OKN gain as the ratio of nystagmus slow-phase velocity and stimulus velocity. Blocks where subjects did not have OKN were detected off-line and removed from the analysis. From the additional recordings of the OKN velocity test, we calculated the maximal OKN velocity for each participant.

### 2.5.2 fMRI data analysis

#### Age-related changes of the positive and negative BOLD responses

Data processing was performed using statistical parametric mapping software (SPM5, <http://www.fil.ion.ucl.ac.uk/spm>), implemented in Matlab (The Mathworks Inc., USA). The functional MRI data were realigned using a mean image as a reference in order to correct for head motion. The high resolution T1 image from every subject was coregistered to the mean image of the motion corrected functional image volumes. T1 images were then segmented into grey and white matter using unified segmentation (Ashburner and Friston, 2005). The normalization parameters obtained during the segmentation step were used to perform spatial normalization of the EPI volumes to the Montreal Neurological Institute (MNI) template (Friston et al., 1995). Therefore, all coordinates in this paper refer to the MNI coordinate system. After normalization, the EPI volumes had a voxel size of  $3 \times 3 \times 3$  mm<sup>3</sup>. In order to attenuate high-frequency noise, data sets were smoothed using an isotropic Gaussian kernel with a size of 8 mm FWHM.

The data from 23 subjects had to be excluded from further analysis due to the following quality criteria: stimulus correlated head movement (7 subjects), head movement larger than 2mm per TR (1 subject), insufficient quality of eye movement recordings due to insufficient pupil recognition (4 subjects), fatigue (8 subjects) and misunderstanding of the experimental instructions (3 subjects).

---

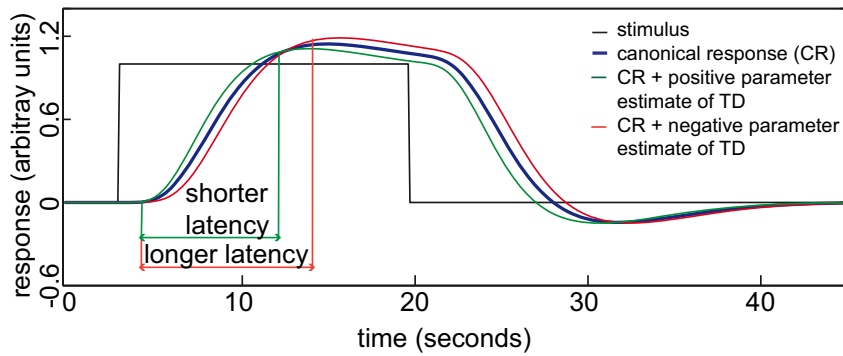
Single subject statistical analysis was performed for each experiment separately. Statistical parametric maps (SPMs) were calculated on a voxel-by-voxel basis by using a general linear model with a canonical hemodynamic response function (HRF) and its temporal and dispersion derivative (Henson et al., 2002). The head movement parameters that have been obtained in the realignment step were included as additional regressors of no interest. An orthogonality matrix was computed, depicting the magnitude of the cosine of the angle between each pair of columns in the model design matrix. Data with  $\cos > 0.6$  between the regressors of interest and any of the head movement regressors were not included in the further analysis due to stimulus correlated head movements. Contrast images were generated as linear combinations of the parameter estimates for the contrasts of interest. The model for the OKN experiment contained regressors modeling the blocks of OKN stimulation: OKN canonical HRF, OKN temporal derivative, OKN dispersion derivative. Blocks of insufficient performance (see 2.5.1) were included as additional regressors of no interest.

The model for the finger-tapping experiment contained the regressors TAP canonical HRF, TAP temporal derivative and TAP dispersion derivative, which modeled the blocks of motor activity. The model for the checkerboard experiment contained the regressors FLICKER canonical HRF, FLICKER temporal derivative and FLICKER dispersion derivative, modeling the blocks of flickering checkerboard stimulation.

In each model t-contrasts were defined to obtain contrast images with the effects of each regressor separately. For each experiment, the following contrasts were created: positive BOLD response (PBR) (revealing positive estimate of the canonical HRF), positive latency to peak (revealing positive estimate of the temporal derivative) and positive dispersion (revealing positive estimate of the dispersion derivative). For more clarity, a positive estimate of the temporal derivative reveals a shorter latency to peak of the BOLD response, compared to the prediction posed by the canonical HRF model. A negative estimate of the temporal derivative on the other hand, fits a longer latency to peak. Regarding the estimate of the dispersion derivative, a positive estimate fits a narrower BOLD response compared to the canonical HRF model, while a negative estimate of the dispersion derivative fits a wider BOLD response (Fig. 2.1).

The amount of percent BOLD signal change for the motor task in the finger-tapping experiment was calculated from the local maximum in the hand motor area of every subject. Percent BOLD signal change for the checkerboard task was calculated from the

### A. Canonical response + temporal derivative (TD)



### B. Canonical response + dispersion derivative (DD)

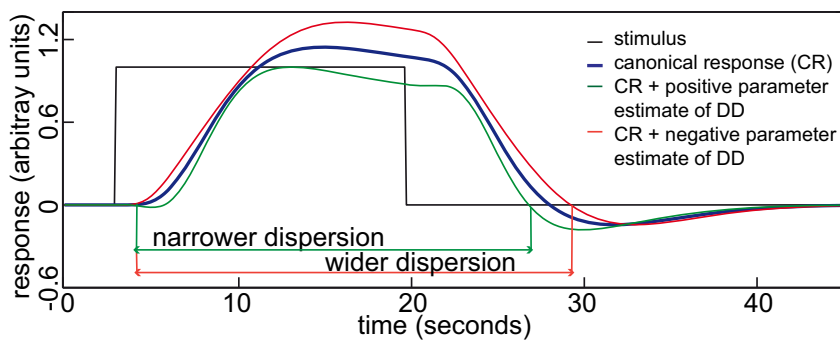


Figure 2.1: Exemplary canonical hemodynamic response function (CR) combined with temporal and dispersion derivatives. Incorporation of the derivative terms allows to model for variations in subject-to-subject and voxel-to-voxel responses. The temporal derivative (TD) allows the peak response to vary by plus or minus one second, the dispersion derivative (DD) allows the width of the response to vary by a similar amount. Positive estimate for TD corresponds to fit a response that occurs earlier compared to the CR. Positive estimate for DD corresponds to a narrower response (Ashburner et al., 2009). A) Variation of response latency by positive or negative TD parameter estimate. B) Variation of response width by positive or negative DD parameter estimate.).

---

local maximum in the primary visual cortex. In order to use age, OKN gain, maximal OKN velocity, percent of BOLD signal change during finger-tapping and percent of BOLD signal change during checkerboard stimulation as covariates in the second level analysis, we performed Spearman's rank correlation test to test whether there is any correlation between age and the other variables. The t-contrast images obtained by the single subject analysis were entered into a second level statistical analysis to test for group effects on a between subject basis (Frison and Pocock, 1992; Woods, 1996). For the OKN experiment, separate one-sample t-tests were performed for the OKN canonical HRF, OKN temporal derivative and OKN dispersion derivative. The test for the canonical HRF contained one contrast image (OKN PBR) from every subject and the additional covariates age, OKN gain, maximal OKN velocity, percent of BOLD signal change during finger-tapping and percent of BOLD signal change during checkerboard stimulation. The tests for the temporal and dispersion derivative contained one contrast image (OKN positive latency to peak or OKN positive dispersion, respectively) from each subject and the covariates age, OKN gain and maximal OKN velocity.

For the finger-tapping and checkerboard experiments, separate one-sample t-tests were performed for the canonical HRF, temporal derivative and dispersion derivative, using one contrast image from every subject (TAP PBR or FLICKER PBR, TAP latency to peak or FLICKER latency to peak and TAP dispersion or FLICKER dispersion, respectively). Age was included in each test as additional covariate.

For all three experiments, we tested for positive and negative main effects of each regressor (canonical HRF, temporal derivative and dispersion derivative), as well as positive and negative correlation of these effects with age. When testing for the effects of the temporal and dispersion derivatives, we used the statistical maps of the OKN PBR contrast or OKN NBR contrast as a region-of-interest (ROI) mask, in order to test only voxels where either positive estimate or negative estimate of the canonical HRF was found. A threshold of  $p < 0.05$  (corrected for multiple comparisons using the FDR-method) was used to test for significance. In the following text we will refer to the positive estimate of the canonical HRF as PBR amplitude and negative estimate of the canonical HRF as NBR amplitude. Positive or negative estimate of the temporal derivative is referred to as PBR shorter or longer latency to peak, respectively, and positive or negative estimate of the dispersion derivative as narrower or wider PBR dispersion, respectively.

We further wanted to test if there was a significant difference between the effects of age on the PBR latency to peak or dispersion found in the OKN experiment and those found

in the checkerboard and finger-tapping experiment. Therefore, from each experiment we used the parameter estimates from the estimated global maximum for the contrasts reflecting correlation between age and PBR latency to peak or dispersion. These values together with the subjects' age were then used to construct a covariance matrix of age, OKN and checkerboard variables and a covariance matrix of age, OKN and finger-tapping variables. We performed a likelihood ratio test for each covariance matrix to test the null hypothesis that the regression slopes of age and the other two variables in the matrices were identical. The same analysis was also used to test whether the regression slope of age and PBR latency to peak in hMT/V5 differed from the regression slope in the cortical areas showing significant age-related changes.

In order to get a clearer depiction of the age-related differences in the hemodynamic response function (HRF) we additionally divided the subjects in three age groups (Group 1: 20 to 39 years, Group 2: 40 to 59 years and Group 3: 60 to 76 years) and reconstructed the profile of the individual HRF for every subject based on the parameter estimates for canonical HRF, temporal derivative and dispersion derivative. From these reconstructed hemodynamic responses, we calculated a group-mean response along with its standard deviation. The plots showed that separate brain areas have different overlaps of the mean HRF and its standard deviation between the groups (Fig. 2.2).

We were interested in testing whether these effects can have an influence on the estimation of the age differences in PBR or NBR amplitude. For this purpose, we additionally performed a full-factorial, one-way between-subjects ANOVA in order to test for the main effects of the OKN canonical HRF regressor in each group individually, and then test for differences in the PBR or NBR amplitude between the groups. We therefore, used the OKN PBR contrast images from the single subject analysis, along with OKN gain, maximal OKN velocity, percent of BOLD signal change during checkerboard and percent of BOLD signal change during finger-tapping as covariates of no interest. The following contrasts were computed: OKN PBR and OKN NBR for each group separately, and contrasts testing for pair-wise differences in OKN PBR or OKN NBR between each pair of groups. A threshold of  $p < 0.05$  (FDR corrected) was used to test for significance.

In order to assess general age-related changes of grey and white matter volume, we performed voxel-based morphometry (VBM), using the optimized method of Good (Good et al. 2001) on the high resolution T1 weighted images. We then correlated local grey matter and white matter volume with the subjects' age.

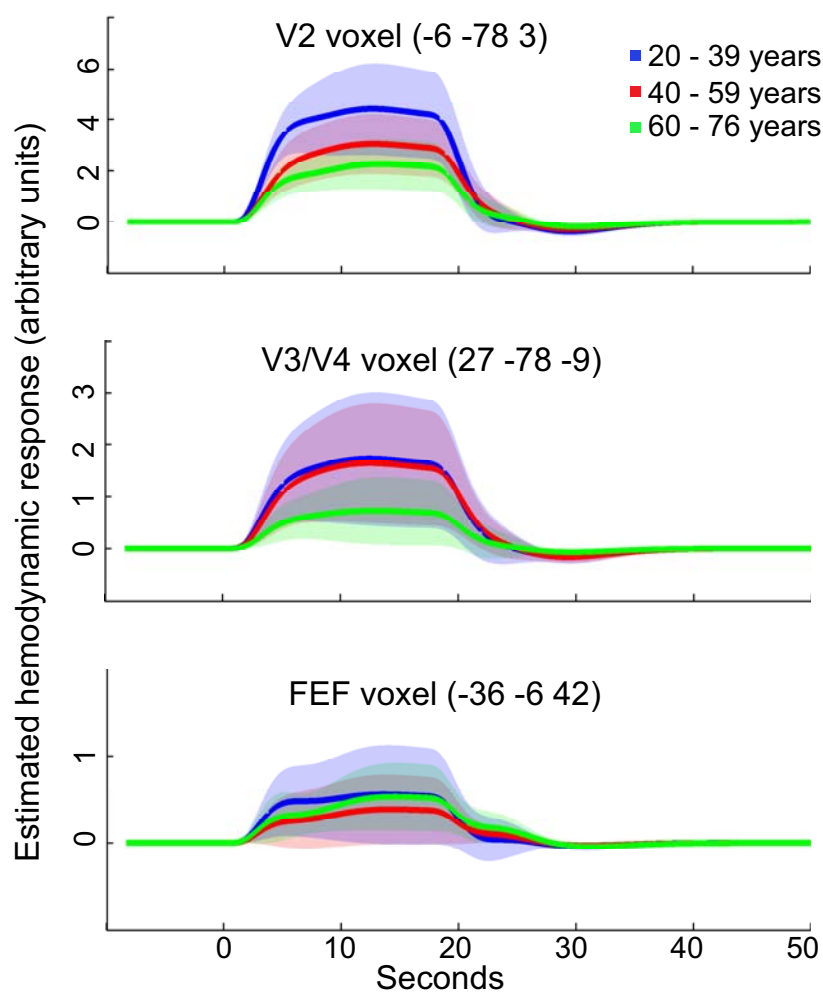


Figure 2.2: Estimate of the mean hemodynamic response relative to stimulus onset and its standard deviation during OKN in three age groups/ranges. Lines depict mean of estimated response during OKN in each of the groups; colored bands depict standard deviations. Exemplary voxels were selected from the extrastriate visual cortex (V2, V3V4) and frontal cortex (FEF).

### Age-related changes in the temporal variability of the BOLD response

As a measure for the temporal variability of the BOLD response in each voxel during an imaging run, we used the method described in (Garrett et al., 2010) to calculate the signal's standard deviation (SD). For calculation of the signal's SD the smoothed and normalized images from each imaging run as obtained by the preprocessing steps in 2.5.2 were used. For the OKN experiment, both directions of the stimulation were treated as one equal stimulus condition (horizontal movement towards right and towards left). Blocks of stimulation or rest were additionally normalized and concatenated in order to correct for large block offsets as described in detail in (Garrett et al., 2010). For this purpose, the signal was converted into percent of mean global signal, and the mean signal in each stimulation block was subtracted from the signal in each voxel. After block concatenation, the SD for each voxel was calculated across this concatenated mean-block corrected time series, resulting in two images per subjects (SD\_stimulation and SD\_rest) which were then used to test for within-group and between-group effects.

As head motion during the scanning procedure can be a source of signal variance in fMRI time series (Friston et al., 1996), it is necessary to control for motion effects when estimating changes in SD. In order to do this, we calculated the Center of Mass (COM) of all inbrain voxels for each subject. Cumulative displacement of this coordinate over the whole measurement (COM-displacement) was computed from the head motion parameters (translations and rotations) that had been estimated in the realignment step (see 2.5.2). The vector of COM-displacement values from all subjects was then used to explore the correlation between age and head motion, and later control for motion effects in the between-group analyses. A Spearman rank correlation test revealed a significant positive correlation between age and COM-displacement. Therefore, in order to use COM-displacement as a covariate in the between-group analyses, the COM-displacement vector and the age vector were orthogonalized using principal component analysis (PCA). The resulting vector of COM-displacement scores was then entered as a covariate of no interest in the imaging data between-group analyses.

The SD\_stimulation and SD\_rest images from each subject were included a paired t-test used to assess the differences in variability between stimulation and rest in all subjects. The test was performed for each experiment separately and contained two contrasts: SD\_stimulation - SD\_rest and SD\_rest - SD\_stimulation. In order to assess age-related changes in variability during stimulation and during rest, the SD\_stimulation and SD\_rest images from each subject were included in separate one-way between-subjects ANOVAs to test for differences between each pair of groups (Group 1: 20 - 39 years, Group 2: 40

- 59 years and Group 3: 60 - 76 years) in SD\_stimulation or SD\_rest, respectfully. Each between-subject ANOVA contained the orthogonalized COM-displacement vector from the respective experiment as a covariate of no interest in order to control for the effects of head motion. For the OKN experiment, OKN gain and maximal OKN velocity were used as additional covariates of no interest. A threshold of  $p < 0.05$  (FDR corrected) was used to test for significance.

We were interested in exploring whether the age-related changes found in the signal's SD occur in areas showing PBR or NBR during stimulation. Therefore, we used the statistical maps of the OKN PBR and OKN NBR contrasts from the OKN canonical HRF one-sample t-test (see 2.5.2) as an inclusion mask for ROI analyses. Anatomical localizations of the results from each analysis were determined using the Harvard-Oxford Cortical Structural Atlas, the Harvard-Oxford Subcortical Structural Atlas, the Juelich Histological Atlas and the Cerebellar Atlas in MNI152 in FSLView 3.1. (<http://www.fmrib.ox.ac.uk/fsl/fslview/atlas.html>).



## 3 Results

### 3.1 Video-oculography data

Analysis of the eye movement recordings showed that the applied visual stimulation elicited OKN and that all subjects included in the analysis were able to accurately perform the task. The mean OKN gain for the whole group was  $0.7 \pm 0.2$  (range from 0.1 to 1.2), the mean frequency of resetting saccades was  $2.9\text{Hz} \pm 0.5$ ; (range from 0.9 to 4.1) and the mean amplitude of saccades was  $3.2^\circ \pm 0.9$  (range from 1.7 to 5.7). The OKN velocity test revealed mean maximal OKN velocity of  $26^\circ/\text{s} \pm 8.9$  (range from 10.2 to 47.6).

### 3.2 Covariates analysis

The Spearman rank correlation test showed no significant correlation between age and OKN gain or maximal OKN velocity (age/gain  $r_s = 0.09$ ,  $p=0.55$ ; age/maximal OKN velocity  $r_s = 0.05$ ,  $p=0.70$ ). The mean percent BOLD signal change during checkerboard stimulation for the whole group was  $2.96\% \pm 1.25$  (range: 1.15 to 5.82), and the mean percent BOLD signal change during the finger-tapping task was  $2.02\% \pm 0.77$  (range: 0.74 to 4.33). No significant correlation between age and these two variables was found (age/percent BOLD signal change during checkerboard stimulation  $r_s = 0.04$ ,  $p=0.77$  and age/percent BOLD signal change during finger-tapping stimulation  $r_s = -0.01$ ,  $p=0.91$ ).

### 3.3 Dynamics of the positive BOLD response (PBR) and their age dependencies

#### 3.3.1 Group fMRI data analysis of PBR amplitude, latency to peak and dispersion

##### OKN experiment

The OKN experiment revealed a symmetrical bilateral pattern of PBR in the primary visual cortex and the adjacent visual areas in the occipital cortex and parietal cortex (Fig. 3.1). Additionally, PBR was found bilaterally in the parietal eye field (PEF), the frontal eye field (FEF) and supplementary eye field (SEF), the frontal orbital cortex, as well as in the lateral geniculate body (Suppl. Tab.1). All the areas showing PBR during OKN also showed shorter latency to peak, compared to the estimate predicted by the

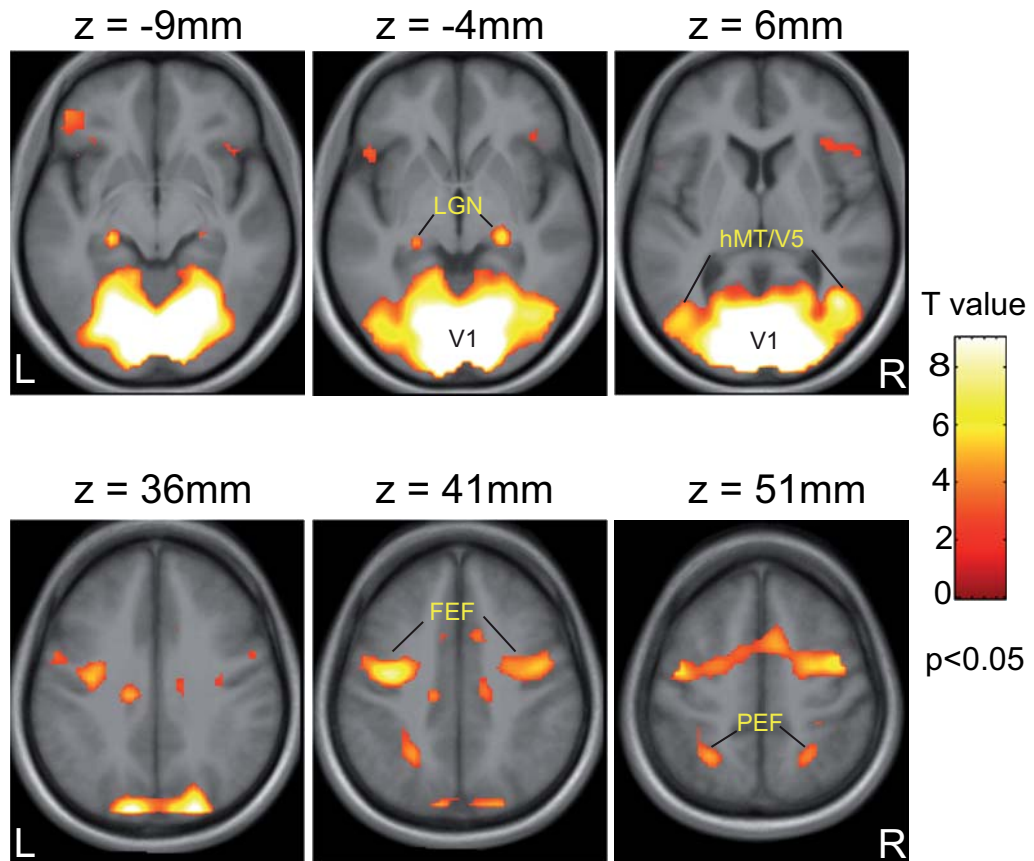


Figure 3.1: Positive BOLD response (PBR) during OKN compared to viewing a static pattern ( $p < 0.05$  FDR) overlaid on transversal sections through a group mean anatomical image. Key: LGN - lateral geniculate body, V1 - primary visual cortex (occipital cortex), hMT/V5 - human analogue of medial temporal/medial superior temporal cortex, FEF - frontal eye field, PEF - parietal eye field.

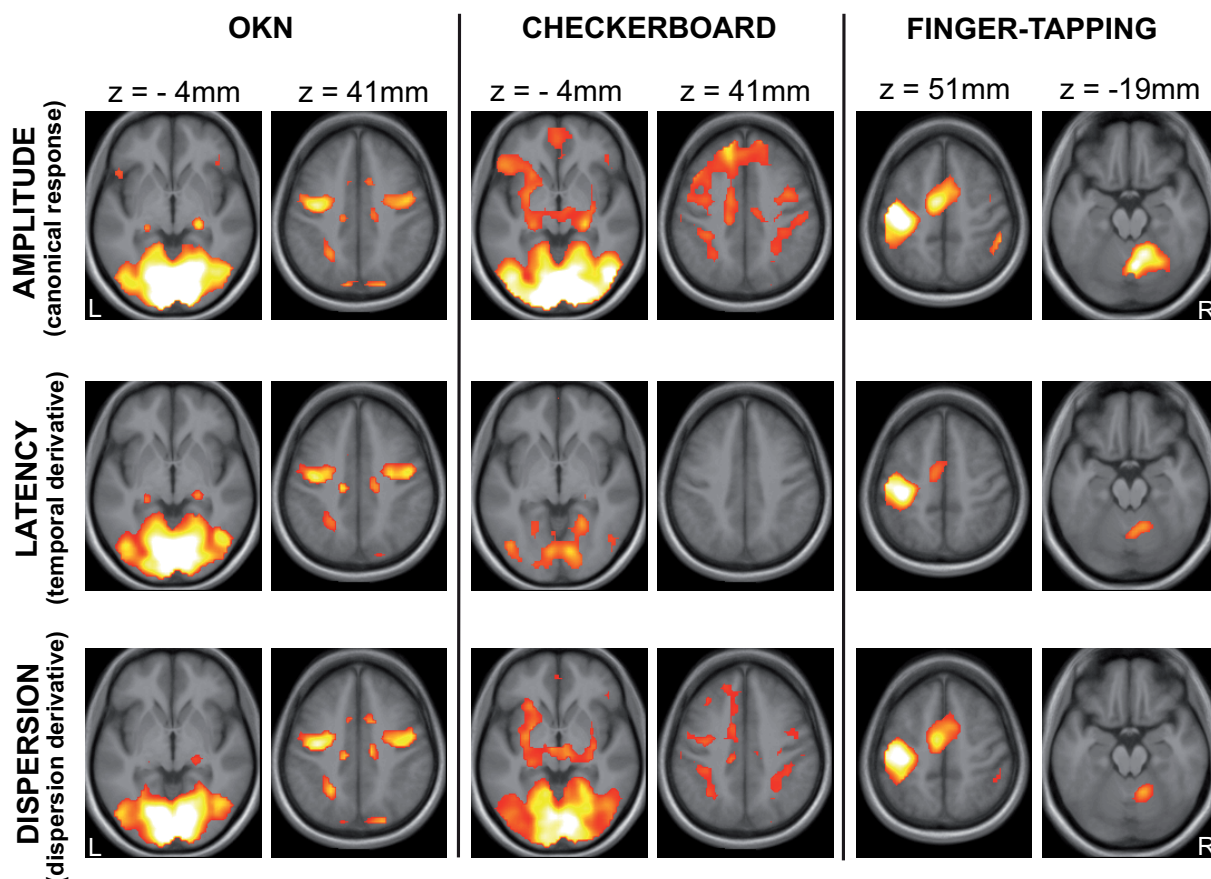


Figure 3.2: Comparison of PBR dynamics for the three experiments: OKN, checkerboard and finger-tapping ( $p < 0.05$  FDR). OKN (left): shorter latency and wider dispersion in lateral geniculate body, occipital cortex, frontal eye field and parietal eye field. Checkerboard (middle): shorter latency in occipital areas and wider dispersion in almost all areas showing PBR. Finger-tapping (right): shorter latency and wider dispersion in almost all areas showing PBR (Table1).

canonical model of the hemodynamic response function (HRF), except for the frontal orbital cortex bilaterally (Fig. 3.2, Suppl. Tab.1), which at lower statistical threshold (uncorrected,  $p < 0.001$ , cluster size  $\geq 5$ ) showed longer latency to peak. Wider dispersion of PBR compared to the one predicted by the canonical model of HRF, was also found in all of the areas showing PBR (Fig.8, Suppl. Tab.1), except for the frontal orbital cortex bilaterally. None of the areas showing PBR during OKN showed narrower dispersion of the signal.

### Checkerboard experiment

In the checkerboard experiment PBR during flickering checkerboard stimulation was found bilaterally in the primary visual cortex and adjacent visual areas in the occipital and

parietal cortex, lateral geniculate body, FEF and SEF, as well as the putamen and frontal orbital cortex. In both hemispheres, area V1/BA17, V2/BA18 and hMT/V5 showed shorter PBR latency to peak. The right inferior frontal gyrus, as well as the right putamen and right superior parietal lobule showed longer PBR latency to peak (Suppl. Tab.2). Additionally, wider PBR dispersion was found in most of the areas activated during checkerboard stimulation (Fig. 3.2, Suppl. Tab.2).

### **Finger-tapping experiment**

In the finger-tapping experiment the motor task elicited a well known pattern of PBR in the hand motor area in the left precentral gyrus (BA4), as well as the basal ganglia, the cingulate gyrus, the corticospinal tract and the cerebellar cortex (V/VI) bilaterally (Fig. 3.2, Suppl. Tab.3). The left precentral gyrus and several other areas showed shorter PBR latency to peak compared to the canonical model of the HRF. We found no areas showing longer PBR latency to peak. Furthermore, wider PBR dispersion was found in the left precentral and postcentral gyrus, cingulate gyrus bilaterally and the right cerebellar cortex (Fig. 3.2, Suppl. Tab.3). There were no areas showing narrower PBR dispersion compared to the canonical HRF model.

### **3.3.2 Age-related changes of PBR dynamics**

#### **OKN experiment**

The data from the OKN experiment showed no significant change of the PBR amplitude with age. Only a trend of decrease in PBR amplitude with increasing age was found in the intracalcarine cortex bilaterally, the left occipital pole (BA18/V2), and the right optic radiation (uncorrected,  $p < 0.001$ , cluster size  $\geq 5$ ). We found significant positive correlation between age and PBR latency to peak in several areas of the visual cortex (Fig. 3.3). These included the intracalcarine cortex (V1/BA17), the lingual gyrus (V2/BA18), the occipital pole (V1/V2), the occipital fusiform gyrus (V3/V4), the lateral occipital cortex (superior division), the lateral geniculate body, the FEF and the PEF bilaterally (Suppl. Tab.4). From all areas showing PBR during OKN, hMT/V5 was the only area that did not show any age-related change of the PBR latency to peak. The additional analysis of the regression slopes in hMT/V5 and in the areas showing age-related changes of PBR latency to peak (see 2.5.2) showed significant differences between hMT/V5 and all the areas with aging effects ( $p < 0.001$ ). Since these areas are unlike hMT/V5 related to saccades (Bttner and Bttner-Ennever, 2006), we wanted to investigate whether age-related changes in the saccadic frequency and amplitude can be detected. Therefore, we tested the correlation between age and the mean saccadic frequency and mean saccadic

---

amplitude using Spearman's rank correlation test. The test revealed no significant correlation (age/mean saccadic frequency  $r_s = 0.01$ ,  $p=0.93$  and age/mean saccadic amplitude  $r_s = 0.12$ ,  $p=0.41$ ). Significant decrease of the PBR dispersion with increasing age was found bilaterally in the intracalcarine cortex and occipital pole, as well as the superior division of right lateral occipital cortex (Fig. 3.3, Suppl. Tab.4).

The estimated mean HRF and its standard deviation (Fig. 2.2 in 2.5.2) in all of the brain areas with significant age related changes during OKN showed that separate brain areas have different overlaps of the mean HRF and its standard deviation between the three age groups. In order to test whether any differences in PBR amplitude between the groups can be detected when modeling the BOLD response with only the canonical HRF, we additionally performed a one-way, between subjects ANOVA using only the OKN PBR contrast. This revealed a comparable activation pattern in all three age groups. Accordingly, the contrasts for group differences in PBR amplitude did not reveal any significant results. Only a trend for an age-related decrease of PBR amplitude (uncorrected,  $p < 0.001$ , cluster size  $\geq 5$ ) was revealed by the contrast Group 1 - Group 3 (the left occipital pole, the right occipital fusiform gyrus and the intracalcarine cortex bilaterally) and the contrast Group 2 - Group 3 (the right intracalcarine cortex).

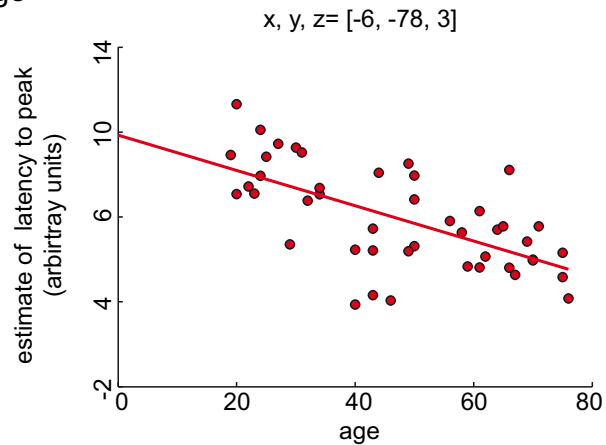
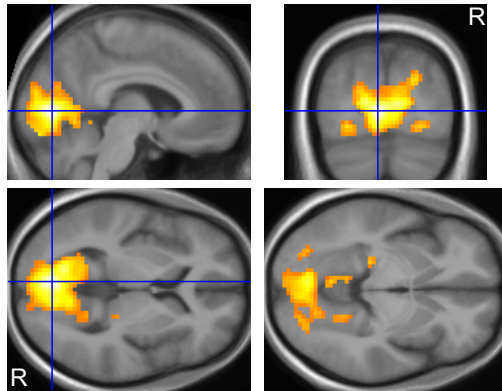
### **Checkerboard experiment**

The data from the checkerboard experiment showed no significant age-related change of PBR amplitude, latency to peak or dispersion. A trend of decrease of PBR amplitude with increasing age (uncorrected,  $p < 0.001$ , cluster size  $\geq 5$ ) was found in the paracingulate gyrus, the middle temporal gyrus, the putamen and the lateral occipital cortex (inferior division) bilaterally, as well as in the left occipital pole, the left occipital fusiform gyrus (V3/V4), and the right inferior frontal gyrus (pars triangularis). Similarly, a non-significant decrease of PBR latency to peak with increasing age was found in the right occipital pole and the inferior division of the right lateral occipital cortex (V4), while non-significant increase of PBR latency to peak was found in the right optic radiation and the right intracalcarine cortex (V1/BA17). Additionally, we found a non-significant decrease of PBR dispersion with increasing age in the right optic radiation.

### **Finger-tapping experiment**

Data from the finger-tapping experiment revealed no significant age-correlated change of PBR amplitude, latency or dispersion. A non-significant increase of PBR latency to peak with increasing age was found in the hand motor area of the left precentral gyrus (BA4p)

## A. Increase of PBR latency to peak with age



## B. Decrease of PBR dispersion with age

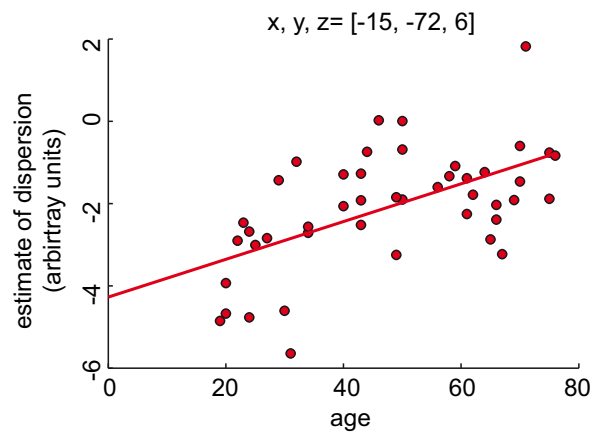
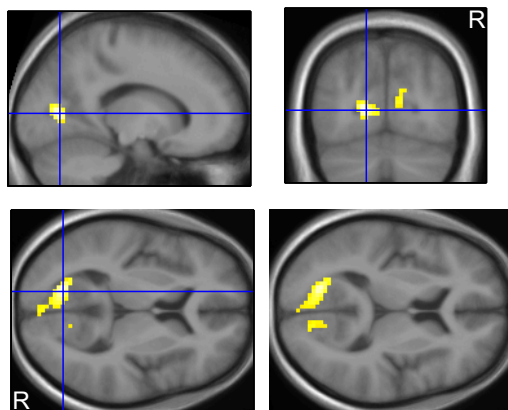


Figure 3.3: Change of PBR latency to peak and PBR dispersion with age during OKN ( $p < 0.05$  FDR). A) Increase of PBR latency to peak with age in lateral geniculate body, and occipital cortex (V1, V2, V3/V4) (left). Plot of parameter estimate of temporal derivative against age (right). Decrease of parameter estimate reveals increase of PBR latency to peak with age. B) Decrease of PBR dispersion in the occipital cortex (V1, V2 and the superior division of the right lateral occipital cortex) (left). Plot of parameter estimate of dispersion derivative against age (right). Increase of parameter estimate reveals decrease of PBR dispersion with age.

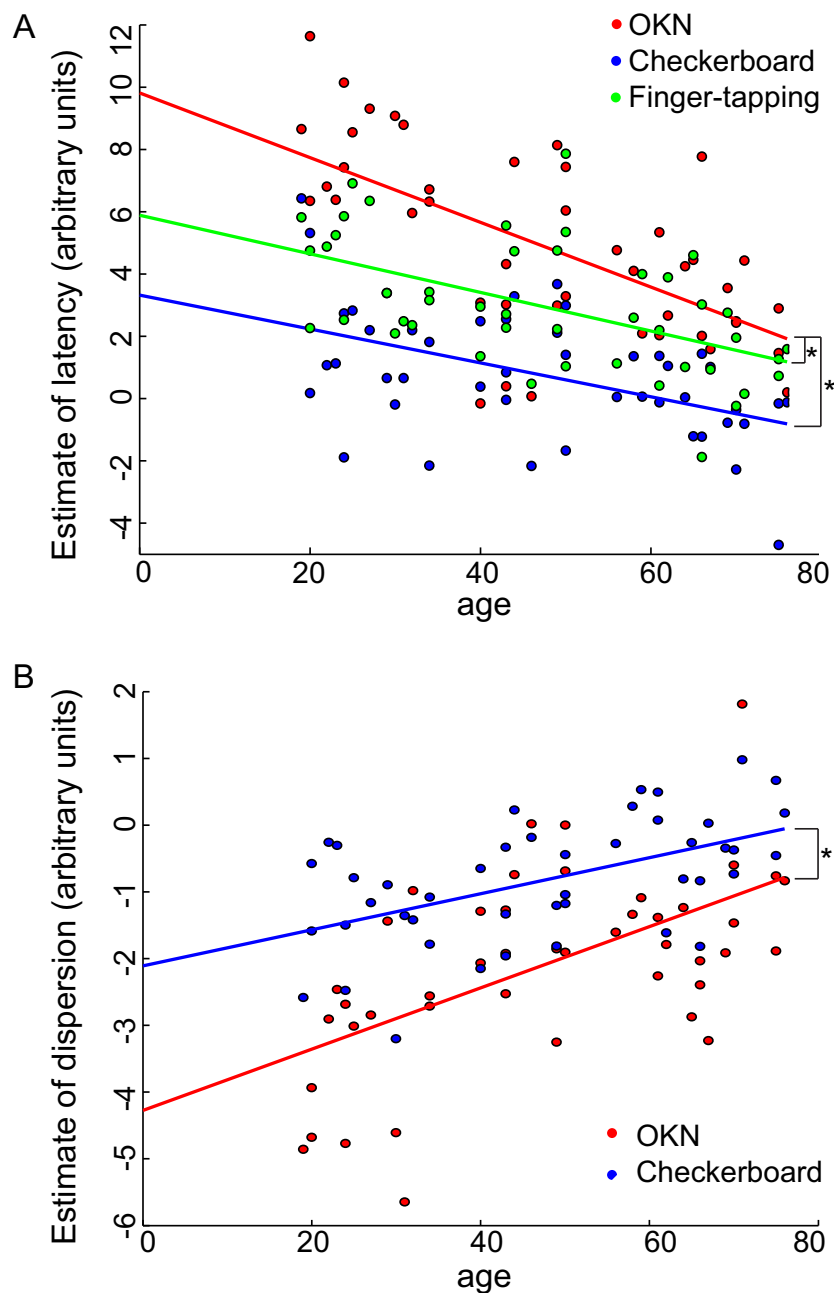


Figure 3.4: Regressions between age and PBR latency to peak (A) and PBR dispersion (B) in the respective global activation maximum of the different experiments. Okn voxel  $x, y, z = -6, -78, 3$ , checkerboard  $x, y, z = 18, -66, 9$ , and finger-tapping  $x, y, z = -36, -24, 51$ . Points: estimate of PBR latency to peak and PBR dispersion for each subject. Lines: linear fit for regressions between these estimates and age. There is a significant difference between regression slopes in OKN and the two control experiments ( $p < 0.001$ ). In B) only regression slopes from OKN and checkerboard experiments are shown.

and in the right cerebellar hemisphere (V).

We further tested if the correlation between age and PBR latency to peak or dispersion found in the OKN experiment was significantly different from the correlation between age and these variables found in the checkerboard and finger-tapping experiment. A likelihood ratio test for the covariance matrices of these variables revealed that the regression slope of age and PBR latency to peak from the OKN experiment was significantly different from the regression slope of age and PBR latency to peak found in the checkerboard and finger-tapping experiment. (OKN/checkerboard  $p=1.1063e-009$ ; OKN/finger-tapping  $p=6.0017e-011$ ) (Fig. 3.4). Furthermore, the regression slope of age and PBR dispersion in the OKN experiment was significantly different from the regression slope of age and PBR dispersion in the checkerboard experiment (OKN/checkerboard  $p < 0.001$ ).

### **3.4 Dynamics of the negative BOLD response (NBR) and their age dependencies**

#### **3.4.1 Group fMRI data analysis of NBR amplitude, latency to peak and dispersion**

##### **OKN experiment**

The OKN experiment revealed a typical bilateral pattern of NBR in the superior and inferior division of the lateral occipital cortex, the inferior and superior parietal lobules, the superior temporal gyrus, the posterior cingulate gyrus, the insular cortex, the temporo-occipital part of the inferior and middle temporal gyrus, the temporo-occipital fusiform cortex, the putamen and the precuneus (Fig. 3.5). Additionally, most of these areas showed longer NBR latency to peak than predicted by the estimate of the canonical HRF. Only the putamen bilaterally showed shorter latency to peak. Furthermore, the inferior parietal lobule, the precuneus, the posterior division of the cingulate gyrus and the middle frontal gyrus in both hemispheres, showed a narrower NBR dispersion than predicted by the canonical HRF model. Wider NBR dispersion was found only in the putamen bilaterally (Fig. 3.6, Suppl. Tab.5).

##### **Checkerboard experiment**

The flickering checkerboard stimulation elicited NBR in the anterior and posterior division of the callosal body and the precuneus bilaterally, as well as in the right thalamus and left superior parietal lobule. Additionally, the NBR in the anterior division of the callosal body had a narrower dispersion than predicted by the estimate of the canonical HRF

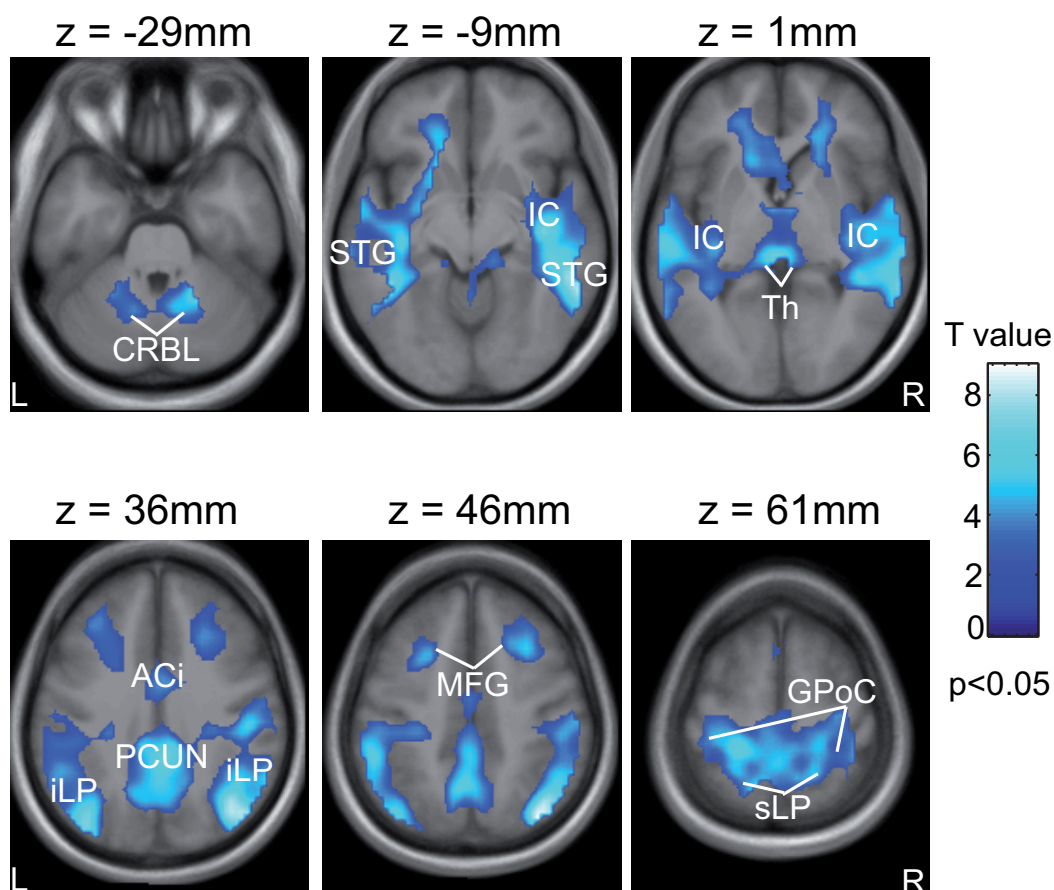


Figure 3.5: Negative BOLD response (NBR) during OKN compared to viewing a static pattern ( $p < 0.05$ , FDR) overlaid on transversal sections through a group mean anatomical image. OKN elicited BOLD signal decreases in areas known to constitute the multimodal vestibular network. Key: CRBL - cerebellum, STG - superior temporal gyrus, IC - insular cortex, Th - thalamus, PCUN - pre-cuneus, iLP - inferior parietal lobule, sLP - superior parietal lobule, ACi - anterior cingulum, MFG - middle frontal gyrus, GPoC - postcentral gyrus.

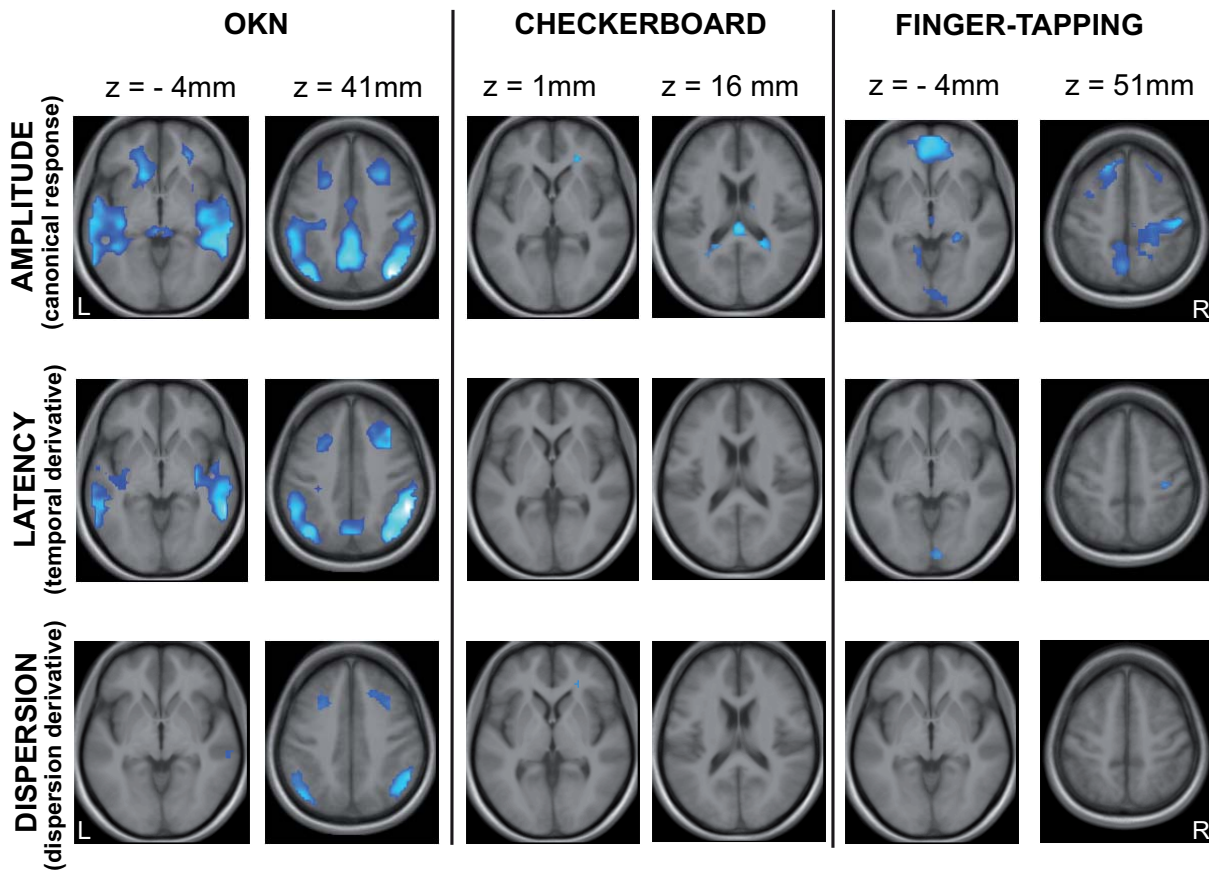


Figure 3.6: Comparison of NBR dynamics for the three experiments: OKN, checkerboard and finger-tapping ( $p < 0.05$  FDR). OKN (left): longer latency to peak in the insular cortex, temporal-occipital part of the inferior temporal gyrus, inferior lobule and precuneus bilaterally; narrower dispersion in the temporal-occipital part of the inferior temporal gyrus and inferior parietal lobule. Checkerboard (middle): except for the anterior division of the callosal body, no other areas showed difference in NBR dynamics compared to the prediction of the canonical model of HRF. Finger-tapping (right): longer latency to peak in the postcentral gyrus and the occipital pole of the right hemisphere.

---

model (Fig. 3.6, Suppl. Tab.6). There were no areas showing longer or shorter NBR latency to peak, or wider NBR dispersion than predicted by the canonical HRF.

### **Finger-tapping experiment**

The motor task in the finger-tapping experiment elicited a bilateral NBR in the frontal pole, the superior and middle frontal gyrus, the anterior division of the cingulate gyrus and precuneus. Furthermore, NBR was found in the precentral and postcentral gyrus, the occipital pole, the inferior parietal lobule and the central opercular cortex in the right hemisphere, as well as in the superior division of the lateral occipital cortex, occipital fusiform gyrus, lingual gyrus, middle temporal gyrus and the frontal orbital cortex in the left hemisphere. Longer NBR latency to peak was detected in the right postcentral gyrus and the right occipital pole, as well as in the left occipital fusiform gyrus. There were no areas showing shorter NBR latency to peak or wider or narrower NBR dispersion than predicted by the canonical HRF. Only at lower statistical threshold (uncorrected,  $p < 0.001$   $k \geq 5$ ) a narrower NBR dispersion was found in the left frontal pole and superior frontal gyrus (Fig. 3.6, Suppl. Tab.7).

### **3.4.2 Age-related changes of NBR dynamics**

#### **OKN experiment**

The data from the OKN experiment revealed no significant age-related change of NBR amplitude, latency to peak or dispersion. A trend of decrease of NBR amplitude with increasing age (uncorrected,  $p < 0.001$ , cluster size  $\geq 5$ ) was found in the left temporo-occipital fusiform cortex and the inferior division of the left lateral occipital cortex. The additionally performed one-way, between subjects ANOVA revealed a similar pattern of NBR in the Group 1 and Group 2 ( $p < 0.05$ , FDR), whereas the NBR pattern in Group 3 was reduced and detected at a lower statistical threshold (uncorrected,  $p < 0.001$ , cluster size  $\geq 5$ ). Surprisingly, however, the contrasts for group differences, revealed no significant difference in NBR amplitude between Group 3 and the other two groups. Only at a lower statistical threshold (uncorrected,  $p < 0.001$ , cluster size  $\geq 5$ ) Group 2 showed lower NBR than Group 1 in the right precuneus, and Group 3 showed lower NBR than Group 1 in the temporo-occipital fusiform gyrus bilaterally, and lower NBR than Group 2 in the right temporo-occipital part of the middle temporal gyrus.

#### **Checkerboard experiment**

The data from the checkerboard experiment revealed no significant age-related change of NBR amplitude, latency to peak or dispersion. A decrease of NBR amplitude with

increasing age was detected only at a lower statistical threshold (uncorrected,  $p < 0.001$ , cluster size  $\geq 5$ ) in the precuneus and superior parietal lobule bilaterally.

### **Finger-tapping experiment**

The finger-tapping experiment showed no significant change of NBR amplitude, latency to peak or dispersion with increasing age. Only a trend (uncorrected,  $p < 0.001$ , cluster size  $\geq 5$ ) of age-related decrease of NBR amplitude was found in the superior parietal lobule and the precentral gyrus of the right hemisphere.

### **3.4.3 Voxel-based-morphometry**

The VBM analysis revealed a general age-related reduction of grey and white matter all over the brain. Consequently, this included all brain areas found activated during the tasks.

## **3.5 Temporal variability of the BOLD signal (SD) and its alteration with age**

### **3.5.1 Differences between the temporal variability during stimulation and during rest**

#### **OKN experiment**

A paired-t-test revealed significantly higher SD during rest than during optokinetic stimulation, as shown by the SD<sub>rest</sub> - SD<sub>stimulation</sub> contrast in the whole brain analysis (Fig. 3.7). The ROI analysis with the OKN PBR and the OKN NBR contrast images showed that higher SD during the rest condition was present in areas with PBR, as well as in areas showing NBR during OKN (Suppl. Tab. 8). There were no areas showing higher SD during stimulation than during rest.

#### **Checkerboard experiment**

The paired-t-test for the checkerboard experiment showed no significant difference between SD<sub>rest</sub> and SD<sub>stimulation</sub> in the whole brain analysis. At lower statistical threshold (uncorrected,  $p < 0.001$ , cluster size  $\geq 5$ ) the SD<sub>stimulation</sub> - SD<sub>rest</sub> contrast revealed higher SD during stimulation in both cerebellar hemispheres, the thalamus and the callosal body bilaterally, as well as in the premotor cortex, superior division of the lateral occipital cortex and the central opercular cortex in the right hemisphere and the hippocampus in the left hemisphere. The ROI analyses revealed that out of these areas, the thalamus

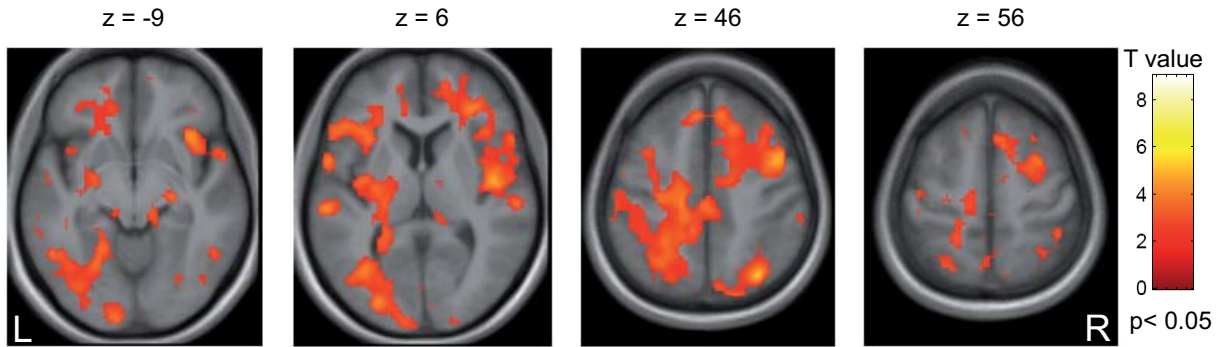


Figure 3.7: Areas showing higher temporal variability of BOLD signal during blocks of rest (static pattern) compared to blocks of stimulation (horizontal optokinetic stimulation) in the OKN experiment ( $p < 0.05$ , FDR). The statistical map showing voxels with higher  $SD_{rest}$  than  $SD_{stimulation}$  is overlaid on transversal sections through a group mean anatomical image. Among other areas, the thalamus, insular cortex, superior parietal lobule, inferior division of the lateral occipital cortex, occipital pole, superior temporal gyrus, middle frontal gyrus and precentral gyrus showed higher variability of the BOLD signal during rest than during to optokinetic stimulation.

bilaterally and the right callosal body were showing NBR during checkerboard stimulation. With the ROI analysis using the FLICKER NBR contrast the difference between SD during stimulation and SD during rest in these areas reached the significance threshold of  $p < 0.05$ , FDR corrected. The  $SD_{rest} - SD_{stimulation}$  contrast showed higher SD during rest in the right occipital pole (uncorrected,  $p < 0.001$ , cluster size  $\geq 5$ ), and ROI analyses revealed that this was an area where PBR was elicited during checkerboard stimulation.

### Finger-tapping experiment

The paired-t-test for the finger-tapping experiment revealed significantly higher SD during rest than during stimulation in the right insular cortex. The ROI analysis with the TAP-PBR contrast revealed additional areas where such significant difference was observed: central opercular cortex bilaterally and precentral gyrus, postcentral gyrus, juxtapositional lobule, and thalamus in the left hemisphere. No significant results were found for the contrast  $SD_{stimulation} - SD_{rest}$ . No areas with NBR during finger-tapping were found to show any difference between  $SD_{stimulation}$  and  $SD_{rest}$ .

### 3.5.2 Age-related changes of the temporal variability during stimulation and during rest

#### Correlation analysis of head motion and age

A Spearman rank correlation test revealed a significant positive correlation between the head motion as classified by COM displacement during each experiment and age (OKN  $r_s = 0.42$ ,  $p = 0.003$ ; checkerboard  $r_s = 0.31$ ,  $p = 0.03$ ; finger-tapping  $r_s = 0.43$ ,  $p = 0.003$ ). Therefore, the COM displacement vectors from each experiment and the age vector were orthogonalized and the appropriate COM displacement scores after orthogonalization were then used as covariates of no interest in the one-way, between-subjects ANOVA.

#### OKN experiment

The ANOVA test for age differences in SD\_stimulation (OKN) showed significant results for the SD\_Group 3 - SD\_Group 1 contrast in superior temporal gyrus, temporal pole, central opercular cortex, postcentral and precentral gyrus, precuneus, thalamus, and superior frontal gyrus in the left hemisphere (Fig. 3.8 A). Furthermore, higher SD\_stimulation in Group 3 compared to Group 1 was found in the right insular cortex and the planum polare bilaterally. ROI analysis using the OKN PBR and OKN NBR contrast images revealed that all of the areas showing higher SD\_stimulation in Group 3 compared to the Group 1 were areas with NBR during OKN. At lower statistical threshold (uncorrected,  $p < 0.001$ , cluster size  $\geq 5$ ) the SD\_Group 2 - SD\_Group 1 contrast showed an age-related increase of SD\_stimulation in the cerebellum, and the posterior and anterior division of the cingulate cortex in the left hemisphere. The ROI analysis revealed that the former two areas showed PBR, while the latter showed NBR during OKN. Additionally, with this lower statistical threshold the SD\_Group 3 - SD\_Group 2 contrast showed an age-related increase of SD\_stimulation in the left superior frontal gyrus (Suppl. Tab.9).

An ANOVA test for age differences in SD\_rest showed significant results for the contrast SD\_Group 3 - SD\_Group 1 (Suppl. Tab.9). Interestingly, most of the areas found to show age-related increase of SD during rest were the same areas showing an age-related increase of SD during stimulation, as depicted by an overlay of both statistical maps on a common anatomical brain image (Fig. 3.9 A, Suppl. Tab.9). Furthermore, at lower statistical threshold (uncorrected,  $p < 0.001$ , cluster size  $\geq 5$ ) the contrast SD\_Group 2 - SD\_Group 1 showed an age-related increase of SD\_rest in the right insular cortex, in the posterior division of the left cingulate gyrus and the left crus of the cerebellum, while the contrast SD\_Group 3 - SD\_Group 2 revealed an age-related increase in superior frontal gyrus, planum polare, and the optic radiation of the left hemisphere (Suppl. Tab.9).

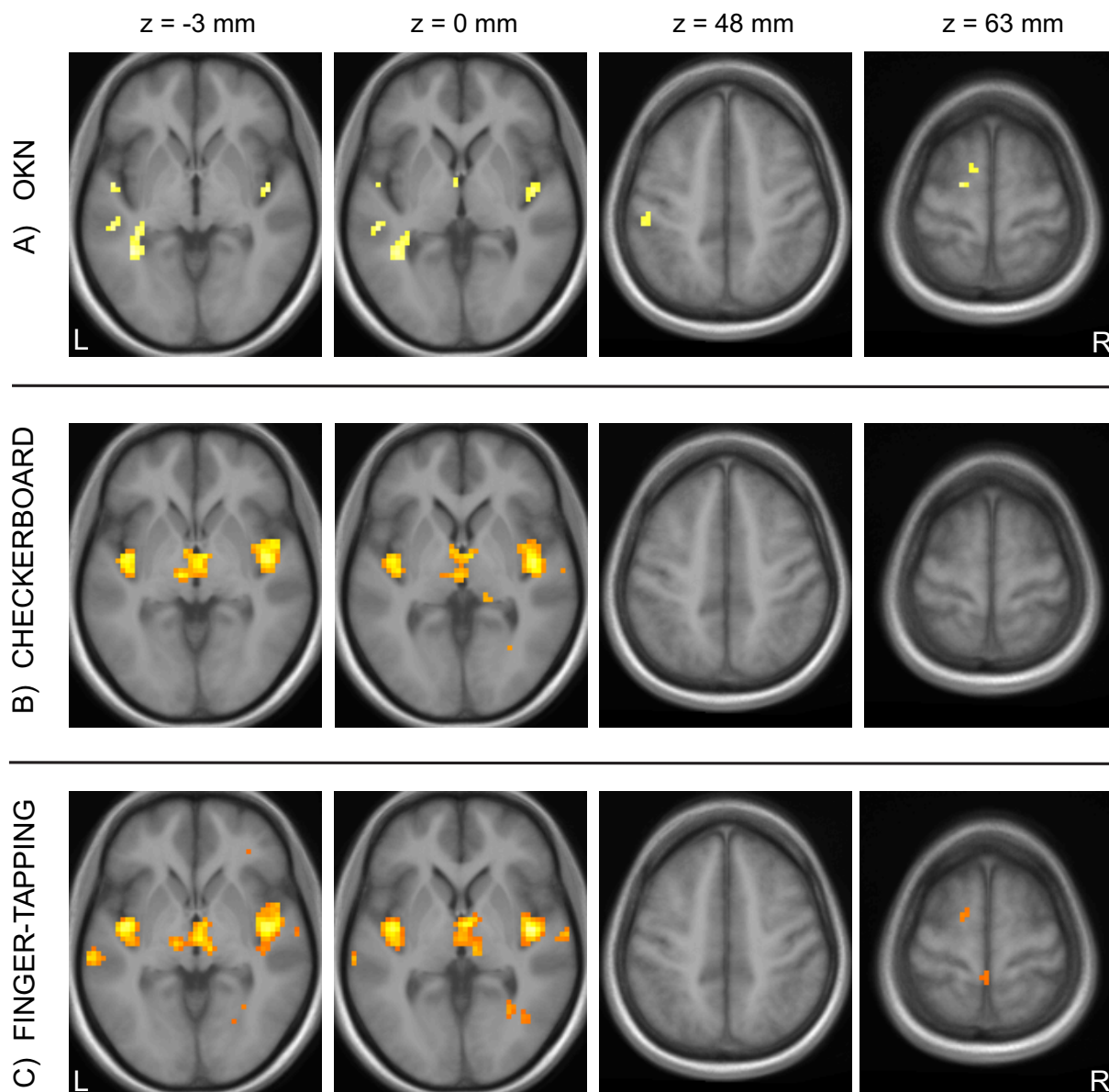


Figure 3.8: Areas showing higher BOLD signal variability during stimulation in Group 3 (60 - 76 years) compared to Group 1 (20 - 40 years) in OKN, checkerboard and finger-tapping experiment ( $p < 0.05$  FDR). A) OKN: age-related increase of BOLD signal variability in insular cortex, planum polare, superior temporal gyrus, postcentral gyrus and superior frontal gyrus. B) Checkerboard (middle): age-related increase of BOLD signal variability in insular cortex and thalamus C) Finger-tapping (bottom): age-related increase of BOLD signal variability in insular cortex, thalamus, superior temporal gyrus and superior frontal gyrus.

As both, SD\_stimulation and SD\_rest showed an age-related increase in the same brain areas we additionally tested whether the observed changes in the signal's fluctuations during blocks of rest could have been affected by the signal in the preceding blocks of stimulation. For this purpose, we performed an ANOVA test for age differences in SD\_rest using only the first block of rest at the beginning of the two imaging sessions in the OKN experiment. This analysis revealed significant results for the contrast SD\_Group 3 - SD\_Group 1 that were consistent with the results from the analyses using all blocks of rest.

### Checkerboard experiment

An ANOVA test for age differences in SD during checkerboard stimulation also showed a significant increase in SD\_stimulation with age. The contrast SD\_Group 3 - SD\_Group 1 revealed higher SD during stimulation in insular cortex, temporal pole, superior temporal gyrus, temporal fusiform complex, hippocampus, thalamus, cerebellum, and the brain stem bilaterally, the left parietal operculum and right inferior parietal lobule in the older subjects (Fig. 3.8 B, Suppl. Tab.10). Furthermore, the contrast SD\_Group 3 - SD\_Group 2 yielded higher SD during stimulation in the elderly subjects in insular cortex bilaterally and the planum polare and hippocampus in the right hemisphere. The contrast SD\_Group 2 - SD\_Group 1 revealed an age-related increase of SD in the superior temporal gyrus, this however, was only seen as a trend (uncorrected,  $p < 0.001$ , cluster size  $\geq 5$ ). ROI analyses showed that out of these areas, only the insular cortex, the hippocampus and the thalamus showed PBR, while all the other areas showed neither PBR nor NBR during checkerboard stimulation. We found no significant decrease of SD\_stimulation with age. A trend, however, of age-related decrease (uncorrected,  $p < 0.001$ , cluster size  $\geq 5$ ) was detected in several brain areas, most of which located in the frontal and temporo-occipital cortex (Suppl. Tab.10). The ROI analysis restricted to areas showing PBR during checkerboard stimulation rendered the age-related decrease in the superior frontal gyrus bilaterally and the posterior part of the right inferior temporal gyrus significant.

The ANOVA test for age-related differences in the SD during rest revealed that most of the areas showing an age-related increase of SD during stimulation, also showed an age-related increase of SD during rest (Fig. 3.9 B, Suppl. Tab.11). The contrast SD\_Group 3 - SD\_group 1 showed significantly higher SD\_rest in Group 3 in insular cortex, temporal pole, hippocampus, thalamus, and cerebellum bilaterally. The contrast SD\_Group 3 - SD\_Group 2 showed an age-related increase of SD\_rest in the insular cortex in both hemispheres as well. The SD\_Group 2 - SD\_Group 1 contrast showed only a trend (un-

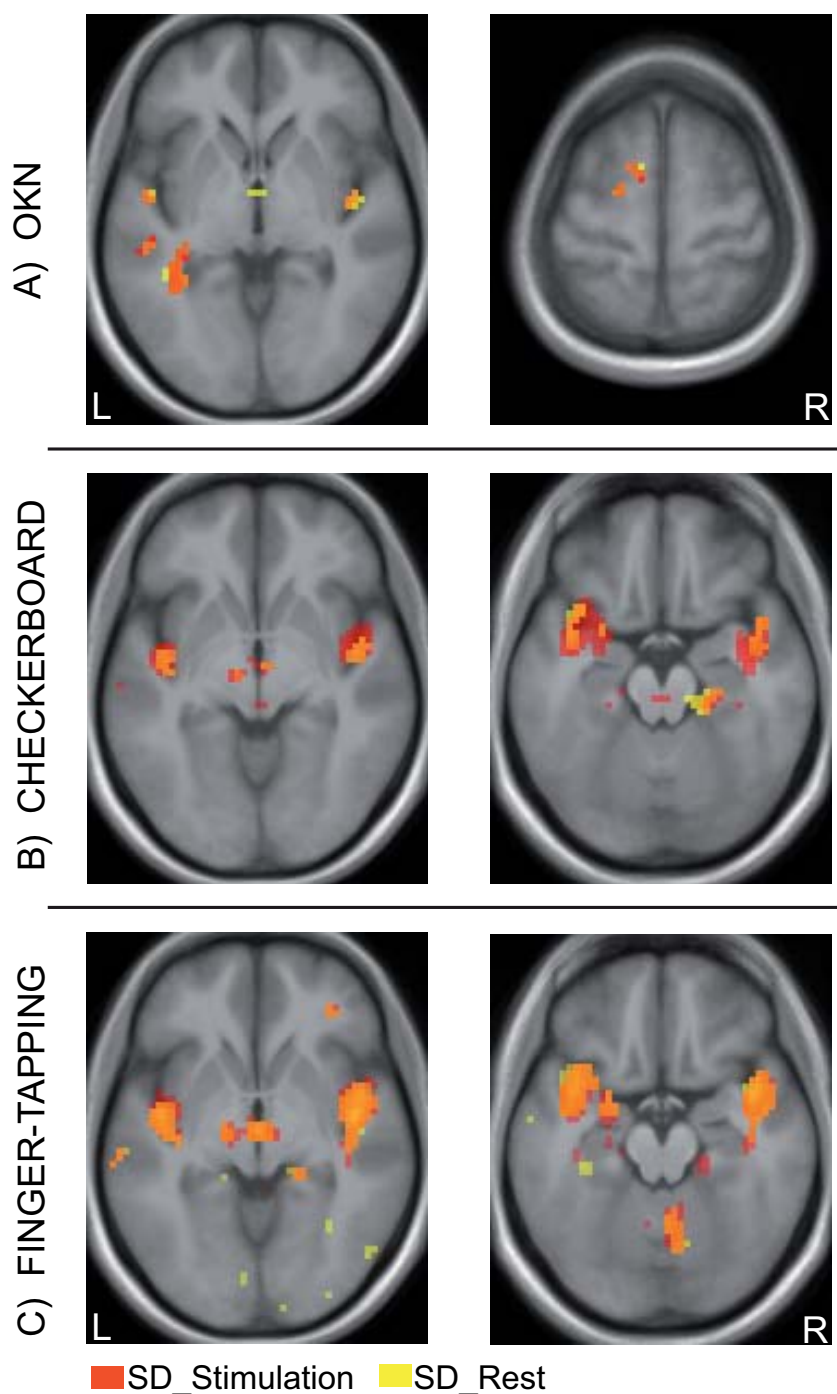


Figure 3.9: Overlaps between statistical maps of age-related increase in BOLD signal variability during stimulation and age-related increase in BOLD signal variability during rest for OKN, checkerboard and finger-tapping experiment ( $p < 0.05$ , FDR). Statistical maps showing higher BOLD signal variability in Group 3 (60 - 76 years) compared to Group 1 (20 - 40 years) during stimulation (red) and during rest (yellow) are overlaid on transversal sections through a group mean anatomical image. A) OKN: age-related increase of BOLD signal variability during stimulation and rest in insular cortex, palmum polare, superior temporal gyrus and superior frontal gyrus. B) Checkerboard: age-related increase of BOLD signal variability during stimulation and rest in insular cortex and temporal pole. C) Finger-tapping: age-related increase of BOLD signal variability during stimulation and rest in insular cortex, temporal pole, hippocampus and cerebellum.

corrected,  $p < 0.001$ , cluster size  $\geq 5$ ) of age-related increase in the left temporal pole and right brain stem. The ROI analyses showed that these areas had neither PBR, nor NBR during checkerboard stimulation. As during stimulation, no significant decrease of SD\_rest with age was revealed by the whole brain analysis. A trend, however, of age-related decrease in SD\_rest (uncorrected,  $p < 0.001$ , cluster size  $\geq 5$ ) was detected in several areas among which: occipital pole, occipital fusiform gyrus, paracingulate gyrus, frontal pole, superior and middle frontal gyrus, putamen, insular cortex, superior parietal lobule, inferior division of the lateral occipital cortex, precentral gyrus, precuneus, and the temporo-occipital fusiform complex (Suppl. Tab.11). The ROI analysis restricted to areas showing PBR during checkerboard stimulation rendered the age-related decrease of SD\_rest in all of the above mentioned brain regions significant.

### **Finger-tapping experiment**

The ANOVA test for age-related differences in SD during stimulation (finger-tapping) showed significantly higher SD in Group 3 compared to Group 1 and Group 2. The contrast SD\_Group 3 - SD\_Group 1 revealed an increase of SD-stimulation with age in the following areas: insular cortex, planum polare, superior temporal gyrus, precentral gyrus, hippocampus, cerebellum, and thalamus in both hemispheres, as well as in left superior frontal gyrus, left central opercular cortex, left middle temporal gyrus, right postcentral gyrus, and right inferior parietal lobule (Fig. 3.8 C). The contrast SD\_Group 3 - SD\_Group 2 showed an age-related increase of SD\_stimulation in the insular cortex and planum polare bilaterally, as well as in the right hippocampus, the inferior division of the right lateral occipital cortex and the right cerebellar hemisphere (Suppl. Tab.12). The contrast SD\_Group 2 - SD\_Group 1 showed only a trend (uncorrected,  $p < 0.001$ , cluster size  $\geq 5$ ) of SD increase with age in the right cerebellar hemisphere and left central opercular cortex. ROI analyses showed that most of the areas with age-related increase in SD during stimulation were also areas showing PBR during finger-tapping. No significant age-related decrease of SD\_stimulation was observed in the whole brain analysis. A trend, however, of age-related decrease (uncorrected,  $p < 0.001$ , cluster size  $\geq 5$ ) was observed in several areas of the frontal, occipital and parietal cortex (Suppl. Tab.12). The ROI analyses revealed that most of these areas showed NBR during finger-tapping, while no age-related decrease of SD\_stimulation was observed in areas with PBR. Furthermore, the ROI analysis restricted to areas with NBR rendered the age-related decrease of SD\_stimulation in the left superior and middle frontal gyrus, left intracalcarine cortex, and right precentral gyrus significant.

The ANOVA test for age-related differences in SD during rest showed a significant increase

---

in Group 3 compared to Group 1 and Group 2. Similar to the age-related differences in SD\_stimulation, the contrast SD\_Group 3 - SD\_Group 1 showed that the SD during rest was higher in the elderly in: insular cortex, planum polare, temporal pole, hippocampus, thalamus, and cerebellum bilaterally, as well as in superior temporal gyrus, precuneus, inferior parietal lobule, occipital pole, and intracalcarine cortex of the right hemisphere, and in middle temporal gyrus and precentral gyrus of the left hemisphere (Fig. 3.9 C, Suppl. Tab.13). The contrast SD\_Group 3 - SD\_Group 2 revealed higher SD\_rest in the elderly in: planum polare bilaterally, insular cortex, precuneus, and inferior division of the lateral occipital cortex in the right hemisphere, as well as superior frontal gyrus and temporal fusiform complex of the left hemisphere. The ROI analyses showed that most of these areas had PBR during finger-tapping, while no age-related change of SD during rest was observed in areas with NBR. No significant age-related decrease of SD\_rest was found in the whole brain analysis. A trend, however, of age-related decrease (uncorrected,  $p < 0.001$ , cluster size  $\geq 5$ ) was observed in several areas of the frontal and parietal cortex (Suppl. Tab.13). The ROI analyses showed that all of these areas had NBR during stimulation, except for the anterior division of the cingulate cortex which showed a PBR. Furthermore, in the ROI analysis restricted to areas with NBR during finger-tapping, the age-related decrease of SD\_rest in the frontal pole and precuneus of the left hemisphere and the paracingulate gyrus bilaterally was significant.

For clearer depiction of the areas showing significant age-related changes of SD in all three experiments, the statistical maps of the SD\_Group 3 - SD\_Group 1 for both, SD during stimulation and SD during rest, were overlaid on the mean anatomical image of the whole group (45 subjects). This showed that in several brain regions, age-related increase of SD during stimulation or SD during rest was observed in all three experiments: planum polare bilaterally, insular cortex in the right hemisphere and left thalamus (Fig. 3.10).

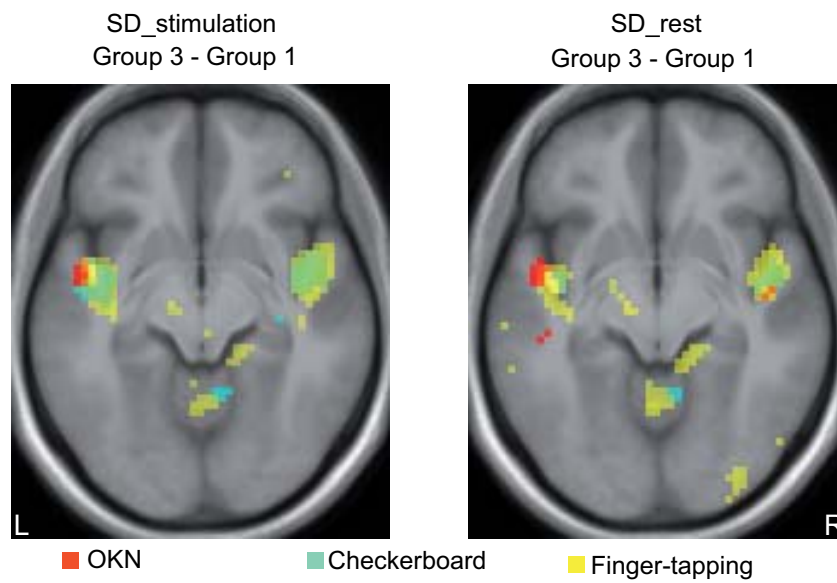


Figure 3.10: Overlaps between the statistical maps of age-related increase in BOLD signal variability from each experiment ( $p < 0.05$ , FDR). The statistical maps from OKN (red), checkerboard (cyan) and finger-tapping (yellow), showing higher BOLD signal variability in Group 3 compared to Group 1 during stimulation (left) and during rest (right) are overlaid on transversal section through a group mean anatomical image. The insular cortex, planum polare and thalamus show an increase of BOLD signal variability in each of the three experiments.

## 4 Discussion

Within the framework of this doctoral thesis we investigated how the cortical visual-vestibular interaction elicited by optokinetic stimulation alters with age in humans. Specifically, we investigated how these changes manifest in fMRI. By applying an experimental paradigm that allowed unaltered OKN performance across all age groups, we were able to offer new insights into the effects of age on the BOLD signal occurring prior to a decrement in oculomotor performance. By exploring the age dependencies of both, the BOLD signal's amplitude and its temporal variability we were able to contribute to the scientific knowledge on the diverse effects of age on distinct features of this signal. This work furthermore offered new information on the age-related changes of the cortical visual-vestibular interaction to be expected in fMRI studies. In the following sections the results from three separate analyses will be discussed in detail and compared to the existing literature.

### 4.1 Age-related changes of the positive BOLD response (PBR) during OKN

The major findings of this analysis were: (1) OKN elicited PBR characterized by shorter latency to peak and wider dispersion compared to the prediction of the canonical HRF model. (2) Increasing age correlated positively with increase in PBR latency to peak and decrease in PBR dispersion despite an unaltered oculomotor performance. (3) The PBR amplitude during OKN performance showed no significant changes with age. (4) No significant age-related changes were observed in the control experiments of pure visual and pure motor tasks. Furthermore, the correlation between age and PBR dynamics in the OKN experiment significantly differed from the one in the two control experiments. Thus, the age-related changes of the PBR dynamics during OKN were specific for this reflexive sensorimotor task.

Since no previous functional imaging study analysed the effects of aging on activations elicited by a reflexive oculomotor task, we compare our findings with the available literature on PBR dynamics during visual and motor tasks, as well as with the changes observed in our two control experiments.

#### 4.1.1 Interpretations of the age-related changes in PBR dynamics

Two distinct aging processes could in principle be accountable for the results obtained from the OKN experiment. First, an unaltered oculomotor performance could indicate an unaltered neural processing, in which case the observed age-related changes in the PBR dynamics reflect changes in the neurovascular coupling with unaltered neural processing. Second, the changes in the PBR dynamics could reflect a cortical adaptive strategy counteracting development of age-related degenerative processes in order to enable maintenance of optimal performance. A combination of these two scenarios, changes in the neural processing and changes in the neurovascular coupling in senescence, could be a possible explanation for the observed alterations in the signal dynamics as well.

Increasing age is associated with degenerative changes in the brain's vasculature, morphology and neural metabolism, which essentially impacts the neurovascular coupling and can therefore, affect the BOLD response. As discussed by D'Esposito et al. (2003) age was shown to correlate with reduction of the vascular reactivity due to atherosclerotic changes, decrease in the resting cerebral blood flow and decrease in the resting cerebral metabolic rate of  $O_2$  consumption ( $CMRO_2$ ), all of which are crucial components of the neurovascular coupling. Previous studies on age-related changes in the BOLD signal have in fact suggested alterations in the neurovascular coupling to be the most possible explanation for the observed signal changes (Taoka et al., 1998; D'Esposito et al., 1999; Huettel et al., 2001; Hesselmann et al., 2001; Harris et al., 2011). A delay in the vascular reactivity during stimulation should theoretically cause an increase in the latency to peak and dispersion of the BOLD signal. In the present study, however, we found bidirectional changes in the signal dynamics: an increase in the PRB latency to peak and a decrease of the PRB dispersion. Therefore, changes in the vascular reactivity can not alone explain our results. Nevertheless, as the dynamics of the BOLD signal are determined by the simultaneous working of both, vascular reactivity and  $CRM O_2$ , it is theoretically possible that disproportional age-related decreases in these components cause the observed changes in the PBR dynamics.

However, the finding that these changes are specific for the OKN task suggests that alteration in the neural processing required for OKN might be a contributing factor. The major difference between OKN and the other two experiments in terms of neural processing is that it requires coupling of visual-motion perception with oculomotor function. Interestingly, we found an increased PBR latency to peak already in the lateral geniculate body (LGN), which indicates a change in an early processing stage in the visual pathway. As previous research has shown that the BOLD signal in early sensory areas

---

correlates better with the local input and the circuits' internal processing than with the circuits' output (Logothetis and Wandell, 2004), it is probable that the increase of the PBR latency to peak in LGN rather reflects a change in the processing of both, feed-forward (retinal) and feed-back (cortical) information in the LGN circuits, than simply a delay in the retinal input to LGN or delay in its output to the cortical areas. In this line of thought, changes in the internal processing of feed-forward and feed-back information could also hold true for the other areas showing age-related changes in PBR dynamics. These alterations in the neural processing during OKN might be an adaptive response to the developing degenerative changes in the brain's vasculature or microstructure, as the performance of the subjects remained unaltered with age. It should be noted, though, that the delay and shorter duration of the PBR response in well-performing elderly, could also mark the beginning of the development of neural dysfunction itself.

Yet, since the BOLD signal is by its nature entirely dependent on the complex mechanisms of coupling the vascular response to the neural function, it is possible that subtle age-related changes in both, neural processing and neurovascular coupling contribute to yield the observed results. A clear separation of the impact from each of these factors poses a great challenge, as they might be dependent on each other. Influence of such multiple factors could, however, better explain not only the results in this study, but also the differences between the results from previous studies in the literature.

An interesting observation in this study was that from all the brain areas activated during OKN, only the hMT/V5 complex did not show any age-related changes in the PBR dynamics. As shown, the regression slope of age and PBR latency to peak in both hMT/V5 areas was significantly different from the regression slopes found in all the other areas showing aging effects. In contrast to all the other areas expressing age-related changes, this area is known to be not involved in the generation or maintenance of saccades (Büttner and Büttner-Ennever, 2006). Thus, the aging effects demonstrated in our study seem to be restricted to the brain network related to saccades, although the saccadic frequency and amplitude of the subjects' OKN remained normal.

#### **4.1.2 Task-specific changes of PBR dynamics with age**

Previous studies on the age dependencies of the BOLD response elicited by simple visual and motor tasks showed heterogeneous results. Huettel et al. (2001) and Richter and Richter (2003) used a checkerboard task to investigate the effects of age on the signal in the visual cortex and found no change in the PBR amplitude with age. However, Huettel et al. (2001) described a significant decrease of the PBR latency and dispersion, whereas

Richter and Richter (2003) found a significant increase of these parameters in advanced age. Taoka et al. (1998) measured the time necessary for the BOLD signal in the precentral gyrus to reach its half-maximal increase after starting a 'hand grip' task, and revealed significant age-related increase of the BOLD signal latency and no change in its amplitude or decay. Raemaekers et al. (2006) investigated the effects of age on the BOLD signal during prosaccades and antisaccades and found an age-related shift in the spatial pattern of the BOLD signal from posterior to frontal areas, as well as an overall decrease of its amplitude with age. Buckner et al. (2000) compared the aging effects on the BOLD response amplitude in the visual and motor cortex during a sensorimotor task (key-press response at the onset of checkerboard stimulation) and found differences between these two regions: the amplitude in the visual cortex decreased with age, while the amplitude in the motor cortex remained intact. The discrepancies between the above mentioned findings, pose the question whether the effects of age on the BOLD signal dynamics depend on global changes in brain structure, vasculature and function, regional changes in these features or on the performed task itself.

Our study showed that the correlation between age and PBR latency to peak or dispersion in the OKN experiment was significantly different from the correlation in the two control experiments. If global vascular changes in the elderly were solely accountable for the alterations in PBR dynamics we would have expected equal effects in all three paradigms. Furthermore, global age-related reduction of grey matter volume can also be excluded as a unique source of our findings, since this would have caused equal effects in the occipital cortex during OKN and checkerboard stimulation. As global changes cannot successfully explain our results, the question arises whether region-specific changes in structure or function would lead to the differences we observed. The finding, however that the occipital cortex in the present study was activated during both, OKN and checkerboard stimulation, but showed age-related differences only during the OKN task renders this possibility unlikely. Thus, general vascular changes, global atrophy or region-specific changes in structure and function may have an effect, but can not solely explain our results. Instead, task-specific changes with age in the neurovascular coupling and/or neural processing required for OKN are the most plausible explanation for the observed alteration of the PBR dynamics.

In summary, this analysis demonstrates that significant age-related changes of the positive BOLD response during OKN occur before any changes in the oculomotor performance can be detected. Furthermore, these changes are specific for the reflexive OKN task and are probably a result of both, age-related changes in the neurovascular coupling, as well

---

as changes in the neural processing during OKN.

## **4.2 Age-related changes of the negative BOLD response (NBR) during OKN**

The main findings of this analysis were: (1) the NBR elicited by OKN had longer latency to peak and narrower dispersion than predicted by the canonical model of HRF. (2) No significant age-related changes of either NBR amplitude, latency to peak or dispersion were detected in the OKN experiment. (3) The two control experiments revealed no significant change in NBR dynamics as well. (4) A trend for age-related decrease of NBR amplitude was detected in all three experiments.

The hypothesis of inhibitory reciprocal visual-vestibular interaction has suggested that the BOLD signal decreases (NBR) during visual optokinetic stimulation reflect inhibition of the vestibular processing in the multisensory vestibular cortex, due to a shift of the sensorial weighting to the more reliable, in this case visual, modality (Dieterich et al., 2003). Such cross-modal inhibition has also been demonstrated for other sensory modalities (Alsius et al. 2005, Haxby et al. 1994, Shulman et al. 1997). It was proposed that in imaging studies such inhibition would be observed as task-specific signal decreases compared to the baseline and would serve to limit the distraction and interference from other sensory modalities (Peiffer et al., 2009).

Previous behavioural and imaging studies on age-related changes in multisensory interactions have suggested that increasing age associates with an increase in multisensory processing (Laurienti et al., 2006; Peiffer et al., 2007, 2009; Zwergal et al., 2010). In terms of fMRI research, this was suggested based on age-related decrease of NBR in task-related brain areas and an appearance of a PBR instead (Zwergal et al., 2010), or as a change in the amplitude and spatial pattern of the NBR in well-performing elderly subjects (Peiffer et al., 2009). If supposed that the task-induced NBR reflects inhibitory effects in a specific cortical network, the above mentioned findings suggest that enhanced multisensory processing is partially modulated by an age-related decline of inhibition. Previous human and animal studies have indeed demonstrated a decrease of the inhibitory processes in advanced age (McDowd and Filion, 1995; Peinemann et al., 2001; Schmidt et al., 2010). Our results, however, revealed no significant age-related changes in either of the NBR dynamics. Although the trend of age-related decrease in NBR amplitude in several multisensory regions is in accordance with the results from the previous studies, it does not offer sufficient support. A possible reason for this could be that the task difficulty posed

by the relatively slow velocity of optokinetic stimulation was not sufficient and challenging enough to trigger significant functional changes in the multisensory vestibular network.

In summary, the results of this analysis offer new insight into the effects of age on the cortical visual-vestibular interaction in fMRI studies. We showed that unlike the PBR in visual and oculomotor cortical areas, the NBR in the multisensory vestibular cortical network does not seem to be age-dependent for a task that is not at the limit of abilities.

### 4.3 Temporal variability of the BOLD signal

The vast majority of fMRI studies has typically focused on average brain activation patterns depicted by the mean of the BOLD signal during a given time course. This tendency originates from the assumption that the BOLD signal's mean conveys the most relevant information and the variability of the signal is regarded to as 'noise'. In this sense, noise is perceived in the sense of random or unpredictable fluctuations that obscure or do not contain meaningful data or other information (Oxford English Dictionary). Previous studies, however, have suggested that the variability in fMRI contains additional information on the functioning of the neural system (Garrett et al., 2010, 2012; McIntosh et al., 2010; Samanez-Larkin et al., 2010; Wutte et al., 2011). Furthermore, it has been shown that the relationship between age and the BOLD signal's variability differs from the relationship with the signal's mean (Garrett et al., 2010; Samanez-Larkin et al., 2010). Therefore, the third objective of this doctoral thesis was to analyse the temporal variability of the BOLD signal and its age dependencies in the OKN experiment. Additionally, we intended to compare these findings with the ones from the two control experiments.

#### 4.3.1 Differences between SD\_rest and SD\_stimulation

The main findings of this analysis were: (1) The OKN experiment revealed significantly higher variability during 'rest' than during stimulation in both, the whole brain and the ROI analysis. (2) The areas showing such difference in variability overlapped with areas showing PBR or NBR during stimulation. (3) The finger-tapping experiment revealed higher variability during 'rest' compared to stimulation in the whole brain analysis. The ROI analysis revealed additional areas with such significant difference between conditions, all of which had PBR during task performance. (4) The checkerboard experiment showed no significant difference between the two conditions in the whole brain analysis. Only a trend of higher variability during 'rest', as well as higher variability during stimulation in different brain areas was detected. The ROI analysis rendered the latter difference significant in areas showing NBR during stimulation.

In a previous study on a similar topic, Garrett et al. (2012) investigated the differences between the signal's variability during blocks of 'rest' (fixation) and during blocks of four different cognitive tasks. Contrary to our results, they found that the BOLD signal variability was significantly higher during the cognitive task blocks compared to the blocks of 'rest'. Furthermore, the areas showing such difference in the transition from fixation to task mostly did not overlap with areas showing task-related changes in the signal's mean. The authors suggested the following explanations for these findings: first, higher variability during task performance could indicate a more sophisticated neural system capable of greater dynamic range, allowing greater range of responses to a greater range of stimuli, second, increase of variability during task performance could be due to bigger stimulus uncertainty and may provide the kinetic energy for the brain networks to achieve a variety of possible functional states (Garrett et al., 2012). This interpretation of signal variability as beneficial to the system builds upon previous work discussing signal fluctuations from the perspective of stochastic resonance (Faisal et al., 2008; McDonnell and Ward, 2011) and was supported by a study from McIntosh et al. (2008). In this work the authors measured the variability of the EEG signal during performance of a face memory task in children and young adults. Their study revealed that higher variability in brain dynamics correlated with lower variability and higher accuracy in task performance. Additionally, the young adults, as representative sample of an 'optimally' developed and matured system, possessed higher signal variability than the children. Therefore, they postulated that an optimal level of internal variability is beneficial to the neural system and might be a key feature governing brain function.

The differences between the results from the OKN and finger-tapping experiment in our study and the findings of Garrett et al. (2012) are intriguing. A possible reason for these differences could lie in the applied experimental paradigms. Namely, the experimental paradigm of Garrett et al. (2012) did not allow the participants to predict which task they would next need to perform, which ensured the stimulus uncertainty and varying cognitive load they suggested accountable for the higher BOLD signal variability during the task blocks (Garrett et al., 2012). Contrary to this, in our study the three experimental paradigms did not pose such stimulus uncertainty, as each type of stimulation was performed in a separate experiment. In the context of the discussion by Garrett et al. (2012), this might indicate that higher BOLD signal variability during task performance can only be detected when stimulus uncertainty exists, and furthermore, it mostly occurs in areas with no task-related changes in the signal's mean. Under conditions, however, where the stimulus uncertainty is minimal, a decrease of variability during task

performance could be beneficial, especially in the areas showing task-related change of the signals mean. Several points, however, argue against such straight-forward explanation. First, the checkerboard experiment in our study showed a trend of bidirectional changes in BOLD signal variability, although the experimental paradigm should not have offered higher uncertainty in stimulus occurrence than the paradigms of the other two experiments. Second, Garrett et al. (2012) did not find any decrease of signal variability during task performance which would support the assumption of variability in task-related areas as 'noise'. The discrepancies between these findings require future exploration of the relationship between BOLD signal variability in task-related and task-non-related brain regions, in the context of stimulus predictability.

#### 4.3.2 Age-related changes of SD\_rest and SD\_stimulation

The main findings from this analysis were: (1) In the OKN experiment variability in both, stimulation and 'rest' blocks increased significantly with increasing age in an extensively overlapping network of areas, most of which known to be part of the multisensory vestibular cortical network. (2) The ROI analysis showed that most of the areas with age-related increase in variability had NBR during OKN. (3) No significant age-related decrease of signal variability was found in the OKN experiment. (4) The two control experiments yielded an age-related increase of signal variability in both, stimulation and 'rest' blocks, in most of the areas observed in the OKN experiment. (5) They additionally showed a trend of age-related decrease in signal variability, mostly found in the frontal cortices. The ROI analyses rendered this age-related decrease in variability as significant in several areas, some of them having PBR during checkerboard stimulation, and some NBR during finger-tapping.

These findings suggest that the age-related changes in the signal variability observed in our study are neither task-specific (as they were detected in almost the same network of areas during three different types of stimulation), nor specific for stimulation per se (as they occurred during the 'rest' condition in the same networks as well). Instead, they seem to be specific to distinct brain areas. The largest brain region showing an age-related increase of variability in all three experiments was the temporal-insular cortex. One explanation for this could be that certain brain regions are more affected by degenerative morphological changes and therefore have greater impact on the changes in signal variability than others. Previous research has, for example, demonstrated that increasing age is associated with grey matter loss, particularly notable in the frontal cortices (Raz et al., 1997). However, the VBM we performed showed a decrease in grey and white matter volume across the whole brain, with no specific spatial pattern. This

---

implies that if atrophy was the source of increased variability in the BOLD signal, such increase would occur in other portions of the brain as well. Yet, as the same results were observed in all three experiments, an effect of grey matter reduction in this region cannot be entirely excluded. The global changes in the vascular dynamics also cannot account for the changes in BOLD signal variability, as the alterations in the vascular response are unidirectional in nature (Handwerker et al., 2007). Another source of variability in fMRI time series is head motion (Friston et al., 1996). Previous research has further shown that head motion during scanning procedure positively correlated with increasing age (Huetzel et al., 2001; D'Esposito et al., 1999). Since we however, controlled for the effects of motion in our analysis, it is unlikely that this factor can explain the increase in variability.

A study by Garrett et al. (2010) has tried to interpret the age-related changes in BOLD signal variability as a reflection of changes in neural function. They investigated the effects of age on the BOLD signal variability during blocks of 'rest' (fixation) and found several areas where the variability increased and other areas where variability decreased in advanced age. In this sense, our results are consistent with their findings, as we also observed such bidirectionality in the changes of variability. However, in our study the spatial network showing age-related increases of variability during 'rest' was more extensive than the network showing variability decreases. Furthermore, some of the areas found to show age-related decrease of variability in the study of Garret et al. showed an increase in our analyses (the middle temporal gyrus, the precentral gyrus, the inferior parietal lobule). Garrett et al. (2010) suggested that the bidirectionality in the age-related changes shows that age-related differences in variability are both, spatially and directionally specific. Furthermore, as younger adults represent the 'optimal' system to which elderly can be compared, this bidirectionality implies that even in young adults variability is heterogeneous across the brain Garrett et al. (2010). The authors suggested that the higher variability in the young adults could be a feature of a more 'sophisticated', 'optimally' operating system, rather than just background noise carrying no meaningful information. They further pointed out that this assumption does not easily account for the brain regions where age-related increase of variability was detected. Discussing from the perspective of 'stochastic resonance', the authors suggested that the increase of signal variability with age might reflect compensating mechanisms counteracting neural dysfunction. In this logic, the decreases of signal variability would then represent reductions in optimal variability levels with age (Garrett et al., 2010). The authors, however, note that greater variability could be naturally beneficial in certain brain regions, while disadvantageous in others.

In our study, the OKN and finger-tapping experiments revealed higher BOLD signal variability in the 'rest' blocks compared to the stimulation blocks in task-related brain areas. This might imply that a decrease of variability is beneficial for optimal task performance during the stimulation period. If the changes in BOLD signal variability should partially reflect functional modulation in the neural circuitry, than the age-related variability increases could reflect deterioration of the circuitry's mechanisms providing optimal 'signal-to-noise' ratio. In this line of thought, the age-related decrease of variability in the frontal regions could then reflect a presence of compensating mechanisms. Yet, it is possible that the optimal level of variability differs between brain regions and any excursions from this level could be a sign of functional decline. Clear interpretation, however, of the BOLD signal variability and its changes with age remains a challenging task for future experiments.

#### 4.4 Conclusions

This thesis demonstrates that age affects the different features of the BOLD signal in a distinct manner. The analyses assessing the dynamics of the mean of the BOLD signal during optokinetic stimulation have revealed task-specific changes in the temporal profile of the PBR in the visual and oculomotor areas, and no significant changes of the NBR in the multisensory vestibular cortical network. Importantly, the age-related changes in the visual and oculomotor system could be detected prior to any decrement in oculomotor performance. While the main areas of the multisensory vestibular cortical network showed no significant age-related changes in the mean of the BOLD response, they revealed a clear increase in its variability in the elderly. Although these changes in variability were not specific for the OKN task, they could have an important impact on the visual-vestibular interaction as they affect crucial regions of the multisensory vestibular network.

#### 4.5 Future research

The present study enabled us to contribute to the scientific knowledge on different aspects of the visual-vestibular cortical interaction in healthy young and older adults. It therefore offered diverse control measures for the investigation of pathological changes in the visual-vestibular interaction. Future studies can build upon these findings and further explore whether and how the mean of the BOLD signal or its variability alter in patients with acute or chronic dysfunctions in the visual and vestibular systems.

## Bibliography

- Allison T, Hume AL, Wood CC, Goff WR (1984) Developmental and aging changes in somatosensory, auditory and visual evoked potentials. *Electroencephalography and Clinical Neurophysiology* 58:14–24.
- Andersson S, Gernand BE (1954) Cortical projection of vestibular nerve in cat. *Acta Oto-laryngologica, Informa Healthcare* .
- Angelaki DE, Cullen KE (2008) Vestibular system: the many facets of a multimodal sense. *Annual review of neuroscience* 31:125–150 PMID: 18338968.
- Ashburner J, Flandin G, Henson R, Kiebel S, Kilner J, Mattout J, Penny W, Stephan K, Gitelman D, Hutton C (2009) SPM5 manual.
- Ashburner J, Friston KJ (2005) Unified segmentation. *NeuroImage* 26:839–851.
- Attwell D, Laughlin SB (2001) An energy budget for signaling in the grey matter of the brain. *Journal of cerebral blood flow and metabolism: official journal of the International Society of Cerebral Blood Flow and Metabolism* 21:1133–1145 PMID: 11598490.
- Baloh RW, Jacobson KM, Socotch TM (1993) The effect of aging on visual-vestibuloocular responses. *Experimental Brain Research* 95:509–516.
- Baloh RW, Enrietto J, Jacobson KM, Lin A (2001) Age-related changes in vestibular function. *Annals of the New York Academy of Sciences* 942:210–219.
- Bear MF, Connors BW, Paradiso MA (2006) *Neuroscience: Exploring the Brain* Lippincott Williams & Wilkins.
- Bense S, Janusch B, Vucurevic G, Bauermann T, Schlindwein P, Brandt T, Stoeter P, Dieterich M (2006) Brainstem and cerebellar fMRI-activation during horizontal and vertical optokinetic stimulation. *Experimental Brain Research* 174:312–323.
- Bense S, Stephan T, Yousry TA, Brandt T, Dieterich M (2001) Multisensory cortical signal increases and decreases during vestibular galvanic stimulation (fMRI). *Journal of Neurophysiology* 85:886–899.

- Bottini G, Sterzi R, Paulesu E, Vallar G, Cappa SF, Erminio F, Passingham RE, Frith CD, Frackowiak RSJ (1994) Identification of the central vestibular projections in man: a positron emission tomography activation study. *Experimental Brain Research* 99:164–169.
- Brandt T, Bartenstein P, Janek A, Dieterich M (1998) Reciprocal inhibitory visual-vestibular interaction. visual motion stimulation deactivates the parieto-insular vestibular cortex. *Brain: a journal of neurology* 121 ( Pt 9):1749–1758 PMID: 9762962.
- Brandt T, Glasauer S, Stephan T, Bense S, Yousry TA, Deutschländer A, Dieterich M (2002) Visual-Vestibular and visuovisual cortical interaction. *Annals of the New York Academy of Sciences* 956:230–241.
- Brandt T (1999) Cortical visual-vestibular interaction for spatial orientation and self-motion perception. *Current Opinion in Neurology* 12:1–4.
- Brandt T, Dieterich M (1999) The vestibular cortex: Its locations, functions, and disorders. *Annals of the New York Academy of Sciences* 871:293–312.
- Bucher SF, Dieterich M, Seelos KC, Brandt T (1997) Sensorimotor cerebral activation during optokinetic nystagmus a functional MRI study. *Neurology* 49:1370–1377.
- Bucher SF, Dieterich M, Wiesmann M, Weiss A, Zink R, Yousry TA, Brandt T (1998) Cerebral functional magnetic resonance imaging of vestibular, auditory, and nociceptive areas during galvanic stimulation. *Annals of Neurology* 44:120–125.
- Buckner RL, Snyder AZ, Sanders AL, Raichle ME, Morris JC (2000) Functional brain imaging of young, nondemented, and demented older adults. *Journal of Cognitive Neuroscience* 12:24–34.
- Büttner U, Büttner-Ennever J (2006) Present concepts of oculomotor organization In *Neuroanatomy of the Oculomotor System*, Vol. Volume 151, pp. 1–42. Elsevier.
- Cabeza R, Anderson ND, Locantore JK, McIntosh AR (2002) Aging gracefully: compensatory brain activity in high-performing older adults. *NeuroImage* 17:1394–1402 PMID: 12414279.
- Cabeza R, Grady CL, Nyberg L, McIntosh AR, Tulving E, Kapur S, Jennings JM, Houle S, Craik FIM (1997) Age-related differences in neural activity during memory encoding and retrieval: A positron emission tomography study. *The Journal of Neuroscience* 17:391–400.

- 
- Cohen B, Matsuo V, Raphan T (1977) Quantitative analysis of the velocity characteristics of optokinetic nystagmus and optokinetic after-nystagmus. *The Journal of physiology* 270:321–344 PMID: 409838.
- Cohen B, Reisine H, Yokota JI, Raphan T (1992) The nucleus of the optic tract: Its function in gaze stabilization and control of visual-vestibular interaction. *Annals of the New York Academy of Sciences* 656:277–296.
- De Sanctis P, Katz R, Wylie GR, Sehatpour P, Alexopoulos GS, Foxe JJ (2008) Enhanced and bilateralized visual sensory processing in the ventral stream may be a feature of normal aging. *Neurobiology of aging* 29:1576–1586 PMID: 17478011.
- Della-Justina H, Pastorello B, Santos-Pontelli T, Pontes-Neto O, Santos A, Baffa O, Colafemina J, Leite J, de Araujo D (2008) Human variability of fMRI brain activation in response to oculomotor stimuli. *Brain Topography* 20:113–121.
- Deshpande N, Patla A (2007) Visual-vestibular interaction during goal directed locomotion: effects of aging and blurring vision. *Experimental Brain Research* 176:43–53.
- D’Esposito M, Deouell LY, Gazzaley A (2003) Alterations in the BOLD fMRI signal with ageing and disease: a challenge for neuroimaging. *Nature Reviews Neuroscience* 4:863–872.
- D’Esposito M, Zarahn E, Aguirre GK, Rypma B (1999) The effect of normal aging on the coupling of neural activity to the bold hemodynamic response. *NeuroImage* 10:6–14.
- Deuschländer A, Bense S, Stephan T, Schwaiger M, Brandt T, Dieterich M (2002) Sensory system interactions during simultaneous vestibular and visual stimulation in PET. *Human Brain Mapping* 16:92–103.
- Dieterich M, Bucher SF, Seelos KC, Brandt T (1998) Horizontal or vertical optokinetic stimulation activates visual motion-sensitive, ocular motor and vestibular cortex areas with right hemispheric dominance. an fMRI study. *Brain* 121:1479–1495.
- Dieterich M (2007) Functional brain imaging: a window into the visuo-vestibular systems. *Current Opinion in Neurology* 20:12–18.
- Dieterich M, Bense S, Stephan T, Yousry T, Brandt T (2003) fMRI signal increases and decreases in cortical areas during small-field optokinetic stimulation and central fixation. *Experimental Brain Research* 148:117–127.
- Faisal AA, Selen LPJ, Wolpert DM (2008) Noise in the nervous system. *Nature Reviews Neuroscience* 9:292–303.

- Frison L, Pocock SJ (1992) Repeated measures in clinical trials: Analysis using mean summary statistics and its implications for design. *Statistics in Medicine* 11:1685–1704.
- Friston KJ, Williams S, Howard R, Frackowiak RS, Turner R (1996) Movement-related effects in fMRI time-series. *Magnetic resonance in medicine: official journal of the Society of Magnetic Resonance in Medicine / Society of Magnetic Resonance in Medicine* 35:346–355 PMID: 8699946.
- Friston KJ, Ashburner J, Frith CD, Poline JB, Heather JD, Frackowiak RSJ (1995) Spatial registration and normalization of images. *Human Brain Mapping* 3:165–189.
- Garrett DD, Kovacevic N, McIntosh AR, Grady CL (2012) The modulation of BOLD variability between cognitive states varies by age and processing speed. *Cerebral Cortex*.
- Garrett DD, Kovacevic N, McIntosh AR, Grady CL (2010) Blood oxygen level-dependent signal variability is more than just noise. *The Journal of Neuroscience* 30:4914–4921.
- Goense JBM, Logothetis NK (2008) Neurophysiology of the BOLD fMRI signal in awake monkeys. *Current biology: CB* 18:631–640 PMID: 18439825.
- Grüsser OJ, Pause M, Schreiter U (1990a) Localization and responses of neurones in the parieto-insular vestibular cortex of awake monkeys (*Macaca fascicularis*). *The Journal of Physiology* 430:537–557.
- Grüsser OJ, Pause M, Schreiter U (1990b) Vestibular neurones in the parieto-insular cortex of monkeys (*Macaca fascicularis*): visual and neck receptor responses. *The Journal of Physiology* 430:559–583.
- Harris JJ, Reynell C, Attwell D (2011) The physiology of developmental changes in BOLD functional imaging signals. *Developmental Cognitive Neuroscience* 1:199–216.
- Hazlett EA, Buchsbaum MS, Mohs RC, Spiegel-Cohen J, Wei TC, Azueta R, Haznedar MM, Singer MB, Shihabuddin L, Luu-Hsia C, Harvey PD (1998) Age-related shift in brain region activity during successful memory performance. *Neurobiology of aging* 19:437–445 PMID: 9880046.
- Henson R, Price C, Rugg M, Turner R, Friston K (2002) Detecting latency differences in event-related BOLD responses: Application to words versus nonwords and initial versus repeated face presentations. *NeuroImage* 15:83–97.
- Hesselmann V, Zaro Weber O, Wedekind C, Krings T, Schulte O, Kugel H, Krug B, Klug N, Lackner KJ (2001) Age related signal decrease in functional magnetic resonance imaging during motor stimulation in humans. *Neuroscience Letters* 308:141–144.

- 
- Heuninckx S, Wenderoth N, Swinnen SP (2008) Systems neuroplasticity in the aging brain: Recruiting additional neural resources for successful motor performance in elderly persons. *The Journal of Neuroscience* 28:91–99.
- Huettel SA, Singerman JD, McCarthy G (2001) The effects of aging upon the hemodynamic response measured by functional MRI. *NeuroImage* 13:161–175.
- Huettel SA, Song AW, McCarthy G (2004) *Functional Magnetic Resonance Imaging* Sinauer Associates.
- Jahn K, Naessl A, Schneider E, Strupp M, Brandt T, Dieterich M (2003) Inverse u-shaped curve for age dependency of torsional eye movement responses to galvanic vestibular stimulation. *Brain* 126:1579–1589.
- Kashou NH, Leguire LE, Roberts CJ, Fogt N, Smith MA, Rogers GL (2010) Instruction dependent activation during optokinetic nystagmus (OKN) stimulation: An fMRI study at 3T. *Brain Research* 1336:10–21.
- Kato I, Ishikawa M, Nakamura T, Watanabe J, Harada K, Kanayama R, Aoyagi M, Koike Y (1994) Quantitative assessment of influence of aging on optokinetic nystagmus. *Acta Otolaryngologica* 114:99–103.
- Kerber KA, Ishiyama GP, Baloh RW (2006) A longitudinal study of oculomotor function in normal older people. *Neurobiology of Aging* 27:1346–1353.
- Kikuchi M, Naito Y, Senda M, Okada T, Shinohara S, Fujiwara K, Hori SY, Tona Y, Yamazaki H (2009) Cortical activation during optokinetic stimulation - an fMRI study. *Acta Otolaryngologica* 129:440–443.
- Konen CS, Kleiser R, Seitz RJ, Bremmer F (2005) An fMRI study of optokinetic nystagmus and smooth-pursuit eye movements in humans. *Experimental Brain Research* 165:203–216.
- Krauzlis RJ (2004) Recasting the smooth pursuit eye movement system. *Journal of Neurophysiology* 91:591–603.
- Lamme VA, Roelfsema PR (2000) The distinct modes of vision offered by feedforward and recurrent processing. *Trends in Neurosciences* 23:571–579.
- Laurienti PJ, Burdette JH, Maldjian JA, Wallace MT (2006) Enhanced multisensory integration in older adults. *Neurobiology of Aging* 27:1155–1163.

- Levine BK, Beason-Held LL, Purpura KP, Aronchick DM, Optican LM, Alexander GE, Horwitz B, Rapoport SI, Schapiro MB (2000) Age-related differences in visual perception: a PET study. *Neurobiology of aging* 21:577–584 PMID: 10924775.
- Li SC, Lindenberger U, Sikström S (2001) Aging cognition: from neuromodulation to representation. *Trends in Cognitive Sciences* 5:479–486.
- Logan JM, Sanders AL, Snyder AZ, Morris JC, Buckner RL (2002) Under-recruitment and nonselective recruitment: dissociable neural mechanisms associated with aging. *Neuron* 33:827–840 PMID: 11879658.
- Logothetis NK (2008) What we can do and what we cannot do with fMRI. *Nature* 453:869–878.
- Logothetis NK, Pauls J, Augath M, Trinath T, Oeltermann A (2001) Neurophysiological investigation of the basis of the fMRI signal. *Nature* 412:150–157.
- Logothetis NK, Wandell BA (2004) Interpreting the BOLD signal. *Annual Review of Physiology* 66:735–769.
- Madden DJ, Turkington TG, Provenzale JM, Denny LL, Hawk TC, Gottlob LR, Coleman RE (1999) Adult age differences in the functional neuroanatomy of verbal recognition memory. *Human brain mapping* 7:115–135 PMID: 9950069.
- Madden DJ, Whiting WL, Provenzale JM, Huettel SA (2004) Age-related changes in neural activity during visual target detection measured by fMRI. *Cerebral Cortex* 14:143–155.
- McDonnell MD, Ward LM (2011) The benefits of noise in neural systems: bridging theory and experiment. *Nature Reviews Neuroscience* 12:415–426.
- McDowd JM, Filion DL (1995) Aging and negative priming in a location suppression task: the long and the short of it. *Psychology and aging* 10:34–47 PMID: 7779315.
- McIntosh AR, Sekuler AB, Penpeci C, Rajah MN, Grady CL, Sekuler R, Bennett PJ (1999) Recruitment of unique neural systems to support visual memory in normal aging. *Current biology: CB* 9:1275–1278 PMID: 10556091.
- McIntosh AR, Kovacevic N, Lippe S, Garrett D, Grady C, Jirsa V (2010) The development of a noisy brain. *Archives Italiennes de Biologie* 148:323–337.
- McIntosh AR, Kovacevic N, Itier RJ (2008) Increased brain signal variability accompanies lower behavioral variability in development. *PLoS Comput Biol* 4:e1000106.

- 
- Oldfield R (1971) The assessment and analysis of handedness: The edinburgh inventory. *Neuropsychologia* 9:97–113.
- Paige GD (1994) Senescence of human visual-vestibular interactions: smooth pursuit, optokinetic, and vestibular control of eye movements with aging. *Experimental Brain Research* 98:355–372.
- Park DC, Polk TA, Mikels JA, Taylor SF, Marshuetz C (2001) Cerebral aging: integration of brain and behavioral models of cognitive function. *Dialogues in Clinical Neuroscience* 3:151–165 PMID: 22034448 PMCID: PMC3181659.
- Peiffer AM, Hugenschmidt CE, Maldjian JA, Casanova R, Srikanth R, Hayasaka S, Burdette JH, Kraft RA, Laurienti PJ (2009) Aging and the interaction of sensory cortical function and structure. *Human Brain Mapping* 30:228–240.
- Peiffer AM, Mozolic JL, Hugenschmidt CE, Laurienti PJ (2007) Age-related multisensory enhancement in a simple audiovisual detection task. *NeuroReport* 18:1077–1081.
- Peinemann A, Lehner C, Conrad B, Siebner HR (2001) Age-related decrease in paired-pulse intracortical inhibition in the human primary motor cortex. *Neuroscience letters* 313:33–36 PMID: 11684333.
- Probst T, Straube A, Bles W (1985) Differential effects of ambivalent visual-vestibular-somatosensory stimulation on the perception of self-motion. *Behavioural brain research* 16:71–79 PMID: 3875354.
- Raemaekers M, Vink M, van den Heuvel MP, Kahn RS, Ramsey NF (2006) Effects of aging on BOLD fMRI during prosaccades and antisaccades. *Journal of cognitive neuroscience* 18:594–603 PMID: 16768362.
- Raichle ME, Mintun MA (2006) Brain work and brain imaging. *Annual review of neuroscience* 29:449–476 PMID: 16776593.
- Rajah MN, D’Esposito M (2005) Region-specific changes in prefrontal function with age: a review of PET and fMRI studies on working and episodic memory. *Brain* 128:1964–1983.
- Rauch A, Rainer G, Logothetis NK (2008) The effect of a serotonin-induced dissociation between spiking and perisynaptic activity on BOLD functional MRI. *Proceedings of the National Academy of Sciences of the United States of America* 105:6759–6764 PMID: 18456837 PMCID: PMC2373337.

- Raz N, Gunning FM, Head D, Dupuis JH, McQuain J, Briggs SD, Loken WJ, Thornton AE, Acker JD (1997) Selective aging of the human cerebral cortex observed in vivo: differential vulnerability of the prefrontal gray matter. *Cerebral cortex (New York, N.Y.: 1991)* 7:268–282 PMID: 9143446.
- Reuter-lorenz PA, Jonides J, Smith EE, Hartley A, Miller A, Marshuetz C, Koeppe RA (2000) Age differences in the frontal lateralization of verbal and spatial working memory revealed by PET. *J. Cognitive Neuroscience* 12:174–187.
- Richter W, Richter M (2003) The shape of the fMRI BOLD response in children and adults changes systematically with age. *NeuroImage* 20:1122–1131.
- Samanez-Larkin GR, Kuhnen CM, Yoo DJ, Knutson B (2010) Variability in nucleus accumbens activity mediates age-related suboptimal financial risk taking. *The Journal of neuroscience* 30:1426–1434 PMID: 20107069.
- Schmidt S, Redecker C, Bruehl C, Witte OW (2010) Age-related decline of functional inhibition in rat cortex. *Neurobiology of aging* 31:504–511 PMID: 18486993.
- Simons B, Büttner U (1985) The influence of age on optokinetic nystagmus. *European Archives of Psychiatry and Neurological Sciences* 234:369–373.
- Snowden RJ, Kavanagh E (2006) Motion perception in the ageing visual system: Minimum motion, motion coherence, and speed discrimination thresholds. *Perception* 35:9–24.
- Stephan T, Deuschländer A, Nolte A, Schneider E, Wiesmann M, Brandt T, Dieterich M (2005) Functional MRI of galvanic vestibular stimulation with alternating currents at different frequencies. *NeuroImage* 26:721–732.
- Straube A, Paulus W, Probst T (1987) Influence of head or trunk oscillations on visually induced self-motion perception in humans. *Neuroscience Letters* 76:245–248.
- Taoka T, Iwasaki S, Uchida H, Fukusumi A, Nakagawa H, Kichikawa K, Takayama K, Yoshioka T, Takewa M, Ohishi H (1998) Age correlation of the time lag in signal change on EPI-fMRI. [Miscellaneous article]. *Journal of Computer Assisted Tomography July* 22:514–517.
- Voss MW, Erickson KI, Chaddock L, Prakash RS, Colcombe SJ, Morris KS, Doerksen S, Hu L, McAuley E, Kramer AF (2008) Dedifferentiation in the visual cortex: An fMRI investigation of individual differences in older adults. *Brain Research* 1244:121–131.

- Ward NS, Frackowiak RSJ (2003) Age-related changes in the neural correlates of motor performance. *Brain* 126:873–888.
- Woods RP (1996) Modeling for intergroup comparisons of imaging data. *NeuroImage* 4:S84–S94.
- Wutte MG, Smith MT, Flanagin VL, Wolbers T (2011) Physiological signal variability in hMT+ reflects performance on a direction discrimination task. *Frontiers in Psychology* 2 PMID: 21852978 PMCID: PMC3151615.
- Zwergal A, Linn J, Xiong G, Brandt T, Strupp M, Jahn K (2010) Aging of human supraspinal locomotor and postural control in fMRI. *Neurobiology of Aging* .



## Acknowledgements

I would like to express my sincere gratitude to those who helped me during the time of my doctoral studies and made this work possible.

I am extremely grateful to my first supervisor, Prof. Dr. Marianne Dieterich, for giving me the opportunity to conduct my research in her group and provided me with her continuous support, expertise and guidance throughout my studies. I would also like to express my gratitude to my second supervisor, Prof. Dr. Thomas Brandt, whose expertise, insightful suggestions and comments shaped the essence of this work. I was most fortunate to have my third supervisor, Dr. Thomas Stephan, without whom this work and my development as a researcher would not have been possible. I am deeply grateful for his constant support, patience, help and encouragement in all the steps of my study.

My sincere appreciation is extended to the Graduate School of Systemic Neuroscience and the Research training group 'Orientation and Motion in Space' for enabling me to conduct my studies and giving me the chance to learn from and be surrounded by inspiring people. I pay special gratitude to Catherine Botheroyd for her selfless support from the very beginning of my studies.

I would also like to thank all my colleagues from our neuroimaging group and the ones from the Forschungshaus for offering me a helping hand in times of need and most of all their friendship.

Last, but not least, my deepest gratitude goes to my family and Lukas Brostek. I cannot express sufficient gratitude to my mother, Prof. Dr. Margareta Balabanova-Stefanova and my sister, M.Sc. Nina Stefanova, for giving me 'roots to grow and wings to fly' in a most loving way. I wholeheartedly thank Lukas Brostek for all the scientific discussions that improved my work tremendously and for his support through thick and thin.



## Appendix

Table 1. Positive BOLD response (PBR), PBR latency to peak and PBR dispersion during stimulation in the OKN experiment

OKN						
PBR Amplitude						
Anatomical area	BA (Functional area)	MNI coordinates x, y, z	Cluster size	t-value	MNI coordinates x, y, z	Cluster size
Occipital pole	BA17/V1	15, -93, 3	<b>5952</b>	18.77	-15, -93, 3	<b>5952<sup>a</sup></b>
Intracalcarine cortex	BA17/V1	18, -78, 12	<b>5952<sup>a</sup></b>	14.12	-18, -78, 12	<b>5952<sup>a</sup></b>
Lingual gyrus	BA18/V2	9, -75, -3	<b>5952<sup>a</sup></b>	20.01	-3, -78, -3	<b>5952<sup>a</sup></b>
Occipital fusiform gyrus	V4/V3v	24, -69, -15	<b>5952<sup>a</sup></b>	16.09	-18, -72, -9	<b>5952<sup>a</sup></b>
Lateral occipital cortex, inferior division	V5 (hMT/V5)	45, -66, 3	<b>5952<sup>a</sup></b>	9.20	-42, -75, 0	<b>5952<sup>a</sup></b>
Superior parietal lobule	BA7a/hIP3(PEF)	27, -54, 51	<b>71</b>	4.31	-27, -54, 48	<b>111</b>
Precentral gyrus	BA6 (FEF)	30, -6, 48	<b>953</b>	6.12	-36, -9, 42	<b>953<sup>a</sup></b>
Precentral gyrus	BA6 (SEF)	6, 3, 57	<b>953<sup>a</sup></b>	3.69	-12, 0, 57	<b>953<sup>a</sup></b>
Frontal orbital cortex /Frontal pole		39, 24, -9	<b>83</b>	3.14	-45, 39, -12	<b>183</b>
Cingulate gyrus, posterior division		12, -18, 42	<b>35</b>	4.01	-9, -21, 42	<b>43</b>
Lateral geniculate body		24, -27, -3	<b>41</b>	5.44	-21, -27, -3	<b>28</b>
<b>PBR with shorter latency to peak</b>						
Occipital pole	BA17/V1	15, -93, 6	<b>5655</b>	7.51	-15, -93, 6	<b>5655<sup>a</sup></b>
Intracalcarine cortex	BA17/V1	18, -78, 12	<b>5655<sup>a</sup></b>	10.11	-18, -78, 12	<b>5655<sup>a</sup></b>
Lingual gyrus	BA18/V2	6, -78, -3	<b>5655<sup>a</sup></b>	13.67	-6, -75, 0	<b>5655<sup>a</sup></b>
Occipital fusiform gyrus	V4/V3v	24, -69, -15	<b>5655<sup>a</sup></b>	9.25	-18, -72, 9	<b>5655<sup>a</sup></b>
Lateral occipital cortex, inferior division	V5 (hMT/V5)	42, -66, 3	<b>5655<sup>a</sup></b>	8.88	-42, -72, 0	<b>5655<sup>a</sup></b>
Superior parietal lobule	BA7a/BA7PC (PEF)	27, -51, 51	<b>66</b>	4.23	-30, -48, 48	<b>106</b>
Precentral gyrus	BA6 (FEF)	30, -9, 45	<b>781</b>	6.52	-39, -12, 42	<b>781<sup>a</sup></b>
Precentral gyrus	BA6 (SEF)	6, 3, 54	<b>781<sup>a</sup></b>	4.32	-12, 0, 57	<b>781<sup>a</sup></b>
Cingulate gyrus, posterior division		12, -18, 42	<b>34</b>	4.14	-9, -21, 39	<b>43</b>
Lateral geniculate body		24, -27, -6	<b>28</b>	5.20	-21, -27, -3	<b>28</b>
<b>PBR with longer duration</b>						
Occipital pole	BA17/V1	9, -90, 3	<b>5230</b>	12.55	-9, -90, 3	<b>5230<sup>a</sup></b>
Intracalcarine cortex	BA17/V1	12, -72, 9	<b>5230<sup>a</sup></b>	15.43	-9, -78, 3	<b>5230<sup>a</sup></b>
Lingual gyrus	BA18/V2	9, -75, 3	<b>5230<sup>a</sup></b>	14.56	-9, -75, 3	<b>5230<sup>a</sup></b>
Occipital fusiform gyrus	V4/V3v	18, -72, 9	<b>5230<sup>a</sup></b>	9.26	-18, -72, 9	<b>5230<sup>a</sup></b>
Lateral occipital cortex, inferior division	V5 (hMT/V5)	42, -63, 3	<b>5230<sup>a</sup></b>	8.48	-45, -72, 3	<b>5230<sup>a</sup></b>
Precentral gyrus	BA4a/BA7a (FEF)	39, -9, 42	<b>942</b>	6.73	-36, -12, 45	<b>942<sup>a</sup></b>
Precentral gyrus	BA6 (SEF)	9, 0, 57	<b>942<sup>a</sup></b>	5.50	-3, 0, 57	<b>942<sup>a</sup></b>
Superior parietal lobule	BA7a/hIP3	27, -54, 51	<b>71</b>	6.87	-24, -54, 45	<b>111</b>
Cingulate gyrus, posterior division		12, -18, 39	<b>35</b>	5.63	-12, -24, 36	<b>43</b>
Lateral geniculate body		21, -27, -6	<b>33</b>	3.41		

p<0.05, FDR corrected, clusters  $\geq 20$ ; <sup>a</sup> part of a cluster





Table 4. Age-correlated change of PBR latency to peak and PBR duration during OKN.

Age-correlated increase of PBR latency to peak						
Anatomical area	BA (Functional area)	Right hemisphere			Left hemisphere	
		MNI coordinates x, y, z	Cluster size	t-value	MNI coordinates x, y, z	Cluster size t-value
Intracalcarine cortex	BA17/V1	9, -69, 9	1943	4.85	-18, -69, 6	1943 <sup>a</sup> 4.56
Lingual gyrus	BA18/V2	6, -78, 3	1943 <sup>a</sup>	5.39	-6, -78, 3	1943 <sup>a</sup> 4.03
Occipital fusiform gyrus	V3/V4	27, -78, -9	1943 <sup>a</sup>	3.1	-30, -81, -9	1943 <sup>a</sup> 3.68
Lateral occipital cortex, superior division		21, -84, 21	1943 <sup>a</sup>	2.86	-21, -84, 19	1943 <sup>a</sup> 2.43
Occipital pole	BA17/V1; BA18/V2	6, -93, 18	1943 <sup>a</sup>	3.21	-9, -93, 15	1943 <sup>a</sup> 2.51
Precentral gyrus	BA6 (FEF)				-36, -6, 42	16 3.43
Superior parietal lobule	hIP3/ 7PC (PEF)				-33, -45, 51	5 2.54
Lateral geniculate body		24, -27, -3	7	2.41	-24, -27, -9	16 3.05
Age-correlated decrease of PBR duration						
Intracalcarine cortex	BA17/V1	9, -75, 12	27	3.65	-15, -72, 6	141 5.15
Occipital pole	BA17/V1; BA 18/V2	0, -90, 6	141	3.56	-3, -90, 18	141 <sup>a</sup> 3.8
Lateral occipital cortex, superior division		18, -84, 21	5	3.41		

p<0.05, FDR corrected; <sup>a</sup> part of a cluster; clusters ≥ 5

Table 5. Negative BOLD response (NBR), NBR latency to peak and NBR dispersion during stimulation in the OKN experiment

OKN							
			NBR Amplitude				
			Right hemisphere		Left hemisphere		
Anatomical area	BA (Functional area)	MNI coordinates x, y, z	Cluster size	t-value	MNI coordinates x, y, z	Cluster size	t-value
Lateral occipital cortex, superior division		36, -72, 42	<b>18046</b>	9.64	-39, -75, 36	18046 <sup>a</sup>	7,26
Lateral occipital cortex, inferior division		54, -63, -9	18046a	2,90	-51, -63, 12	18046 <sup>a</sup>	2,24
Superior parietal lobule	5L	21, -45, 66	18046 <sup>a</sup>	7, 94	-21, -45, 63	18046 <sup>a</sup>	5,30
Inferior parietal lobule	Pgal/Pfm	57, -48, 21	18046 <sup>a</sup>	7,45	-63, -54, 24	18046 <sup>a</sup>	5,47
Inferior temporal gyrus, temporooccip. part		54, -48, -12	18046 <sup>a</sup>	8,30			
Optic radiation		45, -27, -15	18046 <sup>a</sup>	7,31	-36, -24, -9	18046 <sup>a</sup>	6,33
Superior temporal gyrus	H1, H2	54, -18, 9	18046 <sup>a</sup>	7,17	-54, -18, 9	18046 <sup>a</sup>	3,43
Insular cortex		39, -6, 9	18046 <sup>a</sup>	4,08	-39, -12, 9	18046 <sup>a</sup>	3,55
Postcentral gyrus	BA2	42, -36, 57	18046 <sup>a</sup>	5,85	-42, -36, 57	18046 <sup>a</sup>	3,97
Precuneus		15, -51, 21	18046 <sup>a</sup>	4,50	-15, -51, 21	18046 <sup>a</sup>	3,25
Cingulate gyrus, posterior division		6, -39, 36	18046 <sup>a</sup>	6,92	-6, -39, 30	18046 <sup>a</sup>	4,75
Cingulate gyrus, anterior division		3, 12, 30	18046 <sup>a</sup>	2,96	-3, 6, 30	18046 <sup>a</sup>	4,97
Middle temporal gyrus,temporooccip. part		60, -48, -3	18046 <sup>a</sup>	7,24	-60, -48, -6	18046 <sup>a</sup>	5,68
Temporal occipital fusiform cortex		30, -39, -12	18046 <sup>a</sup>	2,64	-30, -45, -9	18046 <sup>a</sup>	2,83
Middle frontal gyrus		30, 25, 42	18046 <sup>a</sup>	4, 36	-30, 24, 42	18046 <sup>a</sup>	2,13
Premotor cotex	BA6	3, 12, 63	<b>25</b>	2,20	-3, 9, 63	25 <sup>a</sup>	2,82
<b>NBR with longer latency to peak</b>							
Inferior parietal lobule		54, -45, 39	<b>5982</b>	9,64	-48, -51, 30	5982 <sup>a</sup>	6,47
Lateral occipital cortex, superior division		33, -72, 48	5982 <sup>a</sup>	8,42	-39, -69, 39	5982 <sup>a</sup>	6,73
Postcentral gyrus		21, -36, 63	5982 <sup>a</sup>	4,13	-36, -27, 54	5982 <sup>a</sup>	5,20
Superior parietal lobule	5L	12, -48, 60	5982a	2,68	-18, -42, 63	5982 <sup>a</sup>	2,80
Inferior temporal gyrus, temporooccip. part		54, -54, -12	5982 <sup>a</sup>	7,51	-51, -60, -9	5982 <sup>a</sup>	4,02
Superior temporal gyrus		48, -15, 3	5982 <sup>a</sup>	3,81	-60, -9, 0	5982 <sup>a</sup>	2,52
Insular cortex		39, -9, 3	5982 <sup>a</sup>	2,70	-39, -18, -3	5982 <sup>a</sup>	2,50
Precuneus		6, -54, 39	5982 <sup>a</sup>	3,52	-3, -54, 36	5982 <sup>a</sup>	2,44
Cingulate gyrus, posterior division		9, -39, 33	5982 <sup>a</sup>	4,63	-3, -39, 33	5982 <sup>a</sup>	2,49
Middle frontal gyrus		39, 15, 45	<b>449</b>	6,64	-27, 12, 48	<b>340</b>	4,74
Middle temporal gyrus,temporooccip. part		60, -45, -3	5982 <sup>a</sup>	8,23	-54, -48, -6	5982 <sup>a</sup>	4,14
<b>NBR with shorter latency to peak</b>							
Putamen		24, 12, 0	<b>50</b>	4,63	-24, 9, -3	<b>28</b>	3,83
<b>NBR with narrower dispersion</b>							
Inferior parietal lobule		54, -51, 42	<b>350</b>	5,76	-42, -72, 39	<b>486</b>	5,22
Precuneus		15, -54, 21	<b>141</b>	3,65	-15, -51, 21	141 <sup>a</sup>	3,59
Cingulate gyrus, posterior division		12, -51, 30	141 <sup>a</sup>	2,84	-6, -54, 30	141 <sup>a</sup>	3,21
Middle frontal gyrus		39, 18, 45	<b>134</b>	4,14	-27, 21, 48	<b>105</b>	4,65
<b>NBR with wider dispersion</b>							
Putamen		24, 12, 0	<b>2</b>	5,35	-21, 6, -6	<b>18</b>	5,76

p<0.05, FDR corrected; <sup>a</sup> part of a cluster

Table 6. Negative BOLD response (NBR), NBR latency to peak and NBR dispersion during stimulation in the checkerboard experiment

<b>CHECKERBOARD</b>									
<b>NBR Amplitude</b>									
<b>Anatomical area</b>	<b>BA (Functional area)</b>	<b>Right hemisphere</b>				<b>Left hemisphere</b>			
		<b>MNI coordinates x, y, z</b>	<b>Cluster size</b>	<b>t-value</b>	<b>t-value</b>	<b>MNI coordinates x, y, z</b>	<b>Cluster size</b>	<b>t-value</b>	<b>t-value</b>
Callosal body, posterior division		3, -30, 12	139	7,12		-3, -27, 12	139 <sup>a</sup>	5,02	
Callosal body, anterior division		24, 36, 0	12	4,86		-15, 33, -9	12	3,97	
Thalamus		3, -6, 6	33	4,37					
Superior parietal lobe									
Precuneus		6, -57, 63	5	4,06		-9, -69, 54	17	4,28	
						-3, -48, 63	1	3,66	
<b>NBR with narrower dispersion</b>									
Callosal body, anterior division		24, 36, 0	5	4,07					

p<0.05, FDR corrected; <sup>a</sup> part of a cluster

Table 7. Negative BOLD response (NBR), NBR latency to peak and NBR dispersion during stimulation in the finger-tapping

FINGER-TAPPING							
NBR Amplitude							
Anatomical area	BA (Functional area)	Right hemisphere			Left hemisphere		
		MNI coordinates x, y, z	Cluster size	t-value	MNI coordinates x, y, z	Cluster size	
						t-value	
Frontal pole		9, 63, 6	<b>2659</b>	5,54	-3, 60, 6	2659 <sup>a</sup>	5,97
Cingulate girus, anterior division		9, 42, 6	2659 <sup>a</sup>	3,42	-6, 42, 3	2659 <sup>a</sup>	4,90
Superior frontal gyrus		24, 27, 42	2659 <sup>a</sup>	5,26	-18, 36, 42	2659 <sup>a</sup>	6,07
Middle frontal gyrus		30, 21, 54	2659 <sup>a</sup>	3,06	-30, 9, 57	2659 <sup>a</sup>	3,38
Precuneus		3, -54, 27	<b>2262</b>	6,76	-3, -60, 48	2262 <sup>a</sup>	6,76
Postcentral gyrus	BA3b	42, -24, 57	2262 <sup>a</sup>	6,13			
Precentral gyrus	BA6	36, -18, 57	2262 <sup>a</sup>	3,81			
Lateral occipital cortex, superior division		15, -96, 18	<b>392</b>	5,13	-51, -72, 27	<b>558</b>	5,78
Occipital pole	V2/BA18	6, -90, -3	392 <sup>a</sup>	3,11			
Occipital pole	V1/BA17						
Lingual gyrus	V2/BA18				-9, -81, -6	392 <sup>a</sup>	2,69
Hippocampus cornu ammonis		27, -33, -9	<b>69</b>	4,85			
Inferior parietal lobule		54, -57, 24	<b>195</b>	4,76			
Central opercular cortex	PGp	42, -15, 18	<b>40</b>	3,76			
Middle temporal gyrus					-60, -15, -15	<b>42</b>	3,56
Occipital fusiform gyrus	V2/BA18				-12, -90, -15	<b>34</b>	2,79
Frontal orbital cortex					-42, 30, -15	<b>38</b>	3,21
<b>NBR with longer latency to peak</b>							
Postcentral gyrus	BA4p	39, -24, 54	<b>39</b>	4,37			
Occipital pole	V1/BA17	6, -90, -3	<b>35</b>	4,35			
Occipital fusiform gyrus					-12, -90, -15	<b>17</b>	4,31

p<0.05, FDR corrected; <sup>a</sup> part of a cluster

Table 8. Differences between temporal variability of BOLD signal during blocks of stimulation and during blocks of rest in OKN experiment

Differences between SD_stimulation and SD_rest in OKN experiment						
SD_rest - SD_stim						
Anatomical area	BA (Functional area)	Right hemisphere			Left hemisphere	
		MNI coordinates x, y, z	Cluster size	t-value	MNI coordinates x, y, z	Cluster size t-value
Inferior frontal gyrus, pars opercularis	BA44	54, 12, 27	11078	4,57	-48, 15, 21	11078 <sup>a</sup> 5,75
Insular cortex		36, 18, -6	11078 <sup>a</sup>	5,38	-42, 12, -9	11078 <sup>a</sup> 2,62
Middle frontal gyrus		36, 6, 51	11078 <sup>a</sup>	4,80	-36, 6, 51	11078 <sup>a</sup> 3,54
Anterior intraparietal sulcus	hIP1/3	33, -51, 42	11078 <sup>a</sup>	2,48	-33, -42, 36	11078 <sup>a</sup> 4,76
Lateral occipital cortex, superior division	A	30, -84, 18	<b>635</b>	2,53	-18, -87, 18	11078 <sup>a</sup> 3,72
Superior temporal gyrus	H1 H2	54, -21, 12	11078 <sup>a</sup>	3,40	-51, -21, 12	11078 <sup>a</sup> 4,60
Lingual gyrus	A	21, -48, -6	11078 <sup>a</sup>	2,48	-21, -48, -12	11078 <sup>a</sup> 4,59
Inferior temporal gyrus,temporooccip. part	D	51, -54, -12	<b>132</b>	4,47	-45, -60, -12	11078 <sup>a</sup> 4,54
Frontal pole		30, 51, 30	11078 <sup>a</sup>	4,45	-18, 48, 33	11078 <sup>a</sup> 2,37
Postcentral gyrus	D	45, -21, 51	11078 <sup>a</sup>	2,54	-57, -18, 39	11078 <sup>a</sup> 4,34
Inferior parietal lobule	D	45, -51, 54	635 <sup>a</sup>	3,86	-45, -51, 51	9 5,58
Occipital pole	A	21, -96, 12	635 <sup>a</sup>	3,74	-21, -96, 12	11078 <sup>a</sup> 2,80
Superior parietal lobule	D	15, -72, 54	635 <sup>a</sup>	2,97	-15, -72, 54	1 2,55
Lateral occipital cortex, inferior division	A	45, -75, -12	132 <sup>a</sup>	3,01	-42, -75, -9	11078 <sup>a</sup> 2,70
Occipital fusioform gyrus	V4	27, -66, -12	132 <sup>a</sup>	2,96	-27, -66, -12	11078 <sup>a</sup> 3,22
Precentral gyrus	BA6	12, -21, 69	<b>36 a</b>	3,61	-12, -21, 66	11078 <sup>a</sup> 2,79
Precentral gyrus	BA6	45, 3, 45	11078 <sup>a</sup>	4,88	-33, -3, 48	11078 <sup>a</sup> 2,98
Temporal pole	D	51, 12, -12	11078 <sup>a</sup>	2,76	-45, 21, -21	<b>85</b> 3,15
Frontal orbital cortex	A	36, 24, -12	11078 <sup>a</sup>	2,70	-36, 18, -18	85 <sup>a</sup> 2,80
Thalamus	D	12, -24, 0	<b>17</b>	3,11	-18, -21, 6	11078 <sup>a</sup> 2,58
Cingulate gyrus, posterior division	D	3, -24, 45	11078 <sup>a</sup>	3,36	-3, -24, 45	11078 <sup>a</sup> 3,82
Cerebellum	D	36, -72, -36	<b>1</b>	2,45	-36, -66, -36	11078 <sup>a</sup> -3,15
Cerebellar hemisphere	D				-24, -51, -24	11078 <sup>a</sup> 2,59

p<0.05, FDR corrected; A = Activated area (PBR), D = Deactivated area (NBR); <sup>a</sup> part of a cluster

Table 9. Differences in temporal variability of BOLD signal during stimulation or rest between three age groups in OKN experiment

Differences in SD_stimulation between groups in OKN experiment						
Anatomical area	BA (Functional area)		Right hemisphere		Left hemisphere	
	SD_Group 2 - SD_Group 1	MNI coordinates x, y, z	Cluster size	t-value	MNI coordinates x, y, z	t-value
Cerebellum, crus I	A	-15, -84, -24	38	4.33		
Cingulate gyrus, posterior division	A	-9, -21, 42	52	4.39		
Cingulate gyrus, anterior division	D*	-6, -6, 39				
<b>SD_Group 3 - SD_Group 1 (p&lt;0.05, FDR)</b>						
Planum polare	D	54, 0, -3	19	4.48		
Insular cortex	D	42, -12, -3	14	3.94		
Superior temporal gyrus, posterior division	D					
Superior temporal gyrus	D*	H1 H2	24	4.72		
Superior frontal gyrus	D	BA6	30	3.65		
Temporal pole	D		21	3.95		
Postcentral gyrus	D	BA2	8	4.39		
Thalamus	D		2	4.29		
Central opercular cortex	D		1	4.11		
Precentral gyrus	D		1	4.09		
Precuneus	D		2	4.04		
Optic radiation	D		34	4.78		
<b>SD_Group 3 - SD_Group 2 (uncorrected p&lt;0.001 k=5)</b>						
Superior frontal gyrus	BA6	-18, -6, 63	14	3.81		
<b>Differences in SD_rest between groups in OKN experiment</b>						
Anatomical area	BA (Functional area)		Right hemisphere		Left hemisphere	
	SD_Group 2 - SD_Group 1	MNI coordinates x, y, z	Cluster size	t-value	MNI coordinates x, y, z	t-value
Insular cortex	D	36, -15, 3	12	3.46		
Cingulate gyrus, posterior division	A					
Cerebellum	A	Crus I				
<b>SD_Group 3 - SD_Group 1 (p&lt;0.05, FDR)</b>						
Planum polare	D	45, -9, -3	28	5.11		
Superior frontal gyrus	A	BA6	40	4.96		
Superior temporal gyrus, posterior division	D		26	4.56		
Postcentral gyrus	D	BA2	27	4.50		
Central opercular cortex	D		8	4.46		
Temporal pole	D		3	4.10		
Insular cortex	D	42, -12, -3	28	4.31		
Thalamus	D	12, -30, 3 *				
Precentral gyrus	D		2	4.21		
Precuneus	D		3	4.01		
Optic radiation	D		31	3.85		
<b>SD_Group 3 - SD_Group 2 (uncorrected p&lt;0.001 k=5)</b>						
Superior frontal gyrus	BA6	-18, -6, 63	16	3.78		
Planum polare	D		17	4.00		
Optic radiation	D		12	3.42		

A = Activated area (PBR), D = Deactivated area (NBR); \* occurring only in ROI analysis using TAP PBR (A) or TAP NBR (D) contrast,<sup>a</sup> part of a cluster

Table 10. Differences in temporal variability of BOLD signal during stimulation between three age groups in checkerboard experiment

Differences in SD_stimulation between groups in checkerboard experiment							
Anatomical area	BA (Functional area)	Right hemisphere			Left hemisphere		
		MNI coordinates x, y, z	Cluster size	t-value	MNI coordinates x, y, z	Cluster size	t-value
	<b>SD_Group 1 - SD_Group 3 ( uncorrected p&lt;0.001 k=5)</b>						
Middle frontal gyrus	A				-27, 27, 48	26	3,51
Frontal pole	A	30, 45, 36	12	3,34	-15, 48, 39	65	3,95
Superior frontal gyrus	A				-3, 48, 45	65 <sup>a</sup>	3,90
Paracingulate gyrus	A	0, 48, -3	16	4,09	-3, 42, -9	16 <sup>a</sup>	3,44
Precuneus					-6, -54, 9	10	3,89
Cingulate gyrus, posterior division					-3, -30, 39	15	3,87
Cingulate gyrus, anterior division					-3, 21, 24	14	3,75
Superior parietal lobule		18, -54, 57	7	3,65			
	<b>SD_Group 1 - SD_Group 2 ( uncorrected p&lt;0.001 k=5)</b>						
Superior frontal gyrus	A <sup>o</sup>	3, 54, 27	24	4,65	-3, 54, 27	24 <sup>a</sup>	3,32
Superior parietal lobule		12, -57, 57	26	4,72	-24, -57, 51	5	3,58
Inferior temporal gyrus,temporooccip. part	A <sup>o</sup>	48, -54, -9	28	4,17			
Lateral occipital cortex, inferior division	A	42, -69, -6	28 <sup>a</sup>	3,80			
Occipital fusiform gyrus	A	21, -72, -9	5	3,68			
Putamen		24, 9, 0	5	3,65			
	<b>SD_Group 2 - SD_Group 3 ( uncorrected p&lt;0.001 k=5)</b>						
Superior frontal gyrus	A*				-6, 54, 33	5	3,51
	<b>SD_Group 2 - SD_Group 1 ( uncorrected p&lt;0.001 k=5)</b>						
Superior temporal gyrus,posterior division		69, -33, 9	5	3,86			
	<b>SD_Group 3 - SD_Group 1 (p&lt; 0.05, FDR)</b>						
Insular cortex	AI	42, -6, -3	280	5,77	-42, -6, -6	267	7,43
Temporal pole		48, 9, -18	280 <sup>a</sup>	4,55	-39, 9, -21	267 <sup>a</sup>	4,71
Hippocampus	Ar	27, -27, -12	45	5,57	-24, -24, -21	7	4,48
Thalamus	A	15, -33, 3	14	4,61	-12, -18, 0	70	3,41
Brain stem		0, -27, -15	17	4,26	-6, -27, -15	17 <sup>a</sup>	3,60
Cerebellum	IX				-6, -54, -39		
Parietal operculum	OP1	9, -54, -9	11	4,04	-57, -24, 15	3	3,41
Cerebellum	V	63, -45, 27	2	3,94			
Inferior parietal lobule	Pfm	69, -30, 9	3	3,83	-63, -21, -6	1	3,71
Superior temporal gyrus, posterior division		36, -30, -18	45 <sup>a</sup>	3,41	-33, -39, -21	2	3,41
Temporal fusiform complex,posterior division							
	<b>SD_Group 3 - SD_Group 2 (p&lt;0.05, FDR)</b>						
Insular cortex		42, -9, -3	69	4,83	-39, 0, -15	9	5,14
Planum polare		51, 0, -6	69 <sup>a</sup>	4,22			
Hippocampus	A*	27, 27, -12					

A = Activated area (PBR), D = Deactivated area (NBR), r - right, l - left; ° significant in ROI analysis using TAP PBR (A) or TAP NBR (D) contrast; \* occurring only in ROI analysis using TAP PBR

Table 11. Differences in temporal variability of BOLD signal during rest between three age groups in checkerboard experiment

Differences in SD_rest between groups in checkerboard experiment						
Anatomical area	BA (Functional area)		Right hemisphere		Left hemisphere	
	SD young group	SD older group	MNI coordinates x, y, z	Cluster size	t-value	Cluster size
Occipital pole	BA18/V2	12, -90, 24	-9, -96, 21	8	3.55	53
Precentral gyrus	BA44		-54, 6, 21			34
Middle frontal gyrus			-27, 24, 45	6	3.47	34
Frontal pole		24, 42, 39	-15, 45, 42			81
Superior frontal gyrus			-6, 51, 30	8	4.24	81 <sup>a</sup>
Lateral occipital cortex, inferior division		24, 6, 0	-45, -72, 3	41	4.10	21
Putamen		3, 48, -3	-3, 45, -3	8	3.77	41 <sup>a</sup>
Paracingulate gyrus		18, -54, 57	-9, -54, 45	5	4.05	11
Superior parietal lobule		36, 21, 3	-18, -63, 6			10
Precuneus	BA17/V1					
Insular cortex						
Intracalcarine cortex						
<b>SD young group - SD middle group ( uncorrected p&lt;0.001 k=5)</b>						
Occipital pole		12, -87, 27	-9, -90, 21	96	3.80	96 <sup>a</sup>
Middle frontal gyrus			-24, 27, 45	65	4.54	32
Lateral occipital cortex, inferior division		51, -60, -6	-42, -66, -12	10	4.28	8
Precentral gyrus		54, 9, 30	-54, 3, 18	29	3.38	21
Insular cortex		36, 18, 3		29	3.54	
Precuneus		9, -57, 60		17	3.99	8
Superior parietal lobule		21, -54, 57	-27, -57, 54	10	3.95	32
Lingual gyrus	BA17/V1		-3, -75, 3	5	3.65	8
Temporal occipital fusiform complex			-39, -60, -12			14
Occipital fusiform gyrus		21, -72, -9	-21, -75, -9			
Inferior frontal gyrus, pars opercularis	BA44	48, 12, 12		65 <sup>a</sup>	3.66	
Putamen		24, 15, 0				5
Superior frontal gyrus		51, -60, 0				
Middle temporal gyrus		3, 60, 27 A				
Frontal pole						
<b>SD middle group - SD older group ( uncorrected p&lt;0.001 k=5)</b>						
Superior frontal gyrus	A		-6, 51, 33	11		11
Paracingulate gyrus	A		-3, 51, 9	16		16
<b>SD middle group - SD younger group ( uncorrected p&lt;0.001 k=5)</b>						
Temporal pole /planum polare		3, -39, -36	-36, 9, -30	5	3.31	6
Brain stem						
<b>SD older group - SD younger group (FDR)</b>						
Insular cortex		42, -3, -12	-39, -3, -12	114	4.56	92
Temporal pole /planum polare		45, 6, -15	-33, 9, -27	114 <sup>a</sup>	4.07	92 <sup>a</sup>
Hippocampus		24, -24, -18	-21, -24, -21	25	4.66	2
Thalamus	A*	6, -6, -3 A*	-3, -3, 0	20	4.73	20 <sup>a</sup>
Cerebellum	IX	6, -51, -36	-9, -51, -39	13	3.85	13 <sup>a</sup>
Cerebellum	I-IV	6, -54, -9		4	3.95	
<b>SD older group - SD middle group (FDR)</b>						
Insular cortex		42, -12, 0	-42, -6, -9	14	4.69	2

A = Activation (PBR), B = Deactivation (NBR), r - right, l - left; ° significant in ROI analysis using TAP PBR (A) or TAP NBR (D) contrast; \* occurring only in ROI analysis using TAP PBR (A) or TAP NBR (D) contrast; <sup>a</sup> part of a cluster

Table 12. . Differences in temporal variability of BOLD signal during stimulation between three age groups in finger-tapping experiment

Differences in SD_stimulation between groups in finger-tapping experiment							
Anatomical area	BA (Functional area)	Right hemisphere			Left hemisphere		
		MNI coordinates x, y, z	Cluster size	t-value	MNI coordinates x, y, z	Cluster size	t-value
Superior frontal gyrus	D°				-3, -39, 42	136	5,12
Middle frontal gyrus	D°				-30, 30, 45	57	4,12
Precentral gyrus	D°			30	4,46		
Intracalcarine cortex	D°				-18, -63, 6	7	3,43
SD_Group 1 - SD_Group 2 ( uncorrected p<0.001 k=5)							
Precentral gyrus				12	4,71		
Superior frontal gyrus					-3, -39, 42	27	4,43
Occipital pole					3, -93, 21	5	3,79
Superior parietal lobule	7PC			10	3,49		
Middle frontal gyrus					-27, 24, 45	19	3,49
SD_Group 2 - SD_Group 3 ( uncorrected p<0.001 k=5)							
Paracingulate gyrus	D				-3, -54, 12	32	4,56
Frontal pole	D				-6, 60, 18	32 <sup>a</sup>	4,18
Precuneus	D			16	4,20	11	4,20
SD_Group 2 - SD_Group 1 ( uncorrected p<0.001 k=5)							
Cerebellum	A	I - IV		20	4,56	6	3,55
Central opercular cortex	OP4				-60, -9, 12		
SD_Group 3 - SD_Group 1 (p<0.05, FDR)							
Planum polare	A			368	4,97	391	5,07
Insular cortex	A			368 <sup>a</sup>	3,84	391 <sup>a</sup>	3,28
Temporal pole	A			368 <sup>a</sup>	5,50	391a	3,59
Amygdala					-24, -3, -21	391 <sup>a</sup>	5,83
Frontal orbital cortex					-36, 21, -24	391a	4,26
Precentral gyrus	A			13	3,41	391 <sup>a</sup>	3,82
Superior temporal gyrus, anterior division				368 <sup>a</sup>	4,02	391 <sup>a</sup>	3,41
Superior temporal gyrus, posterior division				27	4,23		
Thalamus				155	5,61	155a	3,72
Cerebellum	A	I - IV /VI		234	5,50	234 <sup>a</sup>	4,67
Cerebellum		Crus II		2	4,05	3	3,93
Middle temporal gyrus, posterior division					-66, -27, -3	17	4,77
Angular gyrus				9	4,58		
Hippocampus				30	3,82	5	3,53
Brain stem					-27, -21, -15	3	3,81
Postcentral gyrus				15	3,48		
Inferior parietal lobule	A			9	3,67		
Superior frontal gyrus	A				-15, 0, 63	4	3,48
Central opercular cortex	A				-63, -12, 12	4	3,44
SD_Group 3 - SD_Group 2 (p<0.05, FDR)							
Insular cortex	AI			120	5,39	26	4,03
Temporal pole /planum polare	AI			120 <sup>a</sup>	4,14	26 <sup>a</sup>	5,47
Lateral occipital cortex, inferior division	A			10	3,95		
Hippocampus	D			11	4,56		
Cerebellum	A	I - IV		3	4,28		
Juxtapositional lobule	A*	BA6			3, 0, 57		

A = Activated are (PBR), D = Deactivated area (NBR), r - right, l - left, ° significant in ROI analysis using TAP PBR (A) or TAP NBR (D) contrast; \* occurring only in ROI analysis using TAP PBR (A) or TAP NBR (D) contrast; <sup>a</sup> part of a cluster

Table 13. Differences in temporal variability of BOLD signal during rest between three age groups in finger-tapping experiment

Differences in SD_rest between groups in finger-tapping experiment							
Anatomical area	BA (Functional area)	Right hemisphere			Left hemisphere		
		MNI coordinates x, y, z	Cluster size	t-value	MNI coordinates x, y, z	Cluster size	t-value
		<b>SD_Group 3 ( uncorrected p&lt;0.001 k=5)</b>					
Paracingulate gyrus	DI	3, 18, 48	6	4.04	-3, 48, 24	33	4.21
Cingulate gyrus, anterior division	A	9, 12, 39	26	4.12	-3, 9, 39	26	3.75
Middle frontal gyrus	D				-27, 30, 45	18	3.97
Precuneus	D				-18, -60, 6	11	3.77
		<b>SD_Group 1 - SD_Group 2 ( uncorrected p&lt;0.001 k=5)</b>					
Precuneus	D				-15, -6, 9	6	3.89
		<b>SD_Group 2 - SD_Group 3 ( uncorrected p&lt;0.001 k=5)</b>					
Paracingulate gyrus	D°	3, 54, 12	91	3.70	-3, 54, 15	91 <sup>a</sup>	4.86
Frontal pole	D°				-18, 60, 18	91 <sup>a</sup>	4.74
Precuneus	D°				-6, -60, 18	9	3.85
		<b>SD_Group 2 - SD_Group 1 ( uncorrected p&lt;0.001 k=5)</b>					
Cerebellum	Crus II				-9, -81, -39	20	3.93
Cerebellum	A	6, -57, -15	9	3.68			
Temporal pole	V				-42, 15, -27	21	3.90
Vermis	X	0, -51, -33	6	3.86			
		<b>SD_Group 3 - SD_Group 1 (p&lt;0.05, FDR)</b>					
Planum polare	A	45, -9, -3	374	7.09	-45, -9, -3	238	6.12
Superior temporal gyrus, posterior division	A	63, -18, 3	374 <sup>a</sup>	4.91			
Insular cortex	A	45, -3, 0	374 <sup>a</sup>	3.86	-42, -6, -6	238 <sup>a</sup>	6.06
Temporal pole	AI	45, 12, -18	374a	3.88	-36, 21, -24	238 <sup>a</sup>	4.47
Middle temporal gyrus, posterior division					-63, -27, -6	11	4.19
Thalamus		12, -27, 6	313	4.97	-3, -9, 3	313 <sup>a</sup>	3.51
Cerebellum	A	3, -57, -9	313 <sup>a</sup>	3.90	-3, -57, -9	313 <sup>a</sup>	4.54
Cerebellum	A	6, -48, -12	313 <sup>a</sup>	4.46	-3, -48, -9	313 <sup>a</sup>	3.31
Vermis	IX	3, -57, -39	61	3.99			
Cerebellum	AI	9, -81, -39	4	3.99	-3, -81, -33	6	4.05
Cerebellum	Crus I	30, -69, -30	6	3.60			
Hippocampus		18, -33, -6	313 <sup>a</sup>	3.86	-15, -36, -6	1	3.22
Amygdala					-24, -3, -21	36	5.19
Intracalcarine cortex	BA17/N2	24, -63, 3	93	3.49			
Precuneus		3, -54, 66	18	4.24			
Occipital pole	BA18/V2	30, -96, -9	14	3.39			
Brain stem							
Precentral gyrus	AI				-9, -42, -45	61	4.04
Inferior parietal lobule	BA6				-30, -15, 60		
		<b>SD_Group 3 - SD_Group 2 (p&lt;0.05, FDR)</b>					
Planum polare	AI	45, -9, -3	66	5.88	-45, -9, -3	2	4.30
Insular cortex		42, -12, 0	66 <sup>a</sup>	5.18			
Lateral occipital cortex, inferior division	A	45, -66, 0	21	5.46			
Precuneus		6, -54, 66	1	4.26			
Superior frontal gyrus	A				-15, 0, 63	2	4.26
Temporal fusiform complex, posterior division					-36, -30, -18	1	4.15

A = Activated area (PBR), D = Deactivated area (NBR), r -right, l -left; ° significant in ROI analysis using TAP PBR (A) or TAP NBR (D) contrast; \* occurring only in ROI analysis using TAP PBR (A) or TAP NBR (D) contrast; <sup>a</sup> part of a cluster

## Eidesstattliche Versicherung/Affidavit

Hiermit versichere ich an Eides statt, dass ich die vorliegende Dissertation "Age-related changes of the cortical visual-vestibular interaction in healthy subjects" selbstständig angefertigt habe, mich außer der angegebenen keiner weiteren Hilfsmittel bedient und alle Erkenntnisse, die aus dem Schrifttum ganz oder annähernd übernommen sind, als solche kenntlich gemacht und nach ihrer Herkunft unter Bezeichnung der Fundstelle einzeln nachgewiesen habe.

I hereby confirm that the dissertation "Age-related changes of the cortical visual-vestibular interaction in healthy subjects" is the result of my own work and that I have only used sources or materials listed and specified in the dissertation.

Munich, 07.11.2012

Iskra Stefanova

Prof. Dr. Marianne Dieterich conceived of the study. Prof. Dr. Marianne Dieterich, Dr. Thomas Stephan and Iskra Stefanova designed the paradigm. Iskra Stefanova coordinated the study, performed the data acquisition, performed the data analysis and wrote the manuscript. Dr. Thomas Stephan programmed the computer animated visual stimulation and the algorithm for estimation of the temporal variability of the BOLD signal. Dipl- phys. Thomas Dera and Dr. Thomas Stephan programmed the algorithm for the analysis of the VOG data. Dr. Thomas Eggert and Dr. Virginia Flanagan helped with additional statistical analysis (Likelihood ratio test and orthogonalization of vectors). Prof. Dr. Thomas Brandt and Dr. Sandra Becker-Bense were highly helpful in discussing the PBR results.

I hereby confirm the above mentioned contributions to the dissertation "Age-related changes of the cortical visual-vestibular interaction in healthy subjects".

Munich, 07.11.2012

Prof. Dr. Marianne Dieterich

## **Copy-right declaration**

Copyright permission was not required for the use of Figure 1.1 (Krauzlis R.J 2004. *Recasting the smooth pursuit eye movement system*. Journal of Neurophysiology. 91: 591-603) in this doctoral dissertation, as declared by The American Physiological Society.

Copyright permission for the use of Figure 1.2 and 1.3 (Dieterich et al. 2003. *fMRI signal increases and decreases in cortical areas during small-field optokinetic stimulation and central fixation*. Experimental Brain Research 148: 117-127) in this doctoral dissertation was granted by Springer.

Copyright permission for the use of Figure 1.4 (Harris et al. 2011. *The physiology of developmental changes in BOLD functional imaging studies*. Developmental Cognitive Neuroscience 1: 199-216) in this doctoral dissertation was granted by Elsevier.

**ELSEVIER LICENSE  
TERMS AND CONDITIONS**

Nov 05, 2012

---

---

This is a License Agreement between Iskra Stefanova ("You") and Elsevier ("Elsevier") provided by Copyright Clearance Center ("CCC"). The license consists of your order details, the terms and conditions provided by Elsevier, and the payment terms and conditions.

**All payments must be made in full to CCC. For payment instructions, please see information listed at the bottom of this form.**

Supplier	Elsevier Limited The Boulevard, Langford Lane Kidlington, Oxford, OX5 1GB, UK
Registered Company Number	1982084
Customer name	Iskra Stefanova
Customer address	Marchioninistrasse 23 München, 81377
License number	3018320884967
License date	Oct 29, 2012
Licensed content publisher	Elsevier
Licensed content publication	Developmental Cognitive Neuroscience
Licensed content title	The physiology of developmental changes in BOLD functional imaging signals
Licensed content author	Julia J. Harris, Clare Reynell, David Attwell
Licensed content date	July 2011
Licensed content volume number	1
Licensed content issue number	3
Number of pages	18
Start Page	199
End Page	216
Type of Use	reuse in a thesis/dissertation
Intended publisher of new work	other
Portion	figures/tables/illustrations
Number of figures/tables /illustrations	1
Format	both print and electronic
Are you the author of this Elsevier article?	No
Will you be translating?	No
Order reference number	
Title of your thesis/dissertation	Age-related changes of the cortical visual-vestibular interaction in healthy subjects
Expected completion date	Jan 2013

Estimated size (number of pages)	100
Elsevier VAT number	GB 494 6272 12
Permissions price	0.00 EUR
VAT/Local Sales Tax	0.0 USD / 0.0 GBP
Total	0.00 EUR
<a href="#">Terms and Conditions</a>	

## INTRODUCTION

1. The publisher for this copyrighted material is Elsevier. By clicking "accept" in connection with completing this licensing transaction, you agree that the following terms and conditions apply to this transaction (along with the Billing and Payment terms and conditions established by Copyright Clearance Center, Inc. ("CCC"), at the time that you opened your Rightslink account and that are available at any time at <http://myaccount.copyright.com>).

## GENERAL TERMS

2. Elsevier hereby grants you permission to reproduce the aforementioned material subject to the terms and conditions indicated.

3. Acknowledgement: If any part of the material to be used (for example, figures) has appeared in our publication with credit or acknowledgement to another source, permission must also be sought from that source. If such permission is not obtained then that material may not be included in your publication/copies. Suitable acknowledgement to the source must be made, either as a footnote or in a reference list at the end of your publication, as follows:

“Reprinted from Publication title, Vol /edition number, Author(s), Title of article / title of chapter, Pages No., Copyright (Year), with permission from Elsevier [OR APPLICABLE SOCIETY COPYRIGHT OWNER].” Also Lancet special credit - “Reprinted from The Lancet, Vol. number, Author(s), Title of article, Pages No., Copyright (Year), with permission from Elsevier.”

4. Reproduction of this material is confined to the purpose and/or media for which permission is hereby given.

5. Altering/Modifying Material: Not Permitted. However figures and illustrations may be altered/adapted minimally to serve your work. Any other abbreviations, additions, deletions and/or any other alterations shall be made only with prior written authorization of Elsevier Ltd. (Please contact Elsevier at [permissions@elsevier.com](mailto:permissions@elsevier.com))

6. If the permission fee for the requested use of our material is waived in this instance, please be advised that your future requests for Elsevier materials may attract a fee.

7. Reservation of Rights: Publisher reserves all rights not specifically granted in the combination of (i) the license details provided by you and accepted in the course of this licensing transaction, (ii) these terms and conditions and (iii) CCC's Billing and Payment terms and conditions.

8. License Contingent Upon Payment: While you may exercise the rights licensed immediately upon issuance of the license at the end of the licensing process for the transaction, provided that you have disclosed complete and accurate details of your proposed use, no license is finally effective unless and until full payment is received from

you (either by publisher or by CCC) as provided in CCC's Billing and Payment terms and conditions. If full payment is not received on a timely basis, then any license preliminarily granted shall be deemed automatically revoked and shall be void as if never granted. Further, in the event that you breach any of these terms and conditions or any of CCC's Billing and Payment terms and conditions, the license is automatically revoked and shall be void as if never granted. Use of materials as described in a revoked license, as well as any use of the materials beyond the scope of an unrevoked license, may constitute copyright infringement and publisher reserves the right to take any and all action to protect its copyright in the materials.

9. **Warranties:** Publisher makes no representations or warranties with respect to the licensed material.

10. **Indemnity:** You hereby indemnify and agree to hold harmless publisher and CCC, and their respective officers, directors, employees and agents, from and against any and all claims arising out of your use of the licensed material other than as specifically authorized pursuant to this license.

11. **No Transfer of License:** This license is personal to you and may not be sublicensed, assigned, or transferred by you to any other person without publisher's written permission.

12. **No Amendment Except in Writing:** This license may not be amended except in a writing signed by both parties (or, in the case of publisher, by CCC on publisher's behalf).

13. **Objection to Contrary Terms:** Publisher hereby objects to any terms contained in any purchase order, acknowledgment, check endorsement or other writing prepared by you, which terms are inconsistent with these terms and conditions or CCC's Billing and Payment terms and conditions. These terms and conditions, together with CCC's Billing and Payment terms and conditions (which are incorporated herein), comprise the entire agreement between you and publisher (and CCC) concerning this licensing transaction. In the event of any conflict between your obligations established by these terms and conditions and those established by CCC's Billing and Payment terms and conditions, these terms and conditions shall control.

14. **Revocation:** Elsevier or Copyright Clearance Center may deny the permissions described in this License at their sole discretion, for any reason or no reason, with a full refund payable to you. Notice of such denial will be made using the contact information provided by you. Failure to receive such notice will not alter or invalidate the denial. In no event will Elsevier or Copyright Clearance Center be responsible or liable for any costs, expenses or damage incurred by you as a result of a denial of your permission request, other than a refund of the amount(s) paid by you to Elsevier and/or Copyright Clearance Center for denied permissions.

### **LIMITED LICENSE**

The following terms and conditions apply only to specific license types:

15. **Translation:** This permission is granted for non-exclusive world **English** rights only unless your license was granted for translation rights. If you licensed translation rights you may only translate this content into the languages you requested. A professional translator must perform all translations and reproduce the content word for word preserving the integrity of the article. If this license is to re-use 1 or 2 figures then permission is granted for non-exclusive world rights in all languages.

16. **Website:** The following terms and conditions apply to electronic reserve and author

websites:

**Electronic reserve:** If licensed material is to be posted to website, the web site is to be password-protected and made available only to bona fide students registered on a relevant course if:

This license was made in connection with a course,

This permission is granted for 1 year only. You may obtain a license for future website posting,

All content posted to the web site must maintain the copyright information line on the bottom of each image,

A hyper-text must be included to the Homepage of the journal from which you are licensing at <http://www.sciencedirect.com/science/journal/xxxxx> or the Elsevier homepage for books at <http://www.elsevier.com> , and

Central Storage: This license does not include permission for a scanned version of the material to be stored in a central repository such as that provided by Heron/XanEdu.

17. **Author website** for journals with the following additional clauses:

All content posted to the web site must maintain the copyright information line on the bottom of each image, and the permission granted is limited to the personal version of your paper. You are not allowed to download and post the published electronic version of your article (whether PDF or HTML, proof or final version), nor may you scan the printed edition to create an electronic version. A hyper-text must be included to the Homepage of the journal from which you are licensing at <http://www.sciencedirect.com/science/journal/xxxxx> . As part of our normal production process, you will receive an e-mail notice when your article appears on Elsevier's online service ScienceDirect ([www.sciencedirect.com](http://www.sciencedirect.com)). That e-mail will include the article's Digital Object Identifier (DOI). This number provides the electronic link to the published article and should be included in the posting of your personal version. We ask that you wait until you receive this e-mail and have the DOI to do any posting.

Central Storage: This license does not include permission for a scanned version of the material to be stored in a central repository such as that provided by Heron/XanEdu.

18. **Author website** for books with the following additional clauses:

Authors are permitted to place a brief summary of their work online only.

A hyper-text must be included to the Elsevier homepage at <http://www.elsevier.com> . All content posted to the web site must maintain the copyright information line on the bottom of each image. You are not allowed to download and post the published electronic version of your chapter, nor may you scan the printed edition to create an electronic version.

Central Storage: This license does not include permission for a scanned version of the material to be stored in a central repository such as that provided by Heron/XanEdu.

19. **Website** (regular and for author): A hyper-text must be included to the Homepage of the journal from which you are licensing at <http://www.sciencedirect.com/science/journal/xxxxx> . or for books to the Elsevier homepage at <http://www.elsevier.com>

20. **Thesis/Dissertation:** If your license is for use in a thesis/dissertation your thesis may be submitted to your institution in either print or electronic form. Should your thesis be published commercially, please reapply for permission. These requirements include permission for the Library and Archives of Canada to supply single copies, on demand, of the complete thesis and include permission for UMI to supply single copies, on demand, of the complete thesis. Should your thesis be published commercially, please reapply for permission.

## 21. Other Conditions:

v1.6

If you would like to pay for this license now, please remit this license along with your payment made payable to "COPYRIGHT CLEARANCE CENTER" otherwise you will be invoiced within 48 hours of the license date. Payment should be in the form of a check or money order referencing your account number and this invoice number RLNK500886359.

Once you receive your invoice for this order, you may pay your invoice by credit card. Please follow instructions provided at that time.

**Make Payment To:**  
Copyright Clearance Center  
Dept 001  
P.O. Box 843006  
Boston, MA 02284-3006

For suggestions or comments regarding this order, contact RightsLink Customer Support: [customercare@copyright.com](mailto:customercare@copyright.com) or +1-877-622-5543 (toll free in the US) or +1-978-646-2777.

Gratis licenses (referencing \$0 in the Total field) are free. Please retain this printable license for your reference. No payment is required.

---

---

## SPRINGER LICENSE TERMS AND CONDITIONS

Nov 05, 2012

---



---

This is a License Agreement between Iskra Stefanova ("You") and Springer ("Springer") provided by Copyright Clearance Center ("CCC"). The license consists of your order details, the terms and conditions provided by Springer, and the payment terms and conditions.

**All payments must be made in full to CCC. For payment instructions, please see information listed at the bottom of this form.**

License Number	3018320326959
License date	Oct 29, 2012
Licensed content publisher	Springer
Licensed content publication	Experimental Brain Research
Licensed content title	fMRI signal increases and decreases in cortical areas during small-field optokinetic stimulation and central fixation
Licensed content author	Marianne Dieterich
Licensed content date	Jan 1, 0001
Volume number	148
Issue number	1
Type of Use	Thesis/Dissertation
Portion	Figures
Author of this Springer article	No
Order reference number	
Title of your thesis / dissertation	Age-related changes of the cortical visual-vestibular interaction in healthy subjects
Expected completion date	Jan 2013
Estimated size(pages)	100
Total	0.00 EUR
Terms and Conditions	

### Introduction

The publisher for this copyrighted material is Springer Science + Business Media. By clicking "accept" in connection with completing this licensing transaction, you agree that the following terms and conditions apply to this transaction (along with the Billing and Payment terms and conditions established by Copyright Clearance Center, Inc. ("CCC"), at the time that you opened your Rightslink account and that are available at any time at <http://myaccount.copyright.com>).

### Limited License

With reference to your request to reprint in your thesis material on which Springer Science and Business Media control the copyright, permission is granted, free of charge, for the use indicated in your enquiry.

Licenses are for one-time use only with a maximum distribution equal to the number that you identified in the licensing process.

This License includes use in an electronic form, provided its password protected or on the university's intranet or repository, including UMI (according to the definition at the Sherpa website: <http://www.sherpa.ac.uk/romeo/>). For any other electronic use, please contact Springer at ([permissions.dordrecht@springer.com](mailto:permissions.dordrecht@springer.com) or [permissions.heidelberg@springer.com](mailto:permissions.heidelberg@springer.com)).

The material can only be used for the purpose of defending your thesis, and with a maximum of 100 extra copies in paper.

Although Springer controls copyright to the material and is entitled to negotiate on rights, this license is only valid, provided permission is also obtained from the (co) author (address is given with the article/chapter) and provided it concerns original material which does not carry references to other sources (if material in question appears with credit to another source, authorization from that source is required as well).

Permission free of charge on this occasion does not prejudice any rights we might have to charge for reproduction of our copyrighted material in the future.

#### Altering/Modifying Material: Not Permitted

You may not alter or modify the material in any manner. Abbreviations, additions, deletions and/or any other alterations shall be made only with prior written authorization of the author(s) and/or Springer Science + Business Media. (Please contact Springer at ([permissions.dordrecht@springer.com](mailto:permissions.dordrecht@springer.com) or [permissions.heidelberg@springer.com](mailto:permissions.heidelberg@springer.com)))

#### Reservation of Rights

Springer Science + Business Media reserves all rights not specifically granted in the combination of (i) the license details provided by you and accepted in the course of this licensing transaction, (ii) these terms and conditions and (iii) CCC's Billing and Payment terms and conditions.

#### Copyright Notice:Disclaimer

You must include the following copyright and permission notice in connection with any reproduction of the licensed material: "Springer and the original publisher /journal title, volume, year of publication, page, chapter/article title, name(s) of author(s), figure number(s), original copyright notice) is given to the publication in which the material was originally published, by adding; with kind permission from Springer Science and Business Media"

#### Warranties: None

Example 1: Springer Science + Business Media makes no representations or warranties with respect to the licensed material.

Example 2: Springer Science + Business Media makes no representations or warranties with respect to the licensed material and adopts on its own behalf the limitations and disclaimers established by CCC on its behalf in its Billing and Payment terms and conditions for this licensing transaction.

#### Indemnity

You hereby indemnify and agree to hold harmless Springer Science + Business Media and CCC, and their respective officers, directors, employees and agents, from and against any and all claims arising out of your use of the licensed material other than as specifically authorized pursuant to this license.

#### No Transfer of License

This license is personal to you and may not be sublicensed, assigned, or transferred by you to

any other person without Springer Science + Business Media's written permission.

#### No Amendment Except in Writing

This license may not be amended except in a writing signed by both parties (or, in the case of Springer Science + Business Media, by CCC on Springer Science + Business Media's behalf).

#### Objection to Contrary Terms

Springer Science + Business Media hereby objects to any terms contained in any purchase order, acknowledgment, check endorsement or other writing prepared by you, which terms are inconsistent with these terms and conditions or CCC's Billing and Payment terms and conditions. These terms and conditions, together with CCC's Billing and Payment terms and conditions (which are incorporated herein), comprise the entire agreement between you and Springer Science + Business Media (and CCC) concerning this licensing transaction. In the event of any conflict between your obligations established by these terms and conditions and those established by CCC's Billing and Payment terms and conditions, these terms and conditions shall control.

#### Jurisdiction

All disputes that may arise in connection with this present License, or the breach thereof, shall be settled exclusively by arbitration, to be held in The Netherlands, in accordance with Dutch law, and to be conducted under the Rules of the 'Netherlands Arbitrage Instituut' (Netherlands Institute of Arbitration).**OR:**

**All disputes that may arise in connection with this present License, or the breach thereof, shall be settled exclusively by arbitration, to be held in the Federal Republic of Germany, in accordance with German law.**

#### Other terms and conditions:

##### v1.3

If you would like to pay for this license now, please remit this license along with your payment made payable to "COPYRIGHT CLEARANCE CENTER" otherwise you will be invoiced within 48 hours of the license date. Payment should be in the form of a check or money order referencing your account number and this invoice number RLNK500886354.

Once you receive your invoice for this order, you may pay your invoice by credit card. Please follow instructions provided at that time.

#### Make Payment To:

Copyright Clearance Center  
Dept 001  
P.O. Box 843006  
Boston, MA 02284-3006

For suggestions or comments regarding this order, contact RightsLink Customer Support: [customercare@copyright.com](mailto:customercare@copyright.com) or +1-877-622-5543 (toll free in the US) or +1-978-646-2777.

Gratis licenses (referencing \$0 in the Total field) are free. Please retain this printable license for your reference. No payment is required.

---

---